

# **SAFETY OF LITHIUM NICKEL COBALT ALUMINUM OXIDE BATTERY PACKS IN TRANSIT BUS APPLICATIONS**

Timothy Cleary  
Marc Serra Bosch  
Jim Kreibick  
Joel Anstrom

February 2016

## ABSTRACT

The future of mass transportation is clearly moving toward the increased efficiency and greenhouse gas reduction of hybrid and electric vehicles. With the introduction of high-power/high-energy storage devices such as lithium ion battery systems serving as a key element in the system, valid safety/security concerns are presented. This is especially true when the attractive high specific energy and power chemistry, lithium nickel cobalt aluminum oxide (NCA), is used. This chemistry provides great performance but presents a safety and security risk when used in large quantities, such as for a large passenger bus. If triggered, the cell can completely fuel its own fire and this triggering event occurs more easily than one may think.

To assist engineers and technicians in this transfer from primarily the use of fossil fuels to battery energy storage on passenger buses, the Battery Application Technology Testing and Energy Research Laboratory of the Thomas D. Larson Pennsylvania Transportation Institute in the College of Engineering at The Pennsylvania State University partnered with advanced chemistry battery and material manufacturers to study the safety concerns of a NCA battery chemistry for use in transit buses. The research team ran various experiments on cells and modules, studying the rarely considered thermal events or venting events. Special considerations were made to gather supporting information to help better understand what happens, and most importantly how to best mitigate these events and/or manage them when they occur on a passenger bus.

## ACKNOWLEDGMENTS

This report and the supporting work was sponsored by the Mineta National Transit Research Consortium under a University Transportation Centers grant from the U.S. Department of Transportation Research and Innovative Technology Administration, with matching equipment and supplies provided by a manufacturer of advanced chemistry cells.

The Pennsylvania State University's Thomas D. Larson Pennsylvania Transportation Institute (The Larson Institute) administratively supported this work by making facilities and personnel available. The Larson Institute research team expresses special thanks to David Klinikowski, director of the Larson Institute's Federal Transit Administration-sponsored Bus Research and Testing Center (BRTC), for his oversight and guidance during this project, and the BRTC personnel for their assistance in configuring the test site to accommodate this research.

# TABLE OF CONTENTS

<b>List of Figures</b>	<b>6</b>
<b>Executive Summary</b>	<b>11</b>
<b>Introduction</b>	<b>12</b>
<b>I. Literature Review</b>	<b>13</b>
Cell Information	13
Battery Failures and Regulations	17
Design of Experiments	26
<b>II. Material Study</b>	<b>30</b>
Plastic	30
Metal	34
<b>III. Testing Preparation</b>	<b>37</b>
Understanding Cell Construction	37
Machining	37
Data Acquisition Setup	41
Single Cell Testing Design	44
Air Press	48
<b>IV. Single Cell Testing</b>	<b>50</b>
Acetal – Overcharge	50
Acetal - Nail Puncture	54
Acetal - Overcharge and Material Test	56
Pyrophobic - Overcharge	59
Pyrophobic - Nail Puncture	62
Pyrophobic - Overcharge With Housing	65
PET - Overcharge	68
PET - Nail Puncture	72
Teflon - Overcharge	76
Teflon - Nail Puncture	79
Single Cell Conclusions	81
Nail Tip Temperature Measurement	81
<b>V. Module Level Testing Design</b>	<b>85</b>

Manifold Design	86
Cell Separator Design	88
Pressure Release / Check Valve	89
Securing the Module	94
<b>VI. Module Level Testing</b>	<b>95</b>
Single Cell Overcharge in a module with Acetal headers	95
Overcharge of 20 cells in steel enclosure	100
Check valve test	110
<b>VII. Crash Testing</b>	<b>112</b>
Preparation for the truck	112
Pendulum	115
Free Swing Test	117
Battery Pack preparation	119
Impact Test Results and Conclusions	120
<b>VIII. Environmental Impacts</b>	<b>124</b>
<b>IX. Conclusion</b>	<b>126</b>
<b>X. Select Abbreviations and Acronyms</b>	<b>127</b>
<b>XI. Bibliography</b>	<b>128</b>
<b>XII. About the authors</b>	<b>130</b>
<b>XIII. Appendix A – Data Acquisition Scripts</b>	<b>132</b>
<b>XIV. Appendix B – Drawings</b>	<b>133</b>
<b>XV. Appendix C – Specification Sheets</b>	<b>134</b>
<b>XVI. Appendix D - FMVSS STANDARDS</b>	<b>135</b>

# LIST OF FIGURES

Figure 1.	Cell After Venting Event.....	14
Figure 2.	Single Cell Nail Puncture Test.....	15
Figure 3.	Data from Manufacturer Overcharge.....	16
Figure 4.	Molecules Present in Venting Gas.....	17
Figure 5.	Proportion of Vehicles Involved in Traffic Crashes in US .....	18
Figure 6.	Bus occupants dead by initial point of impact.....	18
Figure 7.	Bus occupants injured by initial point of impact .....	19
Figure 8.	Vehicle Standards around the World .....	20
Figure 9.	FMVSS No.305 Tests Conditions.....	22
Figure 10.	Battery Pack on the Roof of the Bus.....	25
Figure 11.	Battery Packs on the Side of the Bus .....	25
Figure 12.	Safety Discussions Prior to Entering the Test Site.....	29
Figure 13.	Commercially Available Polymers .....	30
Figure 14.	Melting Point VS Price and VS Density .....	31
Figure 15.	Melting Points Above Acetal .....	31
Figure 16.	Results of a Single cell Acetal Test.....	32
Figure 17.	Narrowed Material Search .....	33
Figure 18.	Mechanical Properties of POM and PET .....	33
Figure 19.	Results from a Metal Test .....	35
Figure 20.	Aluminum Enclosure After Overcharge Event.....	36
Figure 21.	Acetal Separators After Overcharge Event .....	36
Figure 22.	Cell Internals – Negative Terminal Disassembled .....	37
Figure 23.	Machining Preparation.....	38
Figure 24.	Material Hold Down for Separator Machining.....	39
Figure 25.	Cell Pockets .....	40
Figure 26.	Facing Step.....	40

<b>Figure 27.</b>	<b>Completed Separator .....</b>	<b>40</b>
<b>Figure 28.</b>	<b>PET Machining.....</b>	<b>40</b>
<b>Figure 29.</b>	<b>Welding.....</b>	<b>40</b>
<b>Figure 30.</b>	<b>Complete Assembly.....</b>	<b>40</b>
<b>Figure 31.</b>	<b>Monitoring the data through Vector CANoe.....</b>	<b>41</b>
<b>Figure 32.</b>	<b>Data Can Bus Channels.....</b>	<b>42</b>
<b>Figure 33.</b>	<b>Thermocouple Ranges.....</b>	<b>42</b>
<b>Figure 34.</b>	<b>Arduino Based Isolated Voltage Measurement PCB .....</b>	<b>43</b>
<b>Figure 35.</b>	<b>Initial Single Cell Test Stand Design .....</b>	<b>45</b>
<b>Figure 36.</b>	<b>Cell Enclosure.....</b>	<b>46</b>
<b>Figure 37.</b>	<b>Top Down View of Cell Enclosure .....</b>	<b>47</b>
<b>Figure 38.</b>	<b>Metal Straps.....</b>	<b>48</b>
<b>Figure 39.</b>	<b>Nail Puncture Air Press.....</b>	<b>49</b>
<b>Figure 40.</b>	<b>Single Cell Overcharge Test .....</b>	<b>51</b>
<b>Figure 41.</b>	<b>Data from Initial Overcharge Test .....</b>	<b>52</b>
<b>Figure 42.</b>	<b>Venting Cell – First Test.....</b>	<b>53</b>
<b>Figure 43.</b>	<b>Cell, Hours After Venting Event .....</b>	<b>54</b>
<b>Figure 44.</b>	<b>Acetal Nail Puncture – Cell Temperatures .....</b>	<b>55</b>
<b>Figure 45.</b>	<b>Acetal Nail Puncture – Material Temperatures.....</b>	<b>56</b>
<b>Figure 46.</b>	<b>Acetal Overcharge with Blast Shield Material Test Setup .....</b>	<b>57</b>
<b>Figure 47.</b>	<b>Acetal Overcharge w/ Material – Cell Temperatures.....</b>	<b>57</b>
<b>Figure 48.</b>	<b>Acetal Overcharge w/ Material – Material Temperatures .....</b>	<b>58</b>
<b>Figure 49.</b>	<b>Acetal – Overcharge with Material Test .....</b>	<b>59</b>
<b>Figure 50.</b>	<b>Pyrophobic – Overcharge Setup .....</b>	<b>60</b>
<b>Figure 51.</b>	<b>Pyrophobic – Overcharge Data .....</b>	<b>61</b>
<b>Figure 52.</b>	<b>Pyrophobic – Overcharge Results.....</b>	<b>62</b>
<b>Figure 53.</b>	<b>Pyrophobic – Nail Puncture Data.....</b>	<b>63</b>

Figure 54.	Pyrophobic Material Results .....	64
Figure 55.	Pyrophobic Material After Nail Puncture .....	64
Figure 56.	Pyrophobic – Overcharge with Enclosure Setup .....	65
Figure 57.	Pyrophobic – Overcharge with Enclosure Data .....	66
Figure 58.	Pyrophobic Enclosure Vent Opening .....	67
Figure 59.	Pyrophobic Overcharge with Enclosure Material Results .....	68
Figure 60.	PET – Overcharge Setup .....	69
Figure 61.	PET – Overcharge Data .....	70
Figure 62.	PET – Overcharge Temperature Data .....	70
Figure 63.	PET – Material Result .....	71
Figure 64.	PET – Material Result 2 .....	72
Figure 65.	PET – Nail Puncture Data .....	73
Figure 66.	PET – Positive Venting First .....	74
Figure 67.	PET – Nail Puncture Material Result .....	74
Figure 68.	PET – Nail Puncture Results 2 .....	75
Figure 69.	Blast Radius.....	76
Figure 70.	Teflon - Overcharge Data .....	77
Figure 71.	Teflon Overcharge Material Results .....	78
Figure 72.	Teflon Overcharge Material Data .....	78
Figure 73.	Teflon Overcharge Material Results 2 .....	79
Figure 74.	Teflon – Nail Puncture Data .....	80
Figure 75.	Teflon – Nail Puncture Material Results .....	81
Figure 76.	Nail Tip Temperature Measurement Test Setup .....	82
Figure 77.	Nail Tip Temperature Measurement Test Data .....	83
Figure 78.	Cell and Surroundings After Test .....	84
Figure 79.	Headers Designed for Module Testing.....	85
Figure 80.	CAD of the Battery Pack Assembled .....	86

Figure 81.	CAD of the Manifold Design .....	86
Figure 82.	CAD of the Inside Manifold Design .....	87
Figure 83.	CAD of the Manifold Design w/ Eyebolts.....	87
Figure 84.	CAD of Separator Design w/o Top .....	88
Figure 85.	CAD of the Walls Design .....	88
Figure 86.	Moles of One Cell .....	89
Figure 87.	Trigger.....	90
Figure 88.	Enclosure Pressure Subsystem .....	91
Figure 89.	Check Valve Subsystem .....	91
Figure 90.	Flow Rate Equations. Source: Parker Valves Catalog 4135-CV .....	92
Figure 91.	Full Check Valve Model .....	93
Figure 92.	Simulation Results.....	93
Figure 93.	Handle to lift the Battery Pack up w/ the Forklift.....	94
Figure 94.	Data - Cell Overcharge.....	96
Figure 95.	Data Dummies Cells .....	97
Figure 96.	Bottom Header Temperatures.....	97
Figure 97.	Bottom Header Temperatures (Treated Individually) .....	98
Figure 98.	Bottom Header and the Closest Cell Temperatures.....	99
Figure 99.	Cover Temperatures.....	99
Figure 100.	Enclosure After the Test .....	100
Figure 101.	Battery Pack prior to Testing .....	102
Figure 102.	Overcharge_20_cells_steel_enclosure- First try- Data.....	103
Figure 103.	Overcharge_20_cells_steel_enclosure- Second try- Data .....	104
Figure 104.	Overcharge_20_cells_steel_enclosure- Third try- Data .....	104
Figure 105.	Overcharge_20_cells_steel_enclosure- Data .....	105
Figure 106.	Bottom Header Temperatures.....	106
Figure 107.	Cover Temperatures.....	107

<b>Figure 108.</b>	<b>Steel Temperatures.....</b>	<b>108</b>
<b>Figure 109.</b>	<b>Battery Pack Venting.....</b>	<b>109</b>
<b>Figure 110.</b>	<b>Sequence of the venting process .....</b>	<b>109</b>
<b>Figure 111.</b>	<b>Check Valve Test Exhaust After Test.....</b>	<b>111</b>
<b>Figure 112.</b>	<b>18,400 lbs. GVWR Refrigerated Truck to Simulate Bus .....</b>	<b>113</b>
<b>Figure 113.</b>	<b>Refrigerated Box Remove from Crash Truck.....</b>	<b>113</b>
<b>Figure 114.</b>	<b>I Beam Sections Welded to Chassis Frame.....</b>	<b>114</b>
<b>Figure 115.</b>	<b>Jersey Barriers Mounted onto Truck Chassis .....</b>	<b>115</b>
<b>Figure 116.</b>	<b>Left, Top View of Bumper, Right Bottom View .....</b>	<b>116</b>
<b>Figure 117.</b>	<b>Impact Mass Mounted Bumper and Battery Position .....</b>	<b>116</b>
<b>Figure 118.</b>	<b>Radar Alignment .....</b>	<b>117</b>
<b>Figure 119.</b>	<b>Pendulum Test Swing Setup .....</b>	<b>118</b>
<b>Figure 120.</b>	<b>Impact Accuracy of Pendulum to Battery Position .....</b>	<b>119</b>
<b>Figure 121.</b>	<b>Aluminum Enclosure with Frame Mounting Flanges .....</b>	<b>119</b>
<b>Figure 122.</b>	<b>Battery Module Mounted on Frame with Data Acquisition .....</b>	<b>120</b>
<b>Figure 123.</b>	<b>Camera Layout .....</b>	<b>120</b>
<b>Figure 124.</b>	<b>Fire Fighters Approach Battery Pack after Impact .....</b>	<b>121</b>
<b>Figure 125.</b>	<b>Individual Cell Temperatures during Simulated Crash Event .....</b>	<b>122</b>
<b>Figure 126.</b>	<b>Deformation of bumper and module enclosure .....</b>	<b>122</b>
<b>Figure 127.</b>	<b>Dented battery cell .....</b>	<b>123</b>
<b>Figure 128.</b>	<b>Sample Tube Leading to Gas Sample Bag .....</b>	<b>124</b>
<b>Figure 129.</b>	<b>Gas Chromatography Results .....</b>	<b>125</b>
<b>Figure 130.</b>	<b>Molecules Present in Venting Gas .....</b>	<b>125</b>

## EXECUTIVE SUMMARY

Electrical energy storage is a key component in many of today's advanced vehicles. Lithium nickel cobalt aluminum oxide (NCA) offers great energy and power density but also presents a safety and security risk when used on passenger buses. To assist engineers and technicians in the process of implementing NCA battery systems into heavy vehicles, the Penn State research team with support from MNTRC and research sponsors, tested large format NCA cells and modules under several scenarios and present here in the resulting data.

This report covers a literature review of publicly available information from battery and vehicle manufacturers, presents information on the cells, modules, and materials selected for this research, and finally presents all the results for use in developing safe and secure high-energy / high-power electrical energy storage systems for heavy vehicles.

During this research several groups were invited to witness the battery stress testing, including three local fire companies who were able to participate in the overcharging of a single cell and a crash test of an electrified heavy vehicle.

# INTRODUCTION

This report was written for a broad audience, covering the safety and security concerns when using lithium nickel cobalt aluminum oxide (NCA) cell systems, other research regarding the current regulations, as well as the setup, execution, and results of testing performed by this research group.

After a presentation of the literature review and introduction to the test setup, the report primarily covers the various tests performed and results obtained, specifically the cell and material performance during an overcharge, nail puncture, short circuit, or impact test. This entailed simulating some of the most likely scenarios a passenger bus battery system will likely be exposed to during its service life on the road, charging, or during maintenance.

To safely perform these tests, experts were consulted to determine all the necessary personal-protective equipment, operating distances, preparation, and disposal procedures. This information was made available to all researchers and support personnel. It is not recommended that these tests are performed without properly preparing for the worst-case scenario. Please do not try to repeat these tests without all necessary safety measures in place.

To safely operate a vehicle with large onboard electrical energy storage including hundreds of cells, a battery management system a design capable of handling thermal events for a reasonable amount of time is necessary. Educating the workforce responsible for the safe and secure design, integration, and maintenance of these high-power / high-energy systems is necessary for the long-term success of electric and hybrid electric vehicles using this chemistry. This work strives to support the education effort.

# I. LITERATURE REVIEW

A literature review was conducted to evaluate standards, regulations, and publications to identify research gaps and pursue new innovative safety tests to run on large-format NCA battery cells and packs that are used in bus transit applications.

This section is divided into three subsections. The first contains information necessary to gain familiarity with the cells used in this research. The second goes over the regulations that electrical energy storage manufacturers are facing as well as the problems that transit authorities and firefighters are confronting due to the increase of electric and hybrid vehicles on the road. Finally, the third subsection summarizes the set of test scenarios evaluated by this research group.

## CELL INFORMATION

The collection of information started with the cells themselves, including format, chemistry, and properties that inevitably lead to thermal runaway. However, there are not many studies available on large-format cells used in transit applications, presumably due to recent growth in battery technology. The majority of the publications are on the smaller-format 18650 cells, which contain much less energy and, as a consequence, exhibit less energetic thermal events.

Beyond publications, the research group contacted cell manufacturers for information regarding how to safely operate their batteries and the conditions to be avoided. According to manufacturers, unsafe conditions occur when any cell is operated outside of published temperature, voltage, and or current ranges. If one, or more, of these conditions are experienced by NCA cells they are assumed to be damaged and could possibly enter thermal runaway. Overcharging one or more cells to the point of failure was determined to be a feasible default test since this fits the scope of the project and was safely repeatable within lab facilities and capabilities. It is also reasonably affordable, and representative of many likely scenarios on board electric transit busses. This scenario primary simulates the failure of a battery management system (BMS) to accurately measure cell voltage and/or act on a voltage fault resulting in a cell overcharge.

The data sheet for the cells selected as part of this work, GAIA NCA 45 Ah, provided a well-defined range of operating conditions for voltage, current, and temperature. Failures generally occur when a cell is operated outside its manufacture rating. According to manufacturer's information, the safe cell voltage range is 2 to 4.2V. This is the primary safety limitation. The safe range of operating temperatures is strictly defined as -30°C to 60°C, however this work will show that thermal/venting events occur even with in this range. As far as the current limitations,

values for continuous and peak charge and discharge are detailed within the attached specification sheet and range from 270 (charge) to 1250 (discharge) but are condition and state dependent. A full specification sheet for the large-format cell selected for this research can be found in Appendix C – Specification Sheets.

Generally, when overcharged or mechanically damaged, cell failures are followed by thermal runaway as a result of a cell internal fault, which is one of the most severe failure conditions for this chemistry (Pistoia, 2010).

In general, whenever a charged Li-ion cell is exposed to temperatures above 60°C, there is a risk of initiating a strong exothermic reaction within the cell. The heat generated by these reactions will result in a rise in the cell temperature, which in turn activates heat generation amplitude or additional exothermic reactions that build up pressure in the cell. The cells used in this research are equipped with a safety/pressure burst disc at each terminal side rated at 144-200 psi at room temperature. Figure 1 shows a cell that was overcharged until its burst discs were opened and the cell vented.

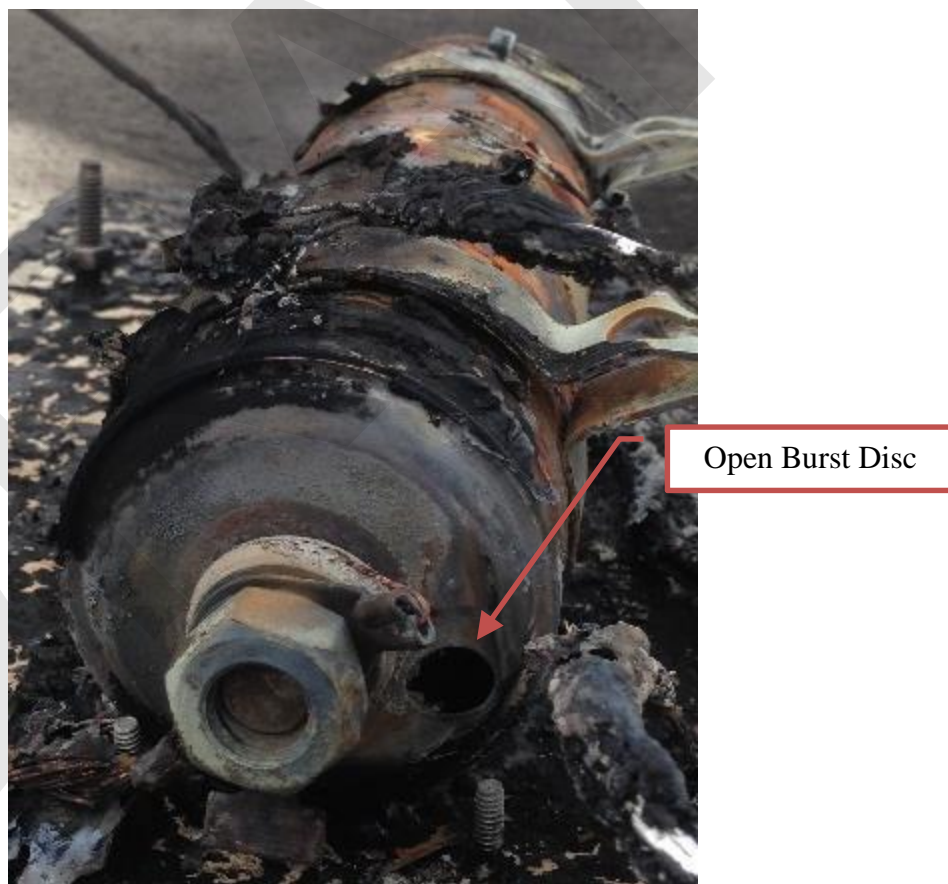


Figure 1. **Cell After Venting Event**

The venting process implies the release of flammable electrolyte, generation of gases, or even a rupture of the cell casing. In most cases, all three happen just about simultaneously. Figure 2 demonstrates the intensity of the venting process, as exhibited by flames and gases energetically flowing out over approximately five seconds.



Figure 2. **Single Cell Nail Puncture Test**

Figure 2 only shows what can happen to one cell, but in heavy buses, battery packs consist of hundreds of cells wired in a series/parallel configuration. In a high-quantity, multi-cell pack, such as an electric bus, the venting of just one cell can propagate its thermal energy to neighboring cells causing, a chain reaction until all cells rupture due to extreme thermal conditions.

Figure 3 presents voltage, current, and temperature from an overcharge test performed by the cell manufacturer. As seen in this figure, a fully charged cell (4.2 V at no load) was continuously charged at 100 A until the battery vented. During the test, the constant current increased voltage to approximately 5.2 V. This high potential between terminals and or other internal phenomena likely caused internal shorts, dropping the cell voltage to below 5 V. Once internal shorts or other energy releasing reactions occur, an abrupt increase in temperature rise/rate is seen.

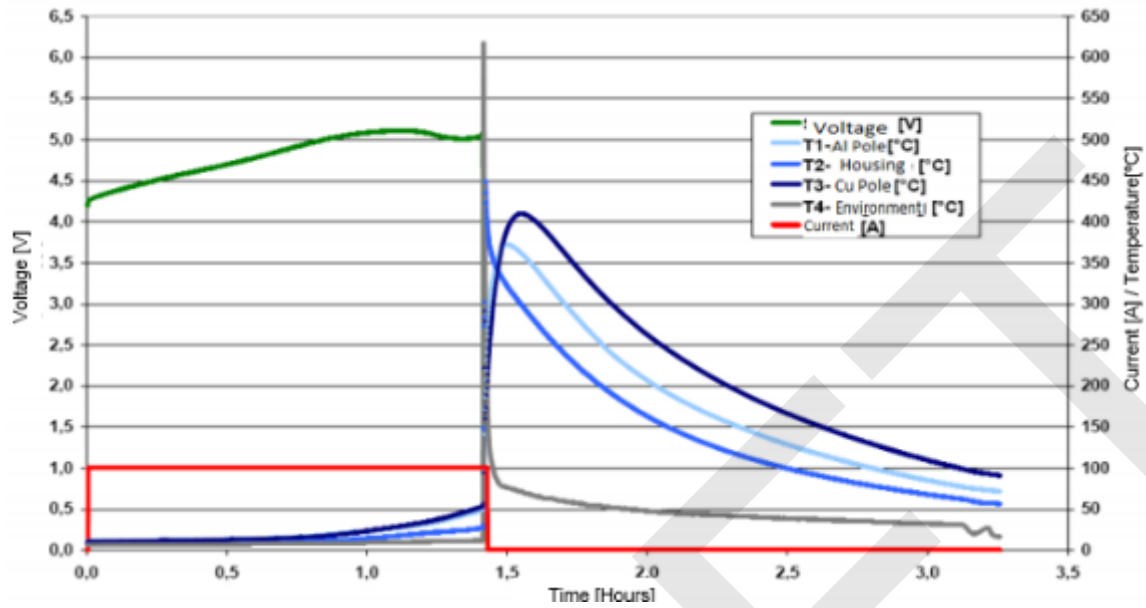
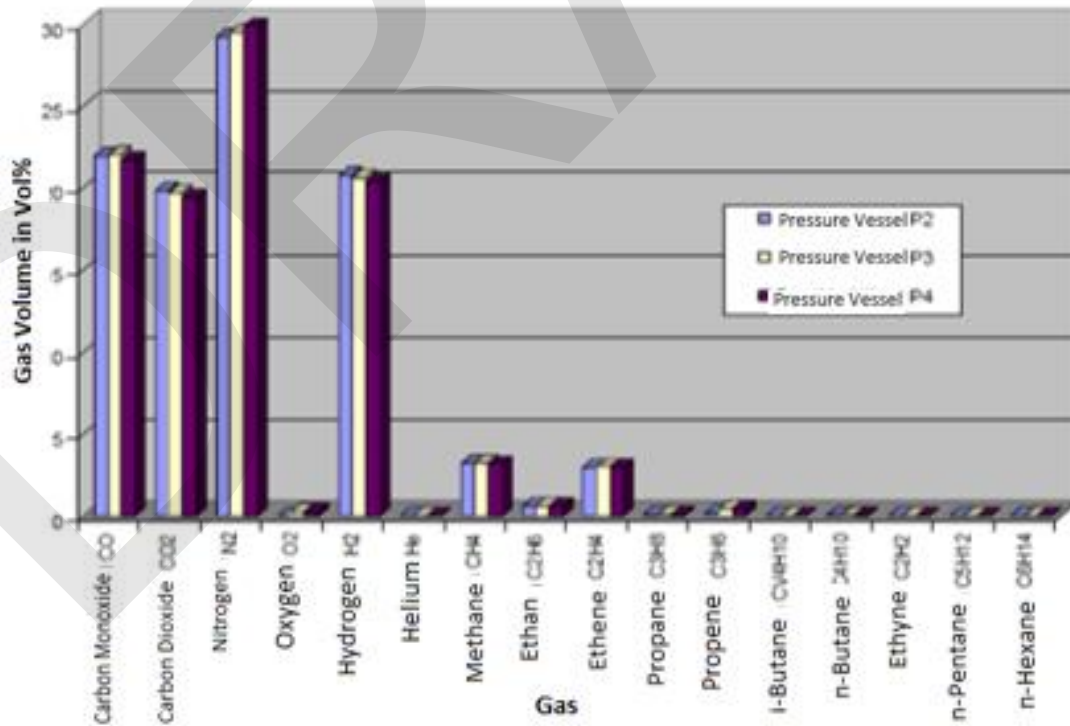


Figure 3. **Data from Manufacturer Overcharge**

Source: GAIA via Lithium Technology Corporation

As a result, when the cell vented, the temperature in the surrounding environment rose immediately to 600°C for a short period of time. Temperature sensors placed on the battery rose to 400-450°C and remained warm, taking several hours to cool down to ambient temperature.



## Figure 4. Molecules Present in Venting Gas

Source: GAIA via Lithium Technology Corporation

Figure 4 shows the molecules present in the venting gasses by percentage of the total volume. The carbon monoxide, carbon dioxide, nitrogen and hydrogen are the principal gases released during the venting of the cell. Nitrogen, hydrogen, and carbon dioxide represent minimal threats to the atmosphere and humans. However, carbon monoxide is toxic.

### **BATTERY FAILURES AND REGULATIONS**

The most common failures in automotive battery systems were researched by contacting car insurance companies and consulting the Pennsylvania Department of Transportation reports. However, significant information was not found, so other publications were examined to determine the forces batteries experience during a crash event, how to reproduce them, and what level of hazard they would represent.

During the process of going over the standards and regulations for electric vehicles (EV) / hybrid electric vehicles (HEV) / pluggable hybrid electric vehicles (PHEV) it became apparent that many associations such as the Society of Automotive Engineers (SAE), National Fire Protective Association (NFPA), and Federal Motor Vehicle Safety Standards (FMVSS) have developed standards; however, information is scattered and varies from association. The researched information was divided into the following topics:

1. Regulations of electrical energy storage in buses
2. First responder strategies / tactics to respond to EV/HEV/PHEV incidents
3. Commercial battery pack characteristics
4. Fire-suppression systems
5. Electric vehicle crashes

### **Government Regulations**

First of all, let's take a look at the statistics of the proportion of vehicles involved in Traffic accidents in US. The data is obtained from the Traffic Safety Facts report which is an annual compilation of motor vehicle crash data presented by the National Highway Traffic Safety Administration (NHTSA).

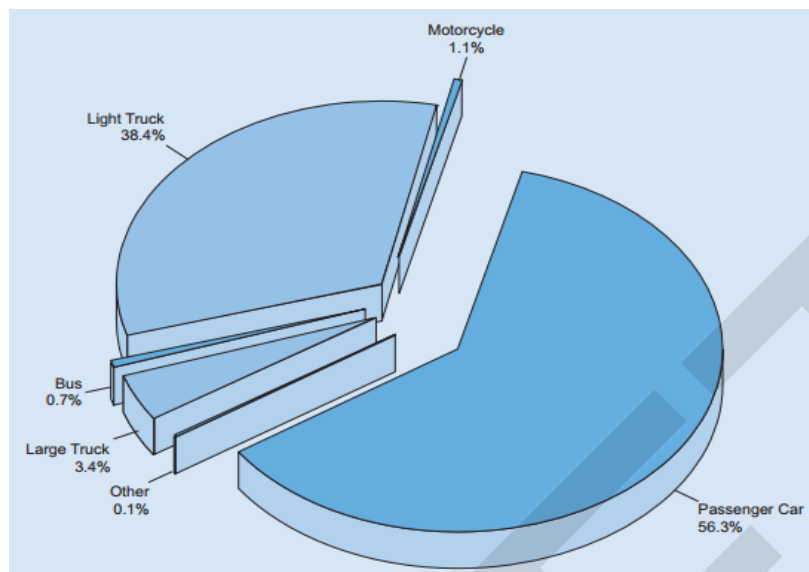


Figure 5. **Proportion of Vehicles Involved in Traffic Crashes in US**

Source: Traffic Safety Facts 2013

Figure 5 shows that buses are involved in less than 1% of accidents compared to passenger cars and light trucks which are the most common vehicles on the road. Figure 6 illustrates the percentage of bus accident fatalities in 2013 based on the initial point of impact.

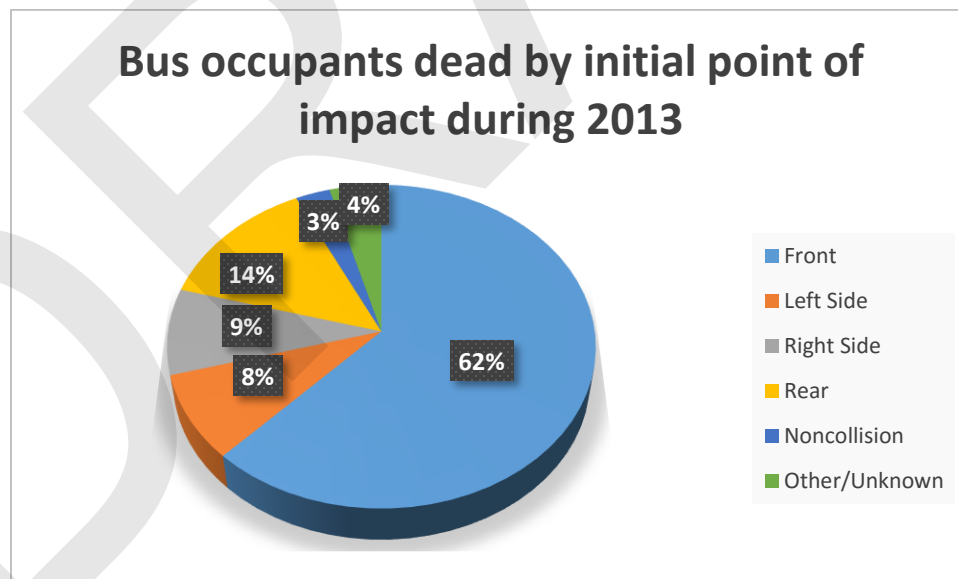


Figure 6. **Bus occupants dead by initial point of impact.**

Source: Data from Traffic Safety Facts 2013

Figure 6 also indicates frontal impacts are the worst case scenario with the highest percentage of fatalities. In 62% of fatal accidents the impact came from the front. Lower fatality rates occur during rear (14%), right side (9%), and left side (8%) accidents. In Figure 7, the same data is presented for injuries and it is observed that the percentages are more equally distributed among each side of the vehicle.

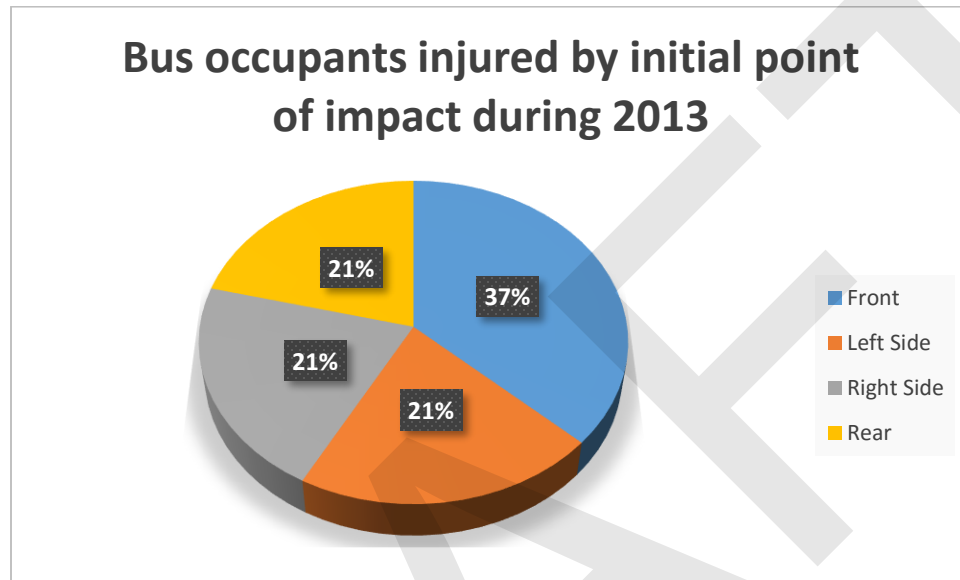


Figure 7. **Bus occupants injured by initial point of impact**

Source: Data from Traffic Safety Facts 2013

In a frontal crash the most common types of injury mechanisms for passengers seated in a Seat-to-Seat configuration are neck flexion or extension. These injuries are due to the combination of the passengers being unrestrained and the low back seat designs (Gerardo Olivares, Vikas Yadav). The Federal Motor Vehicle Safety Standard (FMVSS) No.207 establishes requirements for seats, attachment assemblies, and installation, to minimize the possibility of failure as a result of forces acting on the seat in vehicle impact and the standard FMVSS No.208 regulates the "Occupant Crash Protection" to reduce the number of fatalities and the number and severity of injuries to occupants involved in frontal crashes.

The Federal Motor Vehicle Safety Standards (FMVSS) are the requirements issued by US government to qualify a vehicle before entering the market to insure the vehicles on the road are safe. Compliance with government regulations are analyzed through a set of tests to determine if the vehicle passes or fails. In addition, there are institutes and associations that provide ratings to give the clients some guidelines about the safety of the vehicle. Associations and institutes such as the Insurance Institute for Highway Safety (IIHS) have developed different tests

and ratings to be able to measure and report the safety response of the vehicle during a crash. These associations are well known and respected by consumers.

Figure 8 illustrates the vehicle safety regulations and associations by country. Please, notice that the star indicates association meanwhile § means Government regulation.

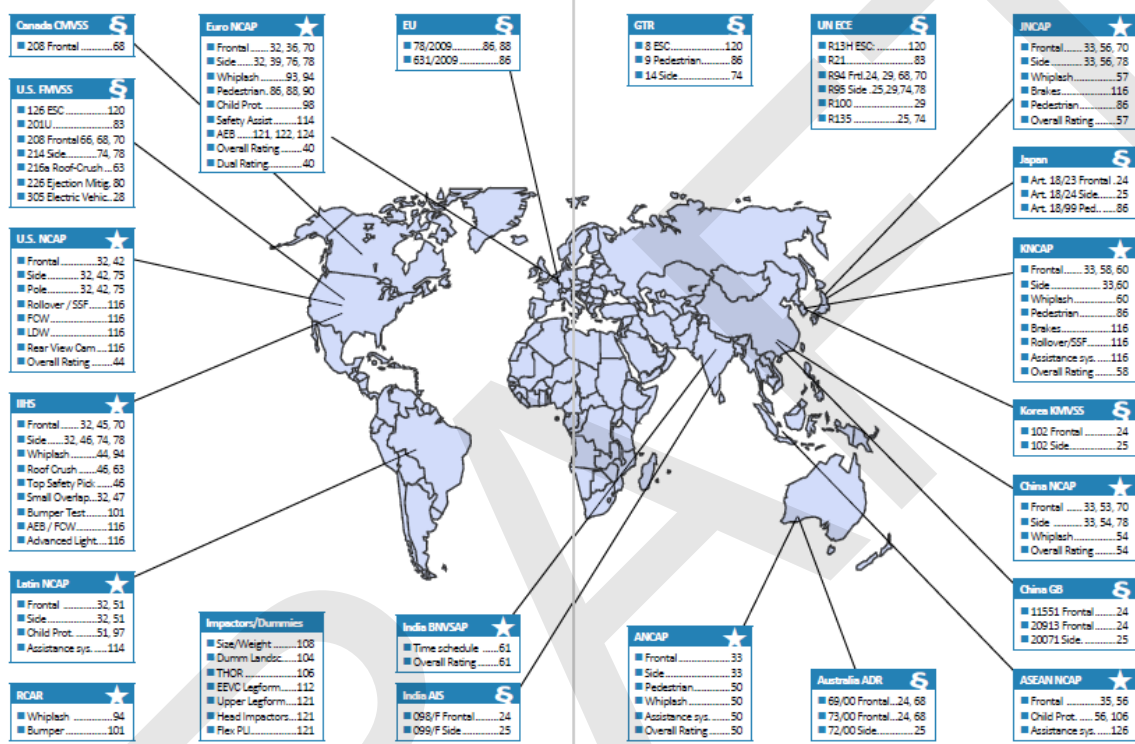


Figure 8. Vehicle Standards around the World

Source: Safety Companion 2016

The U.S. is regulated by the standards under the U.S. FMVSS and several ratings, including the U.S. New Car Assessment Program (NCAP) AND IIHS. Moreover, the UN ECE also applies to US.

### UN ECE:

The United Nations Economic Commission for Europe (UNECE) is the forum where the countries of Western, Central and Eastern Europe, Central Asia and North America, 56 countries in all, come together to forge the tools of their economic cooperation. That cooperation concerns economics, statistics, environment, transport, trade, sustainable energy, timber and habitat (ECE, 2012). The UN ECE

released the Proposal for an Electric Vehicle Regulatory Reference Guide which cites, summarizes, compares and analyzes regulations from the countries that form the UN ECE.

#### *U.S. NCAP:*

The National Highway Traffic Safety Administration's New Car Assessment Program (NCAP) created the 5-Star Safety Ratings Program to provide consumers with information about the crash protection and rollover safety of new vehicles beyond what is required by Federal law. One star is the lowest rating; five stars is the highest. (safercar.gov)

Insurance Institute for Highway Safety (IIHS): The Insurance Institute for Highway Safety is an independent, nonprofit scientific and educational organization dedicated to reducing the losses, deaths, injuries and property damage from crashes on the nation's roads. The Highway Loss Data Institute (HLDI) shares and supports this mission through scientific studies of insurance data representing the human and economic losses resulting from the ownership and operation of different types of vehicles and by publishing insurance loss results by vehicle make and model. (IIHS.org)

#### *FMVSS No 305: SAFETY REQUIREMENTS FOR ELECTRIC VEHICLES*

Scope: Cars, busses, trucks with a GVWR of 4536Kg or less that use electrical components with working voltages higher than **60 volts direct current (VDC) or 30 volts alternating current (VAC)**, and whose speed attainable is more than 40km/h.

#### Requirements:

- Max. 5 liters of electrolyte may spill from the batteries
- There shall be no evidence of electrolyte leakage into the passenger compartments
- All components of the electric energy storage/conversion system must be anchored to the vehicle
- No battery system component that is located outside the passenger compartment shall enter the passenger compartment isolations must be greater than or equal to:
  - 500 ohms/V for all DC high voltage sources without isolation monitoring and for all AC high voltage sources

- 100 ohms/V for all dc high voltage sources with continuous monitoring of electrical isolation
- The voltage of the voltage source ( $V_b$ ,  $V_1, V_2$ ) must be less than or equal to 30 VAX for AC components or 60VDC for DC components

Test conditions:

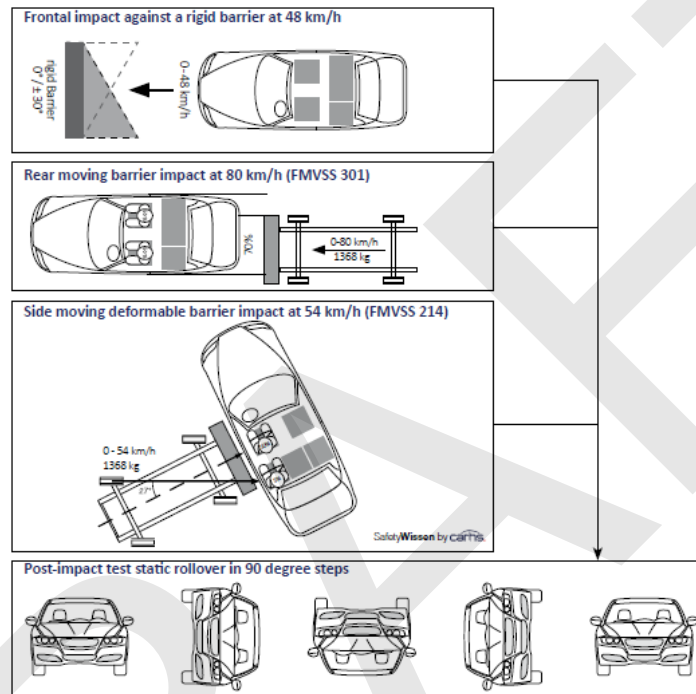


Figure 9. **FMVSS No.305 Tests Conditions**

Source: Safety Companion 2016

Figure 9 details the test conditions of FMVSS No.305. According to the scope it's assumed that this regulation is not applicable to all kinds of buses since for example a full size bus is around 39.000 lbs. so it exceeds the weight specified in the scope so the standard does not cover all the buses.

Buses must also comply with state regulations. In the case of the New York State, there is the Bus & Passenger Vehicle Regulations published by New York State Department of transportation (Transportation, 1999) that establishes a set of requirements, always according to the US Department of transportation (DOT), including:

- Vehicle inspection

- Motor vehicle identification and markings
- Vehicle safety requirements
- Vehicles for transporting the disabled
- Electrical systems
- Electric powered motor vehicles
- Identification of electric vehicles
- Equipment requirements for electric and hybrid-electric buses
- **Batteries and battery compartment**
- Electric propulsion circuit
- Range selectors
- **Electrical overload protection**
- Regenerative braking systems
- Back-up alarm

The Batteries and Battery compartment specifies a set of requirements for the battery pack with respect to crash worthiness including:

- Battery compartment(s) shall be designed and constructed to prevent all battery fluids, such as gel, liquid electrolytes, caustic, reactive or toxic gases or fumes, from entering the passenger compartment when a vehicle is subjected to a moving contoured barrier crash test such that:
  - a) The contoured barrier shall weigh 4,000 pounds and be configured as specified in Figure 2 of FMVSS 301 (49 CFR 571.301)
  - b) The barrier assembly shall be traveling longitudinally forward at any speed up to and including 30 mph at the time of impact
  - c) The barrier assembly may impact the test vehicle at any point and at any angle

Note, that it refers to the FMVSS No. 301 to specify the characteristics of the barrier so it means that the state laws also take into account the FMVSS standards and adapt them.

Furthermore, there is the Standard Bus Procurement Guidelines (SBPG) 2013 released by American Public Transit Association (APTA) (American Public

Transportation Association, 1997) that are a model for solicitation of offers and contracts for the supply of transit buses and also specify requirements about crash.

### **Transit Authorities and First Responders**

This section addresses how first responders perform their duties in response to accidents involving battery powered vehicles. This issue is very general and there no unique answer. However, firefighters are usually the group in charge and manipulate the vehicle to rescue the victims if necessary. This understanding directed the research group to investigate procedures for first responders or firefighters to approach battery systems in a bus crash. Some concerns are ensuring the safety of the responders and accident victims from potential high voltage and exposure to dangerous chemicals.

Further review investigated strategies the fire departments adopted for EV and HEV fires and as a result the training fire fighters are receiving. Although they are already trained to handle conventional vehicles, fire fighters are trained by their department to learn additional procedures to respond to electric vehicles fires. NFPA published a report that developed the technical basis for best practices in emergency response procedures for electric drive vehicle battery incidents. A major conclusion of the study was that EV fires should be treated differently than conventional vehicle fires because more water is required to cool down the battery completely. Usually, an additional engine has to act as an extra water supply since the water is applied for a relatively longer period after the flames are no longer visible. This is because of the possibility of battery cells reigniting after hours of rest. Unless the battery pack has been cooled down sufficiently this is a potential risk. For this reason, NFPA guidelines also recommended burned vehicles be kept at least 50 feet of any combustible material for some time after the event.

Since battery packs are placed in different locations within the vehicle, NFPA published a field guide to determine the location of the high voltage battery within the vehicle and provide guidance to shut down and disable the battery packs and vehicle circuits. NFPA also concluded that the vehicle structure should not be pierced, cut or dismantled because the first responder has the potential to come in contact with high voltage. Current firefighter personal protective equipment (PPE) does not offer the appropriate level of electrical protection. Field experiments have shown there is no adverse electrical current at the nozzle during the firefighting operations (National Fire Protection Association, 2014). However, this information does not provide post-crash procedures or a check list for fire departments and traffic associations to perform after an electric vehicle accident.

## Commercial battery pack characteristics

The amount of energy that needs to be stored in an electric bus requires large battery packs that often cannot be located in one specific location. As a consequence, in many cases it has to be distributed throughout the vehicle.

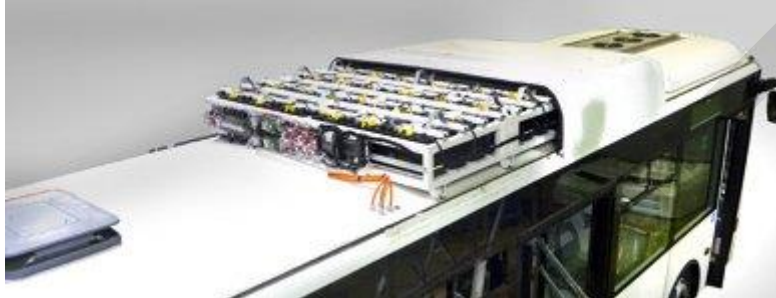


Figure 10. **Battery Pack on the Roof of the Bus**

Source: <http://www.pvi.fr/energie-embarquee-batteries,042.html?lang=en>

The most common locations are the roof and sides. Figure 10 shows a battery pack on the roof of a bus. Roof mounting is also used in buses running on gaseous fuels like compressed natural gas or hydrogen to protect tanks from side impact.



Figure 11. **Battery Packs on the Side of the Bus**

Source:

[http://www.lifeofguanghou.com/node\\_981/node\\_989/node\\_997/node\\_1007/2010/11/19/129014852382496.shtml](http://www.lifeofguanghou.com/node_981/node_989/node_997/node_1007/2010/11/19/129014852382496.shtml)

Alternatively, Figure 11 shows the battery packs mounted on the side. In some cases, cooling systems are also roof-top mounted. Also, the packs have to be properly enclosed and sealed to avoid any contact with water and prevent damage to any electronic components.

This research group expected to find guidelines for commercial battery pack design and recommended materials for bus side panels in order to replicate them for

testing purposes. However, the proprietary nature of bus designs made it very difficult to find information on composites and alloys utilized by the bus industry. Most critically, this investigation centered on which plastic material should be used for cell holders within the battery pack since the material had to have good mechanical, machining, and thermal properties at a reasonable price. Fortunately, we had access to several donated commercial vehicle battery packs which were analyzed in order to design a representative battery pack for testing.

## **Fire Suppression Systems**

According to the NFPA, there is a vehicle fire every two minutes in the US. With an increase in the number of electric vehicles on the road, the fire suppression systems industry and the firefighters and traffic associations have to adopt new procedures to overcome all the challenges they pose.

There is no doubt that the electric vehicle incidents present a challenge to develop new products and materials. The industry is considering two main options: the first one is that the material itself possesses properties to suppress the fire and the second option is that a fire suppression system is incorporated either in or around the battery pack.

However, no regulation is currently proposed that obligates the addition of fire suppression systems to Lithium ion cells or packs and therefore a majority of electrical energy storage manufacturers are not assembling fire suppression systems into their packs in order to control the cost (Fire Protection Engineering, 2012).

## **Electric Vehicle Crash**

Review of battery crash test publications revealed several variants. One variant consisted of bolting down the battery pack while a crash device was impacted into the battery pack. The other variant was completely the opposite in which the battery was moved to impact the crash device. In both variants the vehicle dynamics were neglected (Dr. Lothar Wech, Richard Richter).

In regard to crash velocity, our crash tests were conducted near 20 mph because the literature affirmed that to be a common speed limit in urban environments (Jennifer Chu, 2013).

## **DESIGN OF EXPERIMENTS**

To conclude the literature review, the last task was to define a matrix of battery stress tests or destructive, test to failure tests, that would be within the capability of the researcher facilities, budget and most beneficial to the battery/bus designing

and maintenance community. The set of tests was limited by the number of cells, materials, and time to generate pack design and the stressing mechanisms that the batteries would be submitted. The test matrix included both single cells, ten cell modules, and twenty cell modules to represent sections of a full battery pack found in heavy vehicle systems.

From the literature review, it was understood that during a venting scenario thermal energy is released in the form of visible flames, and smoke. Thermal propagation at the pack level is a serious problem since the thermal energy can propagate to neighboring cells. For this reason, several pack designs were considered to reduce or eliminate thermal propagation by quickly releasing or absorbing the heat from the pack to avoid thermal propagation.

Different enclosure designs were tested including aluminum and steel materials with a variety of emergency venting designs to release or contain gases using a check valve. Polyoxymethylene (POM) commercially known as Acetal, Polyethylene terephthalate (PET) and Polytetrafluoroethylene (PTFE) commercially known as Teflon as well as a special material donated by a research sponsor were the materials selected to be tested. The batteries were submitted to electrical and mechanical abuse through different tests to induce thermal runaway. To replicate electrical abuse tests, the group subjected the batteries to overcharge and nail puncture tests. As a mechanical abuse test, a 20 mph side impact crash test was performed. The following sections detail each test.

### **Overcharge**

As the cell is over charged, lithium ions are irreversibly removed from the positive electrode and deposited as lithium metal on the negative electrode. This de-lithiation of the positive electrode continues as the cell voltage increases during overcharge until eventually the lithium ions are completely depleted from the positive electrode. During the overcharge process, the cell impedance starts to rise due to an increase in the positive electrode material resistance. At the same time, the electrolyte within the cell begins to decompose, coating the active materials and further contributing to the increase in cell impedance. The increasing cell impedance results in an increase in resistive losses in the form of thermal energy. The cell temperature starts to rise rapidly as an exothermic reaction between the de-lithiated positive electrode material and the electrolyte occurs. Once the cell temperature rises above approximately 60°C, the rate of this reaction accelerates generating a large amount of carbon dioxide.

The cell temperature continues to rise until the internal temperature reaches approximately 130–135°C. In this temperature range, the cell separator undergoes a phase transition that closes the porosity of the membrane and impedes the

transport of ions between the electrodes. This engineered safety feature “shuts down” the separator terminating the charge current and ending the overcharge process. In some instances, a “shutdown” of the separator is unable to stop the self-heating of the cell which eventually leads to additional exothermic degradation processes. These “additional” processes are not well understood but if sufficiently activated can continue to generate heat within the cell and can eventually lead to a thermal runaway (Ashis Arora, Noshirwan K. Medora, Thomas Livernois, and Jan Swart., 2010).

### **Nail Puncture**

This test attempts to simulate a cell internal short circuit condition by using a nail to achieve a short between the cell’s positive and negative electrodes. By causing a short between the terminals, there will be a very large short circuit current. Most of this power will be dissipated off in the form of heat in the cell, increasing the temperature of the internal materials, boiling electrolyte and increasing pressure inside the cell. The pressure will only reach at most 200 psi since the burst discs on either terminal of the cell are rated to handle this pressure. A nail puncture test is a standard and was chosen here to replicate damage during a crash event. It was also used to intentionally induce an internal short to dissipate any residual energy and ensure the cells are safe to handle for disposal after overcharge or other non-nail puncture testing.

### **Simulation of Side Impact at 20 mph**

A large impact pendulum located in LTI’s facilities was used to simulate a 20 mph side impact. Direct impact of an SUV bumper was simulated at 20 MPH to replicate the likely scenario of light vehicles crashing into a transit bus on urban streets.



Figure 12. **Safety Discussions Prior to Entering the Test Site**

As part of this test, local fire departments and environmental health and safety personnel were invited as part of a workforce development session. Discussions prior to the testing, seen in Figure 12, were centered around the test setup and plan. Following the test, the emergency responders acted to suppress the event and educate their firefighters on the appropriate response and approach to actual crash situations.

## II. MATERIAL STUDY

At the system level, batteries are composed of cell separators to hold each battery in place, and then an enclosure to protect the batteries and their BMS components from various environmental conditions. Typically, the cell separators and enclosure are not made of the same material due to the different properties a designer looks for from each component. Separators have to be light, low cost, have high impedance and a high melting point. All these requirements are accomplished by a thermoplastic polymer. The material for the enclosure is going to be responsible for absorbing part of the energy in a crash scenario, so it has to be a material with good mechanical properties, low in cost, capable of withstanding high temperatures and as light as possible since the cells make up most of the weight of a battery pack. In this case, the material can be conductive because the cells won't be in contact with the material. Based on these requirements, the ideal material is a metal.

### PLASTIC

Acetal is the commercial name of Polyoxymethylene (POM) and graphing all the polymers of the market, it's clear that there is a linear relation between the product price x density and the melting point. Figure 13 shows this relationship between the melting point, cost, and density.

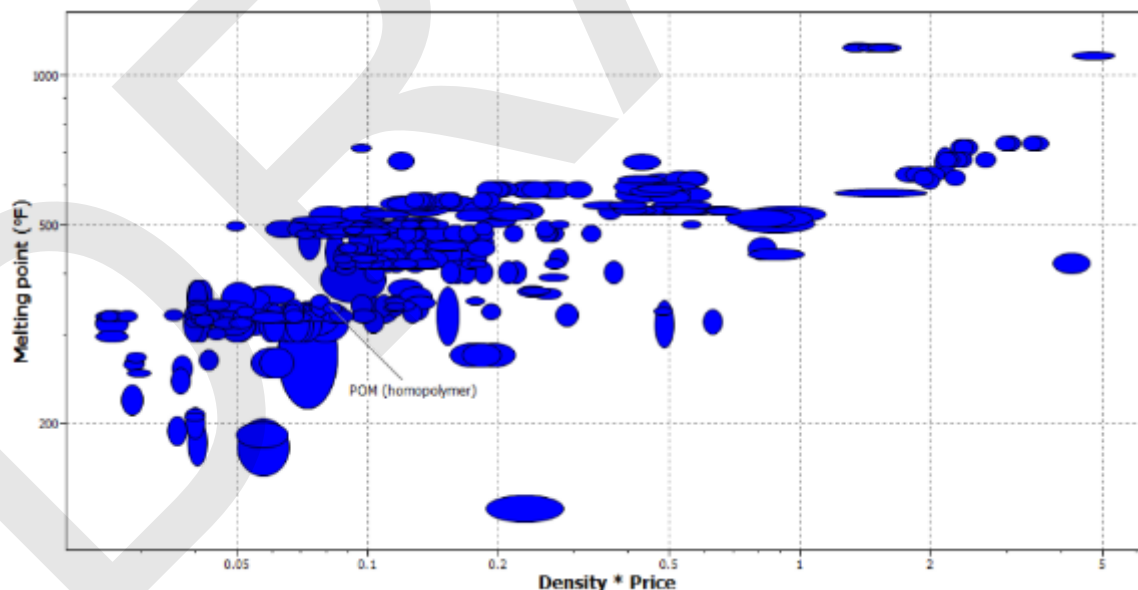


Figure 13. **Commercially Available Polymers**

Graph created w/ CES EduPack-Granta Design

In fact, breaking down the product, as seen in Figure 14, it's noticeable that there is a close link between price and melting point.

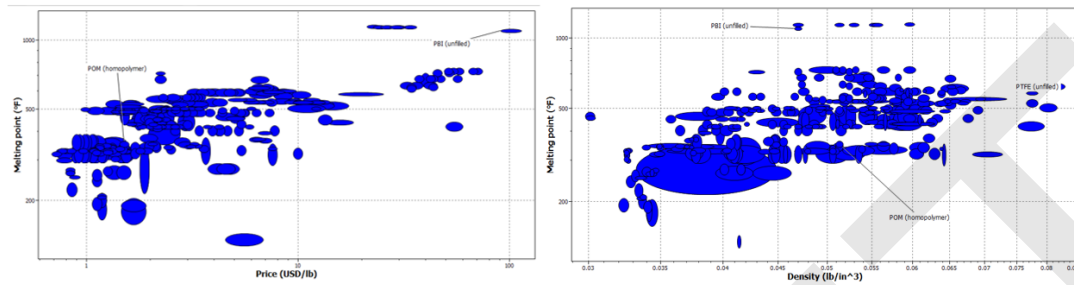


Figure 14. **Melting Point VS Price and VS Density**

Graph created w/ CES EduPack-Granta Design

Thus Acetal initially looks like a good candidate. Nevertheless, the tests performed showed that the flames coming out the battery and its casing temperature after an event are much higher in temperature than the melting point of the Acetal (160°C) so all the Acetal melted and ended up burning until it was gone. Thus, different materials with higher melting point were selected. Using the same relation between price and density versus melting point, the next candidates are sought.

Figure 15 shows materials with a higher melting point than the Acetal. There are several choices but none of which is feasible due to the excessive price or density. Furthermore, the market doesn't demand these materials in the thicknesses needed to build the battery systems tested in the research, making it very difficult to get those specific materials with the thickness needed at an affordable price.

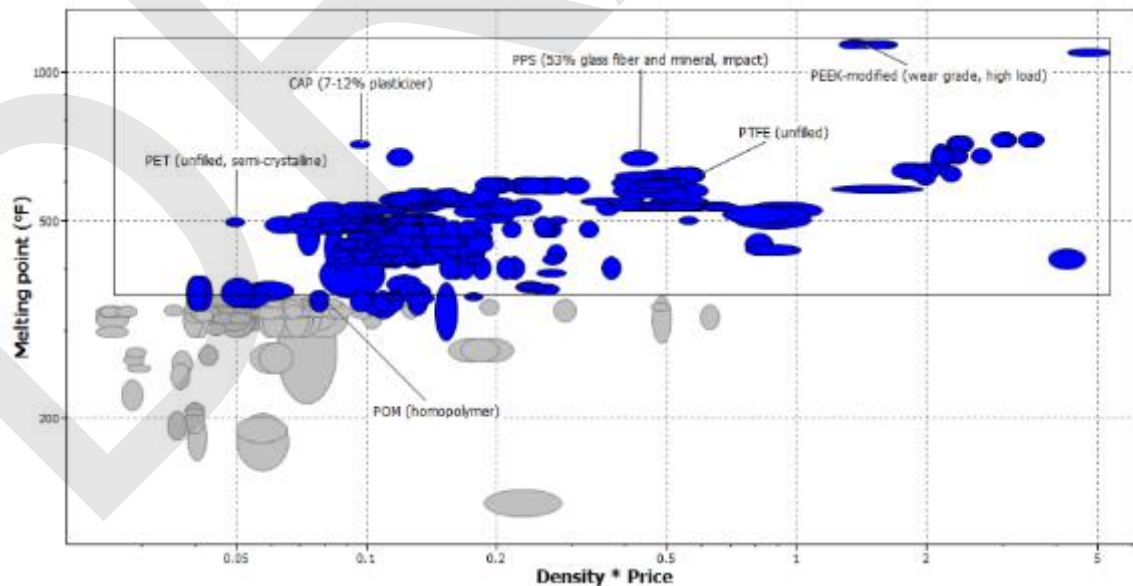


Figure 15. **Melting Points Above Acetal**

Graph created through CES EduPack-Granta Design

Being more restrictive with the product density x price parameter, the Polyphenylene sulfide (PPS) shows up as a possible contender but again it was hard to find a provider that supplies the thickness needed. Then, keeping candidates from the same area the Polytetrafluoroethylene (PTFE) appears, a material often used in the industry because of its great qualities like electrical insulation, inherent flame resistance, low coefficient of friction and obviously the high melting point (338.89°C).

The fact that Teflon (PTFE) is inherently flame resistant makes this material very interesting for the worst case scenario conditions that this research will test. It's expected that this material shouldn't act as a combustible, potentially reducing the length of heat generation and smoke production during an event. Figure 16 shows the results of a single cell test when Acetal was used to hold the cell. The material continued to burn well after the cell vented. Producing smoke for approximately 30 min. after the event and concluding in a complete lack of structural support mechanical separation or electrical isolation.



Figure 16. Results of a Single cell Acetal Test

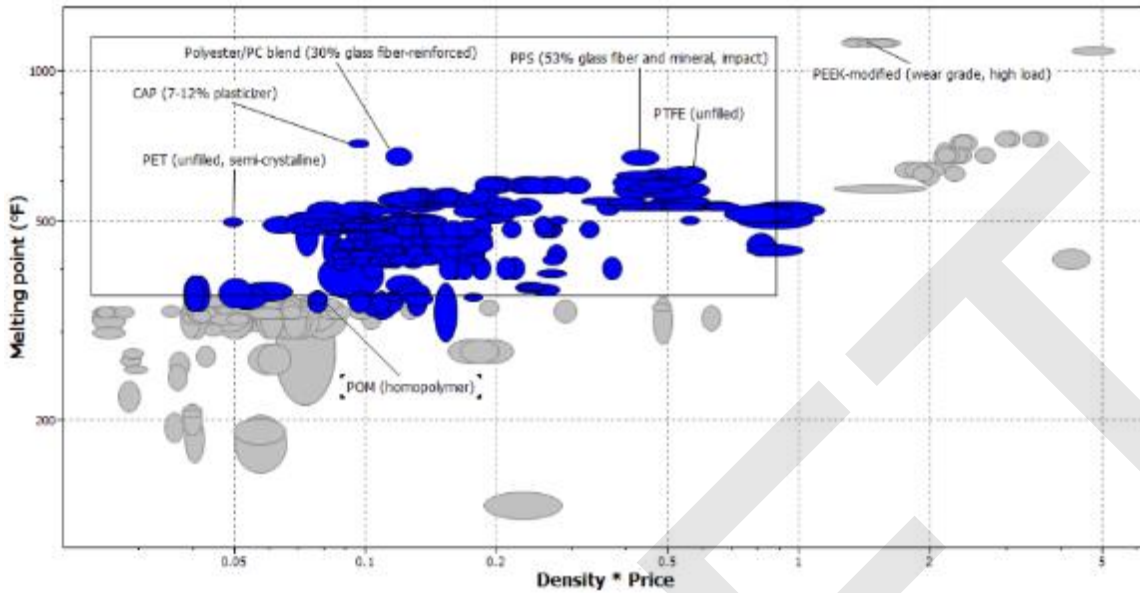


Figure 17. Narrowed Material Search

Graph created through CES EduPack-Granta Design

The Polyethylene Terephthalate (PET), as seen in Figure 17, is also selected based on its high melting point relative to Acetal. It also has a better price/density relationship than the Acetal.

POM (homopolymer)				PET (unfilled, semi-crystalline)			
Price				Price			
Price	* 1.44	- 1.58	USD/lb	Price	* 0.939	- 1.03	USD/lb
Physical properties				Physical properties			
Density	0.0509	- 0.0517	lb/in <sup>3</sup>	Density	0.0495	- 0.0506	lb/in <sup>3</sup>
Mechanical properties				Mechanical properties			
Young's modulus	0.4	- 0.521	10 <sup>6</sup> psi	Young's modulus	0.4	- 0.45	10 <sup>6</sup> psi
Yield strength (elastic limit)	9.5	- 10	ksi	Yield strength (elastic limit)	* 9.43	- 10.2	ksi
Tensile strength	9.7	- 10	ksi	Tensile strength	10.2	- 10.9	ksi
Elongation	10	- 75	% strain	Elongation	65	- 75	% strain
Compressive modulus	0.651	- 0.685	10 <sup>6</sup> psi	Compressive modulus	* 0.4	- 0.6	10 <sup>6</sup> psi
Compressive strength	* 15.7	- 18	ksi	Compressive strength	* 11	- 14.9	ksi
Flexural modulus	0.379	- 0.489	10 <sup>6</sup> psi	Flexural modulus	0.434	- 0.448	10 <sup>6</sup> psi
Flexural strength (modulus of rupture)	13.6	- 16	ksi	Flexural strength (modulus of rupture)	* 10.2	- 10.9	ksi
Shear modulus	* 0.149	- 0.194	10 <sup>6</sup> psi	Shear modulus	* 0.144	- 0.216	10 <sup>6</sup> psi
Bulk modulus	* 0.464	- 0.487	10 <sup>6</sup> psi	Bulk modulus	* 0.717	- 0.753	10 <sup>6</sup> psi
Poisson's ratio	0.33	- 0.35		Poisson's ratio	* 0.381	- 0.396	
Shape factor	5.1			Shape factor	5.7		
Hardness - Vickers	* 19.7	- 24.8	HV	Hardness - Vickers	* 17	- 20	HV
Hardness - Rockwell M	92	- 94		Hardness - Rockwell M	92	- 87	
Hardness - Rockwell R	114	- 126		Hardness - Rockwell R	120	- 125	
Fatigue strength at 10 <sup>7</sup> cycles	* 3.46	- 4.49	ksi	Fatigue strength at 10 <sup>7</sup> cycles	* 2.8	- 4.2	ksi
Mechanical loss coefficient (tan delta)	* 0.0111	- 0.0145		Mechanical loss coefficient (tan delta)	* 0.00966	- 0.0145	

Figure 18. Mechanical Properties of POM and PET

Source: CES EduPack-Granta Design Materials Data Base

As seen in Figure 18, PET has acceptable mechanical properties for cell separation and structural support as well as similar machining properties to Acetal. Another proprietary plastic material manufactured by Pyrophobic Systems was also experimentally analyzed during this work. The results of all materials are presented in each of the test sections to follow.

## METAL

Battery packs made for transit bus applications are typically enclosed in thin sheeting of plastic, composite, steel or aluminum. There hasn't yet been a mass acceptance of any one material. This section aims to address why special considerations should be made for the material selection of the enclosure material.

First, the objective of this material is to possibly supply structural support, if necessary, otherwise at least limit the transfer of smoke, heat or other materials from leaving the battery system in the event of a cell thermal run away. Second, this material needs to be capable of withstanding the environment as most battery systems on passenger buses are located outside the cabin and exposed to moisture and debris. Finally, the material shouldn't melt down during a battery thermal event or other fire on board the vehicle.

A test was performed to evaluate the thermal performance of metals by positioning a sheet of common 6061 aluminum alloy and mild steel at either end of a cell undergoing an overcharge. As Figure 19 shows, the flames that came out from the cell during the venting event melted the Aluminum. This proves that the flames/gasses are hotter than the melting point of the Aluminum which is approximately 600°C. On the other hand, the steel plate was able to withstand the hot gasses and remain intact. A mark where the gasses met the steel can also be seen on the far side of the cell in Figure 19.



Figure 19. **Results from a Metal Test**

This test validated the use of a relatively thin, 1/8" thick, mild steel with approximate melting point of 1300°C when considering materials for exposure to direct venting. If considering a ducting system or isolation within a pack, steel is recommended. Also, for small packs with no isolation, steel should be used to contain the event for as long as possible giving passengers time to evacuate the bus. Otherwise, materials such as aluminum or even plastic will allow the hot gasses to escape immediately and potentially cause more fire damage at a faster rate, thus making evacuation much harder for passengers and allowing less time to safely exit. Also, less time would be available for first responders to contain the event by cooling the pack with water.



Figure 20. **Aluminum Enclosure After Overcharge Event**



Figure 21. **Acetal Separators After Overcharge Event**

A module level test of the same materials produced similar results as seen in Figure 20 and Figure 21. In this case the aluminum inner enclosure was damaged by the intense heat but the steel lid resisted damage. The Acetal battery separators were completely consumed by fire leaving only the stainless steel cell canisters.

### III. TESTING PREPERATION

#### UNDERSTANDING CELL CONSTRUCTION

To prepare for this destructive battery testing an investigation into the particular cell construction and internal configurations was performed.



Figure 22. **Cell Internals – Negative Terminal Disassembled**

To understand the mechanisms inside a cell the research team, partnered with Pennsylvania College of Technology, safely discharged and disassembled a cell. Figure 22 shows the negative terminal of the GAIA cell and inside view of the pressure release and electrical isolators.

#### **MACHINING**

All machining was performed by the students and faculty supported on the project. This section details the work performed to prepare for the various battery system destructive tests presented in this report.

During the fabrication of battery pack parts several processes and machining techniques were used. The cell separators were machined using a CNC mill, the covers and enclosure parts were cut using a water jet and finally the enclosure parts are

welded together using TIG welding. These are processes commonly used in the building of prototype battery systems and typically available to those designing and building these systems for low volume transit buses.

To speed series production and at the same time get accurate dimensions, CNC technology was used to machine the complicated cell separators. Programming for CNC machining was done using MasterCAM software. Figure 23 shows the cut profile as planned prior to machining.

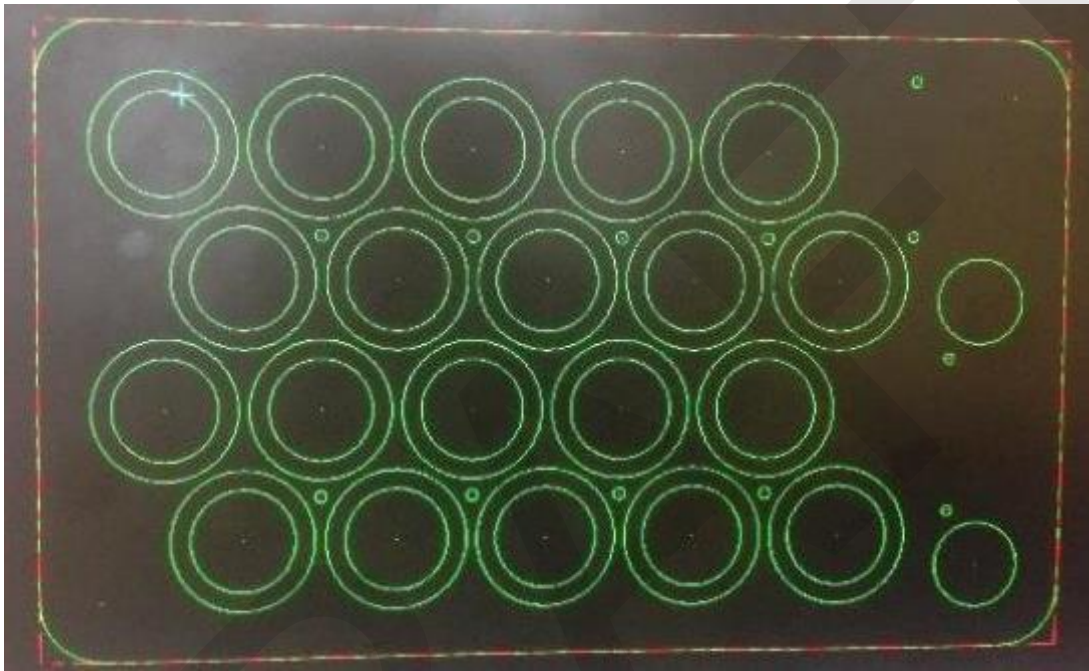


Figure 23. **Machining Preparation**

An aluminum plate was used below the cell separator so that through holes could be machined without bottoming out onto the end mill table. Figure 24 shows the aluminum plate and preparations made on the machines prior to any cutting steps.



Figure 24. **Material Hold Down for Separator Machining**

The following, Figure 25 and Figure 26 show some of the intermediate phases in the machine process while Figure 27 represents the final completed part.

The same steps were followed for all three materials selected for testing. Figure 28 shows the PET material during separator machine. Figure 29 shows a researcher preparing a battery enclosure for module testing while Figure 30 shows the completely machined internal module assembly, top and bottom cell separators and isolation walls.

The parts machined as part of this research were consumed by the battery destructive testing presented in other sections of this report.



Figure 25. **Cell Pockets**



Figure 26. **Facing Step**



Figure 27. **Completed Separator**

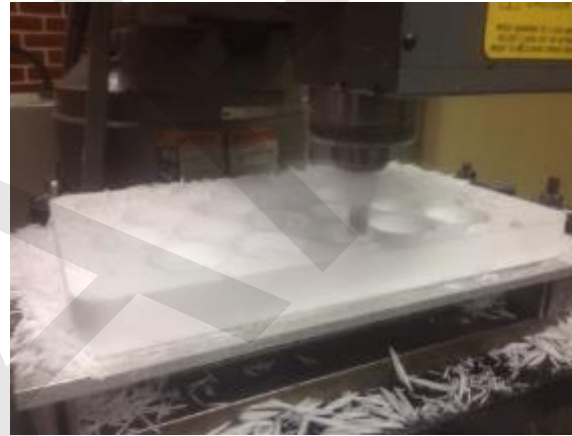


Figure 28. **PET Machining**



Figure 29. **Welding**



Figure 30. **Complete Assembly**

## DATA ACQUISITION SETUP

Data from voltage, current, temperature, and pressure sensors are vital in understanding the processes a cell undergoes during a destructive test. To gather all this information at a high rate and over long distances a Controller Area Network (CAN) bus was setup. All sensors were tied to the CAN bus via custom build embedded devices including necessary signal conditioning and calibration. Each message broadcast from a CAN node was logged using Vector CANtech hardware and software to monitor and capture the data in real time. This data allowed researchers to quantify batteries response under extreme conditions of voltage, current, temperature, and in some cases pressure.

Figure 31 **Error! Reference source not found.** shows a typical CANoe interface set up that logged data from the cells during a test including voltage, current, and temperature in this case. Notice the screen is split into three main windows. The window on the top left graphs the temperature of each sensor versus the test time. The window on the bottom left graphs the voltage and the current. In the case of this nail puncture test no current is flowing therefore the current value is zero. The window on the right displays raw data variables and current values available on the CAN network which are available for graphing.

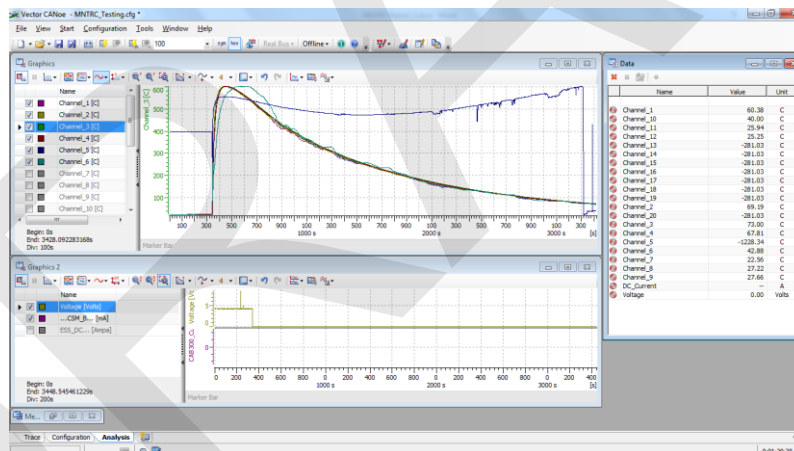


Figure 31. Monitoring the data through Vector CANoe

After a test, data was post processed and exported into a MATLAB format to clean up erroneous signals and apply any necessary scaling. Because of the various bus speeds and conflicting CAN IDs, several channels were required to record all test data.

Channel	Bus Speed	Equipment
1	500 kbps	Current sensor (CAB300)
1	500 kbps	Temperature sensor (18B20 and Thermocouples)
2	250 kbps	Pressure sensor (Honeywell MLH150PGB06A)
2	250 kbps	Voltage

Figure 32. **Data Can Bus Channels**

Figure 32 lists the channels and the bus speeds for each signal. A LEM CAB 300 current sensor was used to measure current with high resolution and accuracy. This current sensor is the same type used in battery monitoring applications where high accuracy and very low offset are required. By collecting accurate current and voltage data during testing it was possible to integrate the amount of energy each battery consumed during a test.

Thermocouples and single wire digital sensors were placed in various locations along both the cell and packaging materials. In early testing, 18B20 digital temperature sensors were employed but these have a limited temperature range of -55 to 125°C. The 18B20 sensor communicated directly to a single board microprocessor system via a digital I/O port and this system relayed signals with a built in CAN node. These sensors were destroyed once the cell vented and data afterwards could not be recorded. The second type of temperature sensor used was a J type thermocouple connected to a CAN based scanner from Axiomatic. J type thermocouples were used for the majority of the testing, except for the instrumented nail test for which K type thermocouples were needed to measure higher temperature values.

Calibration	Tem Range	Std. Limits of Error	Spec. Limits of Error
J	0°C to 750°C (32° F to 1338°F)	Greater of 2.2°C or 0.75%	Greater of 1.1°C or 0.4%
K	-200°C to 1250°C (-328° F to 2282°F)	Greater of 2.2°C or 0.75%	Greater of 1.1°C or 0.4%
E	-200°C to 900°C (-328° F to 1652°F)	Greater of 1.7°C or 0.5%	Greater of 1.0°C or 0.4%
T	-250°C to 350°C (-328° F to 662°F)	Greater of 1.0°C or 0.75%	Greater of 0.5°C or 0.4%

Figure 33. **Thermocouple Ranges**

Figure 33 summarizes the temperature ranges for various thermocouples.

Cell voltage measurements were obtained in three different ways:

- 1) Single cell level: single board computer A/D with CAN conversion and node
- 2) Pack level: I+ME battery management system with CAN node
- 3) Pack level: single board computer A/D with CAN conversion and node

### 1st Setup

Measured cell voltage analog signal at terminals with single board A/D. Value was converted to CAN format and broadcast to the network using a CAN chip add on board. Calibration was checked using a factory calibrated multi-meter.

### 2nd Setup

This setup was used when the test required ten cell voltages or more in a battery pack. An I+ME BMS system employing a master/slave communication network. Each slaves reported up to ten voltages back to the master using an RS485 bus. Two slaves were used to collect 20 voltages in our final tests. Master unit sends out the reported voltage measurements over CAN for logging/monitoring by Vector CANoe setup.

### 3rd Setup

This third setup was necessary because the I+ME BMS hardware is limited to 4.5V per channel/cell and inadequate for pack overcharge tests. Therefore, the team developed their own switching and isolation circuitry to measure each module cell's voltage independently to send one cell voltage at a time to a single board computer (SBC) for A/D input.

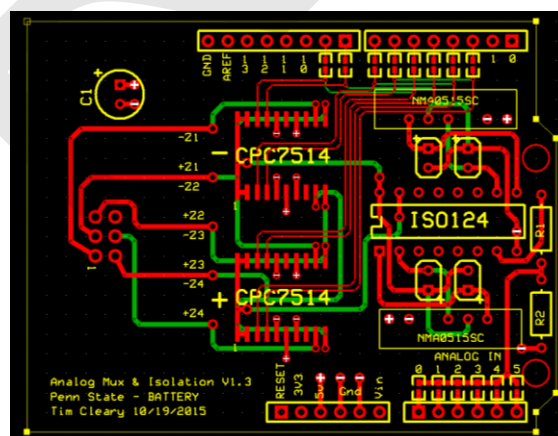


Figure 34. **Arduino Based Isolated Voltage Measurement PCB**

The custom Arduino based board, seen in Figure 34, allowed for high voltage isolation and scalable voltage dividers so that peak voltages during over charge could

be captured. The SBC with isolate voltage measurement PCB converted data to CAN messages for network broadcast and these messages were captured by CA-Noe. Calibration of this device was completed prior to each test.

A pressure sensor was used, when sealed packs were tested, to record how pressure changed inside a battery enclosure before and during an overcharge event. A voltage output single was read by SBC A/D and broadcast to via the high speed can bus, similar to all other sensors. A curve fit calibration was performed to know pressures prior to any testing.

## **SINGLE CELL TESTING DESIGN**

A set of single cell tests were planned prior to module level testing to allow for any information learned to be used in module designs. These tests were used to determine the response of the batteries in accordance with the failure mode they were submitted to and also to discover the performance of the materials tested.

These goals had to be accomplished without compromising the safety. This means the test setup had to be able to secure the cell during venting processes generating unknown forces. Strong battery tie downs were used in early testing. Throughout early testing, experience was gained which fed directly into future designs of the single cell test setup. The first design was a control. The intent was to overcharge a cell to understand the duration of the venting process and magnitude of the resulting forces to ensure all tests could be performed safely.

Two Acetal separators and a base were used to hold the cell. Then two metal straps were also installed to make sure the cell could not escape the test stand. These separators were either bolted down to the platform of an air press or directly to studs in a concrete base.

The majority of the single cell tests were performed on an air press which gave the researchers the ability to push a nail through the cell and release the cell energy in the cases where the initial test failed. This made approaching the cell after a test much safer as one could be confident there is no residual energy remaining. Also, the researchers could visually see the energy escape via a severe venting event.

Figure 35 shows a solid model of the early concepts for a single cell test stand.

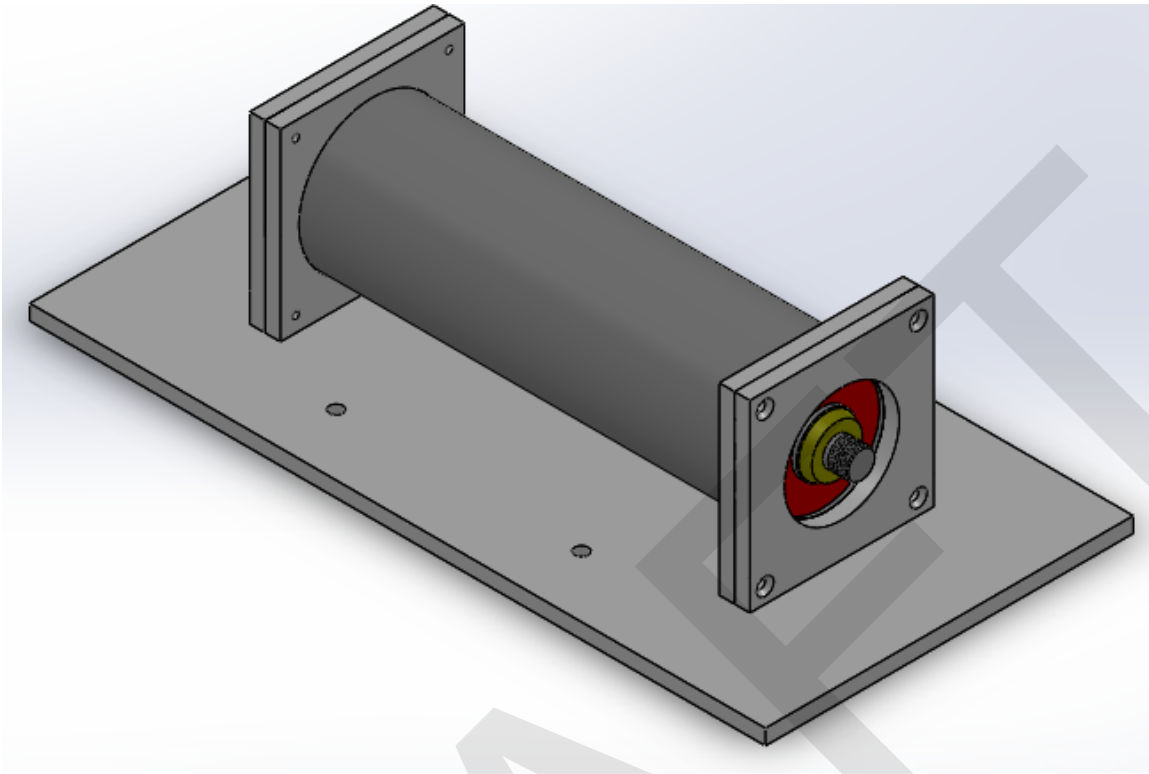


**Figure 35. Initial Single Cell Test Stand Design**

The results of initial testing showed that the Acetal parts used to hold the cell were strong enough but shortly after an event they melted and burned until there was little material remaining.

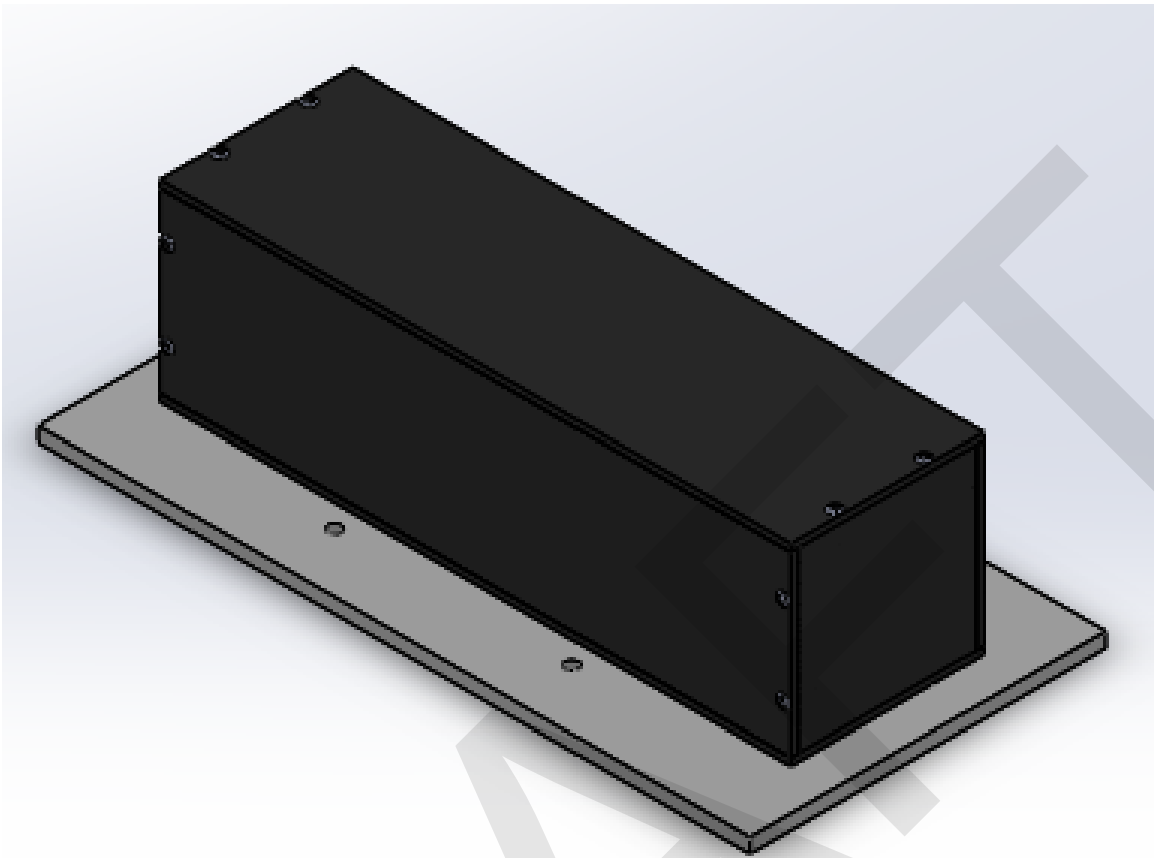


Figure 36. **Cell Enclosure**

Following the initial testing, a cover was designed to enclose a cell and allow for thermal propagation testing. Figure 36 shows the cell enclosure. This enclosure was slightly larger than the cell and was secured to the testing platform using the same methodology as the previous test stand. Figure 37 shows a top down view of the inside of this cell enclosure. Note, the minimal clearances to minimize any gas pressure relief.

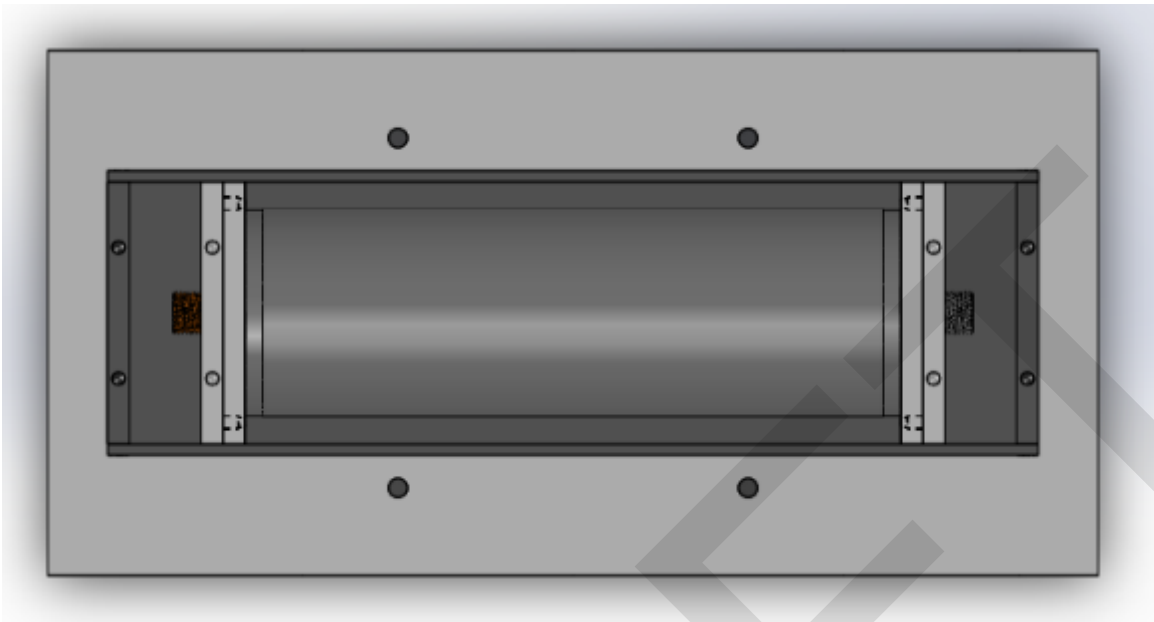


Figure 37. **Top Down View of Cell Enclosure**

### **Holding Cells Down**

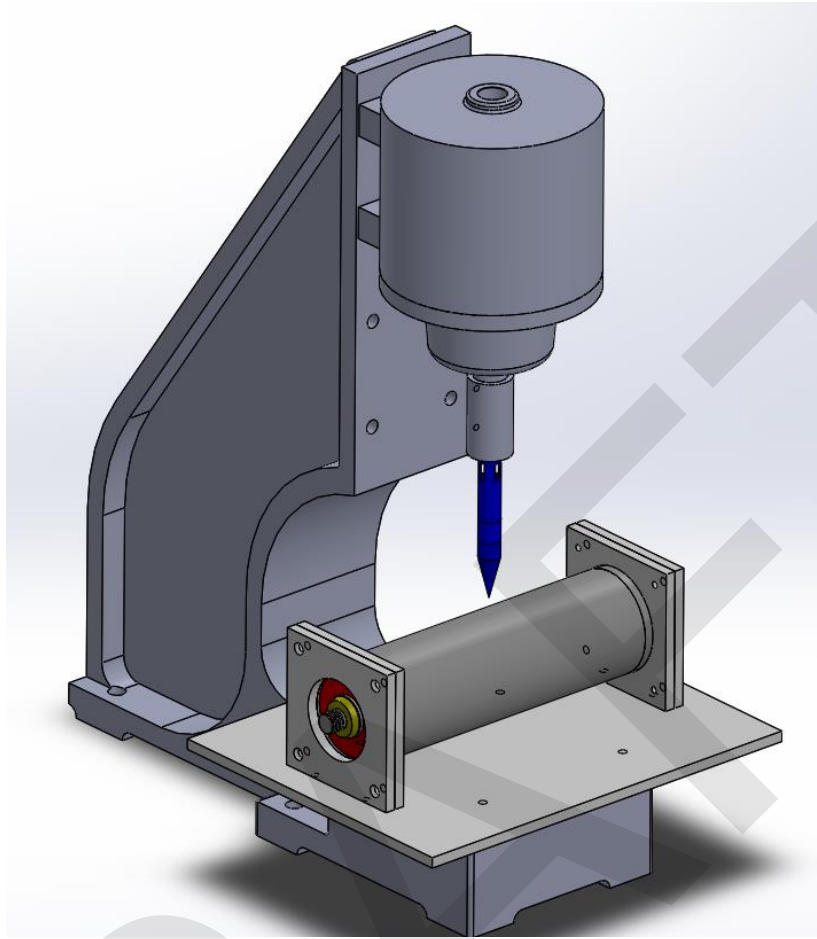
To be sure that a cell would not escape during a venting or nail puncture test, metal bands, seen in Figure 38, were used to secure the cell.



Figure 38. **Metal Straps**

### **AIR PRESS**

A Mead AP-122 air press was purchased to be able to perform nail punctures and end all other cell tests safely. On the base of the air press was threaded to secure the plastic base of the single cell platform.



**Figure 39. Nail Puncture Air Press**

Figure 39 shows the air press system CAD model including a cell and nail. The air press was bolted to a concrete pad and was operated through a system of valves with air pressure supplied by a typical tool compressor.

## IV. SINGLE CELL TESTING

Before larger, module level tested were performed, simpler single cell testing was needed to provide baseline data such as temperatures and material responses. This section details the testing procedures and results of all single cell tests performed on the GAIA 45Ah NCA cell. Prior to all tests, cell capacity was verified to be within 80% of its original manufacture specification as all the used cells in these experiments were donated with unknown State of Health (SOH).

### ACETAL – OVERCHARGE

In this first test, a 20 Ampere load was applied in an overcharge scenario to replicate a hypothetical undetected voltage measurement error during a constant current charge mode. If a battery management system, specifically its analog to digital converter measuring cell voltage, is not accurate, a dangerous charge load may remain active. More intelligent charging systems may measure energy to protect against this but balancing the accuracy of an energy measurement, possible human error in the programming and setup of this feature, hardware failure and ensuring a battery is fully charged is a difficult task. Despite the attention given to this topic, overcharging of cells continues to occur.

Prior to testing, a single cell was fully charged to 100% SOC and/or an open circuit voltage 4.2 V as specified by the manufacture. Upon initial electrical loading the cell entered an overcharged state because the cell was already fully charged. The cell was allowed to continue charging at a constant current of 20 Amperes until cell pressure discs burst. Immediately following the pressure release, charge current reduced to nothing due to the cell becoming an open circuit, likely because of internal damage to electrodes. All the data and setup of this test are presented in this section.

The single cell Acetal test stand was bolted to a large concrete pad with metal straps as previously described. Figure 40 shows the concrete pad and single cell test stand, with charge cables, prior to the start of the first overcharge event.



Figure 40. **Single Cell Overcharge Test**

Data was collected during testing, including seven temperature sensors attached to various areas on the surface of the cell, voltage measured between positive and negative terminals the cell, and current. All this information was gathered by sensors and broadcasted via the Controller Area Network (CAN) while simultaneously being logged by a CAN bus data logger, as discussed in the data acquisition section of this report. Besides recording CAN data, video of the test was also recorded by two stationary high resolution cameras.

Maxwell DS1820 single wire digital temperature sensors were used to capture temperature data during this test. It was not until after this test that it was discovered that these sensors would be insufficient due to their range from  $-55^{\circ}\text{C}$  to  $125^{\circ}\text{C}$ . As a consequence, the sensors were damaged and peak temperatures achieved during venting were not captured. However, the temperatures leading up to this venting event were recorded as they were within range of the sensors.

Figure 41 shows the data recorded via the CAN bus. Cell voltage, all temperatures and cell current up until the venting event were logged.

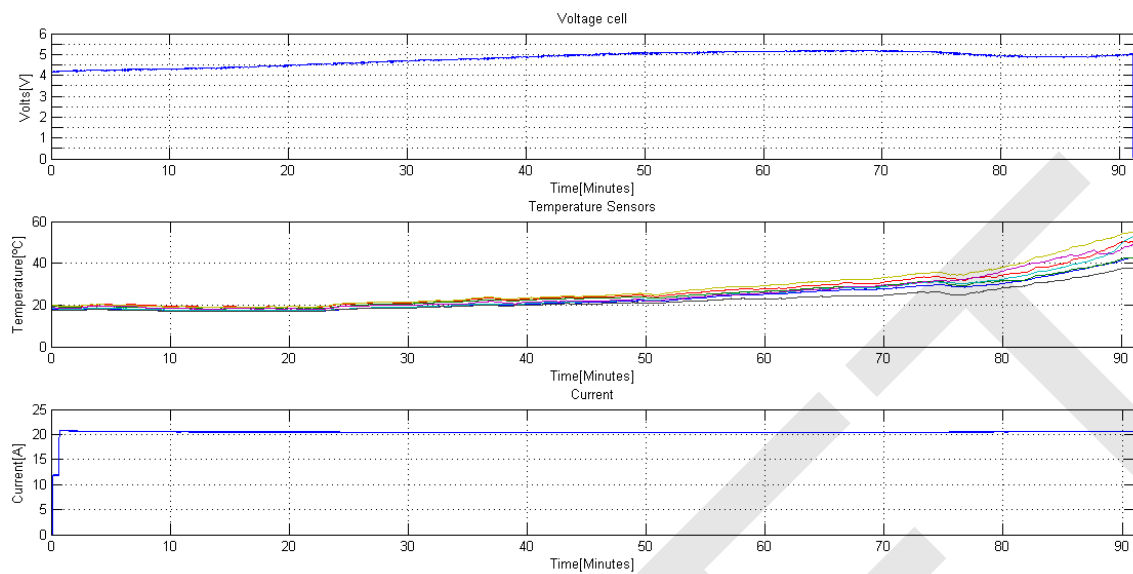


Figure 41. **Data from Initial Overcharge Test**

Note the dip in voltage (top chart) just prior to the venting event. This is a pattern that was repeatedly observed through all tests and the research team is confident indicates the onset of thermal runaway due to the correlation between dip in voltage, and the sharp increase in temperature rate. As the voltage dips and temperatures rates increase, the cell experiences an increase in internal pressure right up until the cells burst discs' brake open and the cell vents. At this point the cell becomes an open circuit and current stops flowing due to internal damage the electrodes are no longer connected. Note that the temperatures seen on the external surfaces of the cell (middle chart) never exceeds 60°C before venting. These particular cells are rated to operate up to 60°C, so a battery management system that uses temperature data would not have triggered a fault condition since the battery is operating within specifications. Note, a potential solution to this problem would be modeling internal cell temperature based on surface and ambient temperature readings as well as current through put over a recent time period.

The battery venting lasted roughly five seconds as indicated by flames and huge clouds of smoke. The magnitude of the event is displayed on Figure 42.



Figure 42. **Venting Cell – First Test**

The single cell was held down to the concrete test pad through an Acetal cell holder and plate. The flames and the high temperature associated with the venting ignited the Acetal plastic which acted as a combustible and burned out until it was completely gone as seen in Figure 43.



Figure 43. Cell, Hours After Venting Event

The cell is also visibly swollen after this test. It's clear to the researchers that if not for its large stainless steel cell casing, the cells casing itself would also likely be completely destroyed. Note, the cells threaded terminals and terminal nuts are intact following this test. The cell burst discs broke as the design intended with the casing ends bulged outward slightly.

### **ACETAL - NAIL PUNCTURE**

Based on the previous test of an overcharge, it was important to then transition to initiating an internal short circuit on the cell to simulate a crash event with battery system penetration.

This early test also served a dual role in testing battery enclosure materials by testing their thermal capabilities and the appropriate thickness of material needed to withstand a direct venting event. As a starting point, sheets of 1/8in thick aluminum alloy, 6061, and a general low carbon steel material were used.

This test also marked the initial use of the air press system designed to press a nail through a cell. For this particular test, only temperature was recorded and J type thermocouples were used. These sensors were located in various areas thorough the surface of the cell including, top of cell by the positive terminal, positive

terminal, negative terminal, top of cell in the center, top of cell by the negative terminal as well as in the surrounding air (ambient), on the aluminum sheet by negative terminal, steel sheet by positive terminal, and aluminum base.

Figure 44 shows cell temperature measurements in two charts. The top is scaled to the highest temperatures while the bottom is scaled to the lower values. The highest values were measured on the top of the cell by the positive and negative terminals peaking at about 273 °C and 175 °C respectively. The bottom chart shows little rise in temperature. Note, this test was performed in -3 °C ambient conditions.

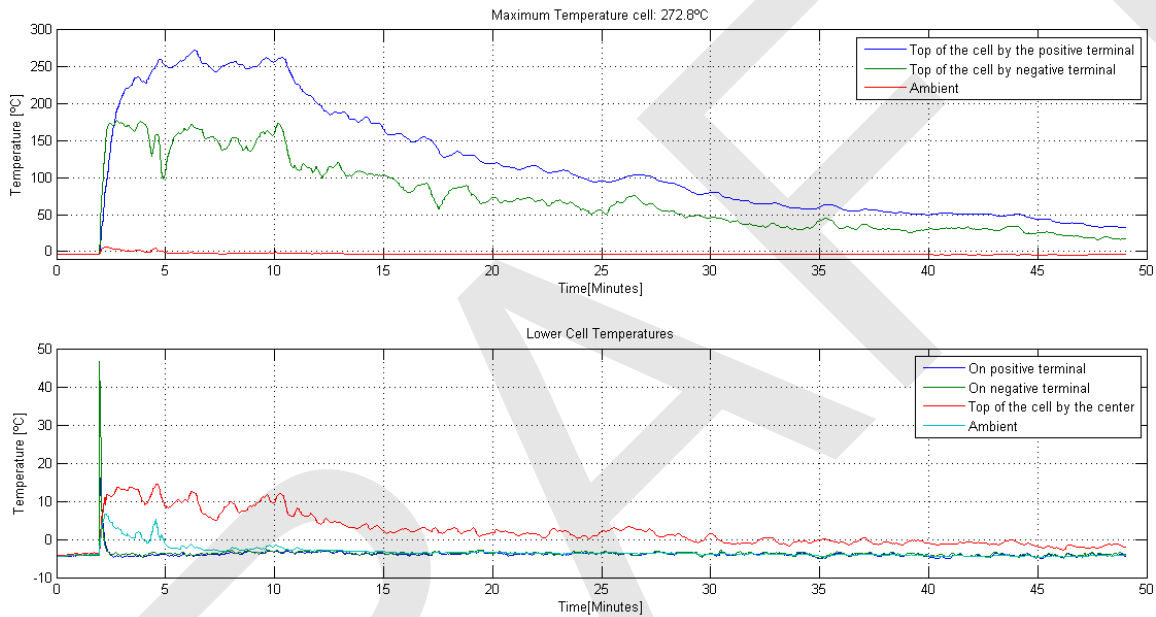


Figure 44. Acetal Nail Puncture – Cell Temperatures

Figure 45 shows the temperature data gathered from surfaces of the aluminum and steel sheets. These sensors are on the opposite side of that which took the direct blast from the cell, through the vent discs. The maximum material temperature was measured to be 32.7°C. Note, these sensors were not directly opposing the point of impact but a few inches away.

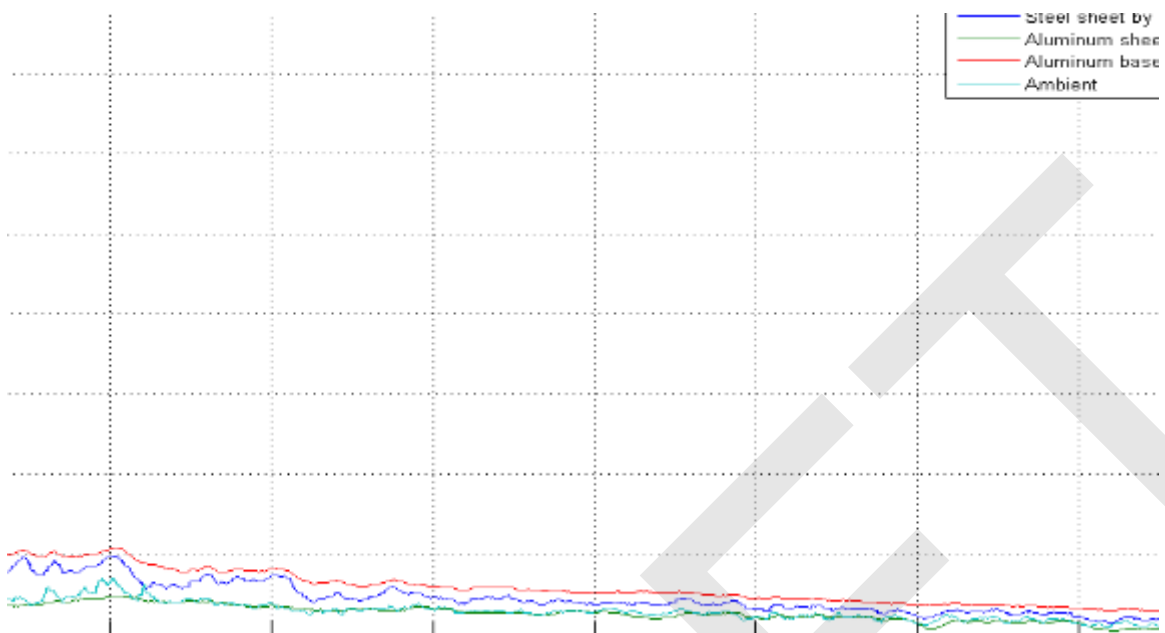


Figure 45. **Acetal Nail Puncture – Material Temperatures**

Material temperatures did not exceed their respective melting points. Note, the scaling is the same as in Figure 44. Material temperatures did not exceed 12C.

### **ACETAL - OVERCHARGE AND MATERIAL TEST**

The nail puncture testing causing a dramatic internal short circuit did not provide the heat necessary to melt nearby metals. Therefore, the objective of this test was to determine if an overcharge would melt the aluminum or steel used to deflect and or redirect the venting, burring electrolyte. An overcharge event is likely to release much more energy than a nail puncture at 100% SOC. As in the previous test, aluminum and steel were placed on either side of the cells, normal to the pressure release discs, in direct line with the venting gasses. These sheets of material were placed at 1.5in from the cell terminal. Approximately where they would be in a pack design for a large bus application to direct venting electrolyte away from other cells.

Figure 46 shows the setup of the cell and blast shield material. Two Acetal separators which were bolted down on an aluminum base held the cell. The aluminum base was mounted on the air press and the blast shield sheets were attached to the base through L type brackets.



Figure 46. **Acetal Overcharge with Blast Shield Material Test Setup**

Temperature sensor location was identical to previous tests and again, just temperature data was logged during this test. These temperature readings are presented through the next few charts. Figure 47 shows two charts with the same data but at different time scales. The top chart shows the entire test from start, through the venting event, and until the end of the cells cool down. The bottom chart highlights the temperature profile immediately following the event.

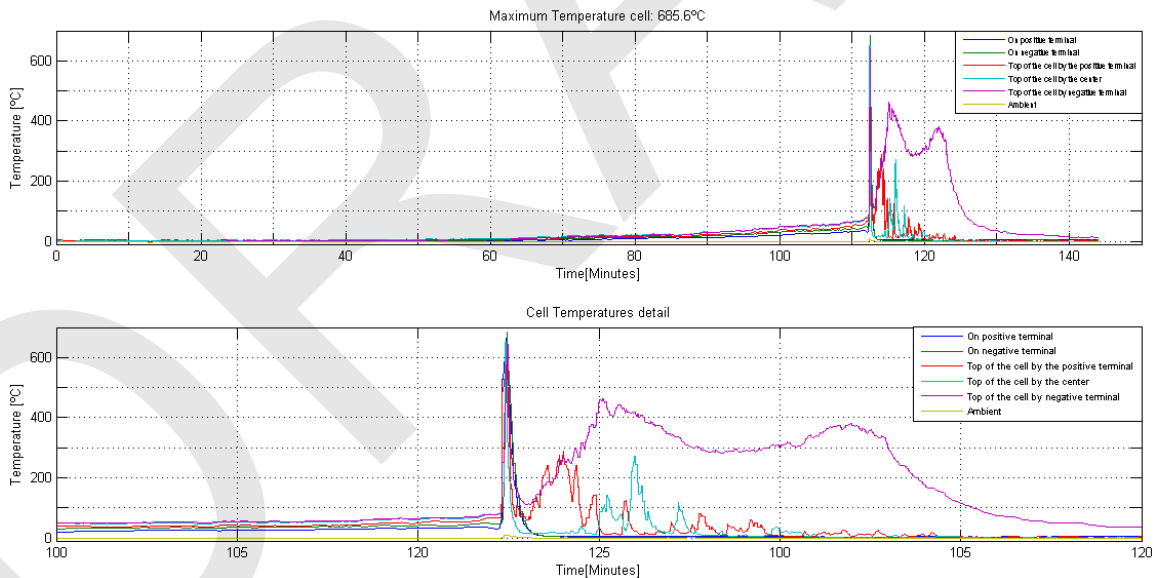


Figure 47. **Acetal Overcharge w/ Material – Cell Temperatures**

Note the spikes in temperature, some sensors reach in excess of 600 °C then are followed immediately by an aggressive cooldown. The second climb in temperature and sustained 300 °C readings are from the combustion of the cell holders made of Acetal material. If Acetal did not burn, then the time during this event in

which the temperatures exceed common vehicle material combustion temperatures would be greatly reduced. In turn reducing the chance of a vehicle fire, or at least limiting the damage and increasing time to evacuate and for emergency responders to cool the pack with water.

The response of the metal is summarized in Figure 48. This first noteworthy point is that the metal exceeds temperature measurements from the cell itself. This is likely a result of the metal blast shields being in direct contact with the venting gasses while the cell surface temperature sensors are likely limited by the insulation properties of the cell casing. These material temperatures are assumed to be much closer to internal cell temperatures than the surface measurements captured from the cells exterior. The aluminum sheet experiences a temperature 100 °C warmer than the steel sheet. One of the causes of this response could be that the cell did not vent uniformly. Also, the thermal distribution properties of each material are substantially different. If the sensors were directly on the opposite side of the impact area more accurate readings would be possible. In reality, the sensors were at different distances from impact point of the gasses which also contributed to this difference.

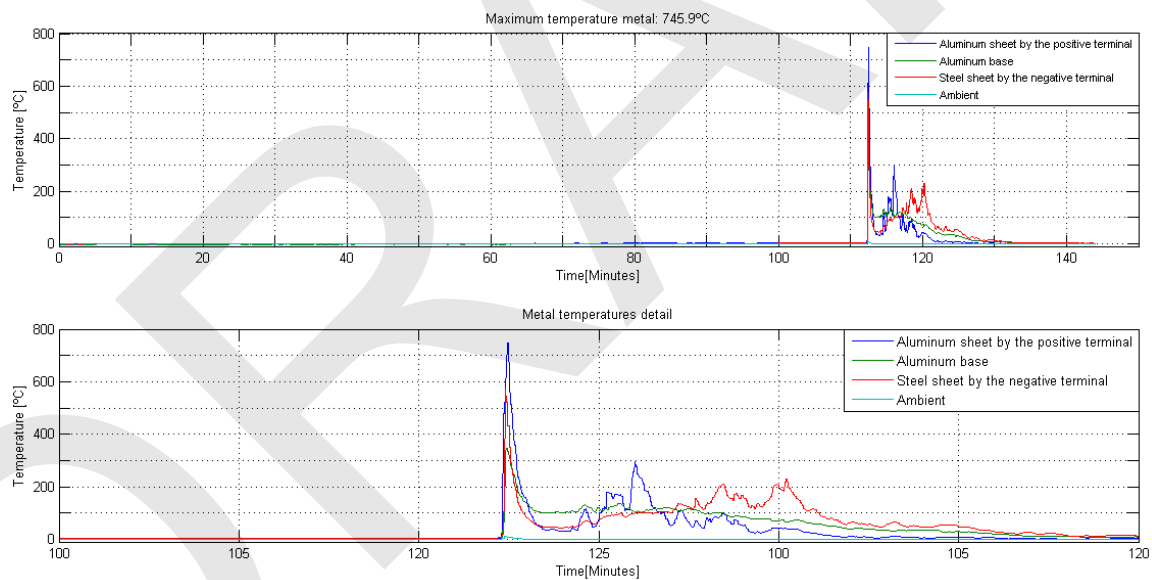


Figure 48. Acetal Overcharge w/ Material – Material Temperatures

According to the measured temperatures and melting point of the aluminum and steel it is not surprising that a 2-inch diameter hole was burned through the aluminum while the steel remained intact.

The venting process for this test was very intense as Figure 49 demonstrates. Although the testing was completed in non-ideal environmental conditions, (very cold, windy weather) it did unexpectedly provide a valuable measurement. The black

smoke escaping the cell stained the snow providing a radius for which to measure the effective distance debris can be expected to travel. Upon visual inspection, the smoke and flames traveled approximately 125 in from each side of the cell or in a radius of the same dimension.



Figure 49. **Acetal – Overcharge with Material Test**

This test resulted in valuable information useful in understanding the magnitude of temperature and burning electrolyte only one 45Ah NCA cell is capable of releasing. This brings up concerns of safety and security when using this type of energy storage system as well as reason to have redundant sensors to ensure accurate measurements during charging.

### **PYROPHOBIC - OVERCHARGE**

Part of this research was to investigate fire suppression systems and fire prevention techniques using new materials and design. Pyrophobic Systems produces proprietary compounds that claim to both absorb, and suppress fires from spreading to adjacent areas. This research team formed a partnership with Pyrophobic by receiving donations of their materials in the form of machined components ready for testing in our single cell scenarios. To thoroughly test this material an overcharge test was commissioned. It is well known from previous tests that the most stressful scenario will occur from an overcharge venting event. For this test the cell was surrounded by a wall of Pyrophobic material with cell separators holding the cell at each terminal. Again the assembly was bolted down to an aluminum base that was also secured down to the air press just in case the cell failed to vent and a nail had to be put through to induce the discharge.



Figure 50. **Pyrophobic – Overcharge Setup**

Temperatures of the walls and cell surface were recorded as well as cell voltage and current. Unfortunately, a sensor placed on the cell and another one on the walls were lost due to the intensity of the event so their data is not available. Other than these two sensors all others were valid throughout the test. The data gathered from these sensors can be seen in Figure 51.

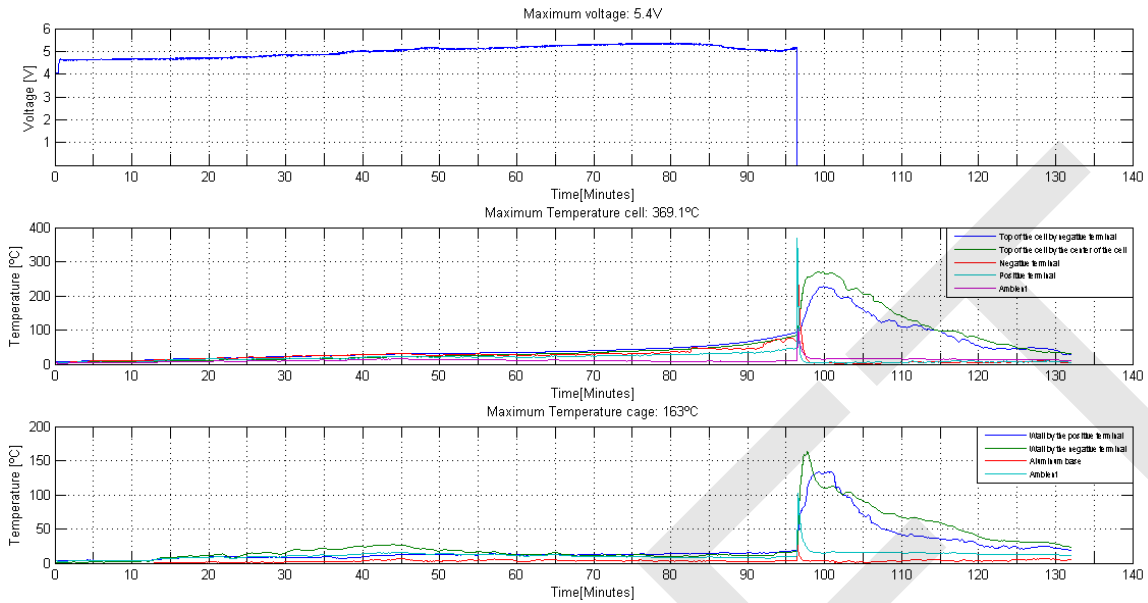


**Figure 51. Pyrophobic – Overcharge Data**

Analyzing the voltage (top chart), notice that the cell was charged before starting the test and at an open circuit voltage of 4.2. Although current is not shown in the data charts, the cell was charged at the typical 20 A constant current which brought the cell up to approximately 5.4V just prior to the typical voltage dip. This dip is followed by the increase in temperature rise then concludes in a powerful overcharge venting event.

It is notable that the venting event resulted in a peak cell surface temperature of approximately 400°C which is considerably lower compared to the earlier tests.



Figure 52. **Pyrophobic – Overcharge Results**

This test resulted in confirming this material as a viable candidate for use with NCA cells, see Figure 52. It is able to maintain structural integrity and not melt or burn during or following an extreme cell venting event.

### **PYROPHOBIC - NAIL PUNCTURE**

The test detailed in this section is the evaluation of the Pyrophobic phase change material under a nail puncture scenario. Temperature sensors were placed on the cell surface as in previous tests as well as all six parts of the cell and wall separators used in this design. To capture the thermal distribution during an event, but to also document how well this material held up to this extreme temperature and force, the temperature sensors were distributed along the cell and the surrounding walls, all made of the same Pyrophobic material. Figure 53 shows the voltage and temperature data recorded during this test.

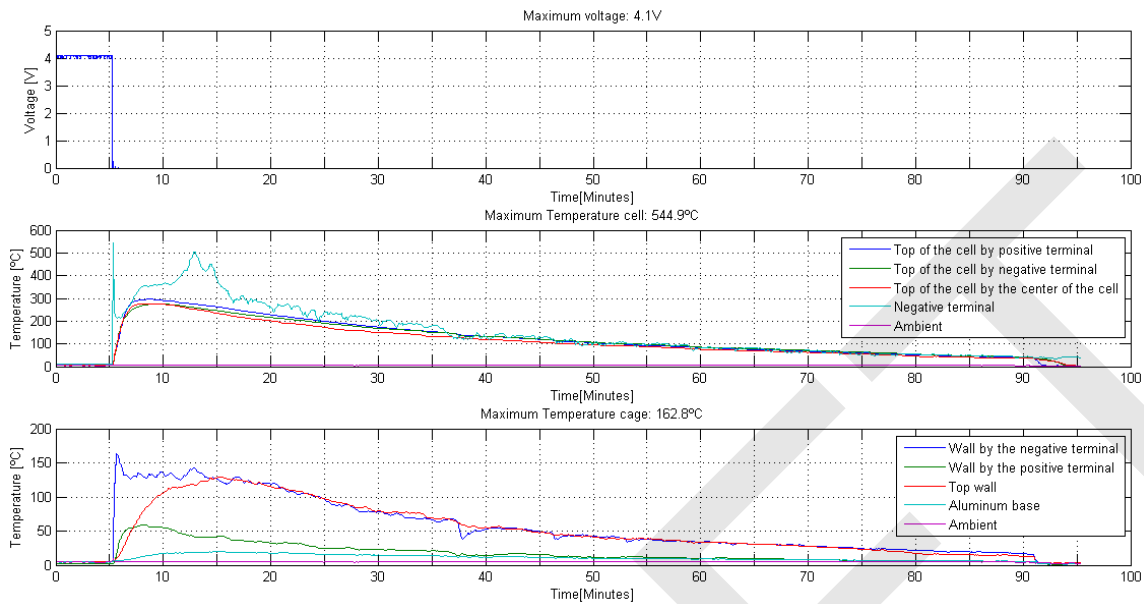


Figure 53. **Pyrophobic – Nail Puncture Data**

The top chart shows cell voltage readings, the middle chart cell surface temperature readings and the bottom chart Pyrophobic material temperature readings. The cell had a steady open circuit, unloaded, voltage of 4.1 VDC up until the nail went through to force the cell in to an extreme short circuit condition. This, as typically seen in these tests, lead to an internal open circuit dropping the measured voltage to 0 VDC. Temperature readings from this test are comparable to the previous Acetal tests but without the second jump in temperature due to burning materials. Cell surface temperatures rose quickly to approximately 300 °C the slowly cooled back to ambient over a 1.5-hour period.

The negative terminal wall heated up as soon as the nail went through the cell. This sensor achieved a peak temperature of 162.8 °C, which is significantly lower than the heat released by the cell. This fact highlights the excellent capabilities of the material to dissipate heat. A sensor on the top of the wall took a bit longer to heat up although it quickly achieved the same temperature as the wall by the negative terminal.

Another notable result was the measurable difference between positive and negative terminals. It seems that the majority of the heat, during this test, came from the negative terminal of the cell so, no surprise that this side of the material showed more damage.

Figure 54 shows both the positive (left) and negative (right) terminal walls/covers. This material, just as with the aluminum and steel blast shields, was in the direct path of the venting, burning, electrolyte released during a nail puncture. As presented above the positive terminal experienced a lower temperature rise compared

to the negative terminal. The images of these terminal covers may show why this happened. The positive terminal cover was quickly punctured by the venting gases while the negative cover seems to have contained these hot gasses and only vented on the side opening of the cell separator.

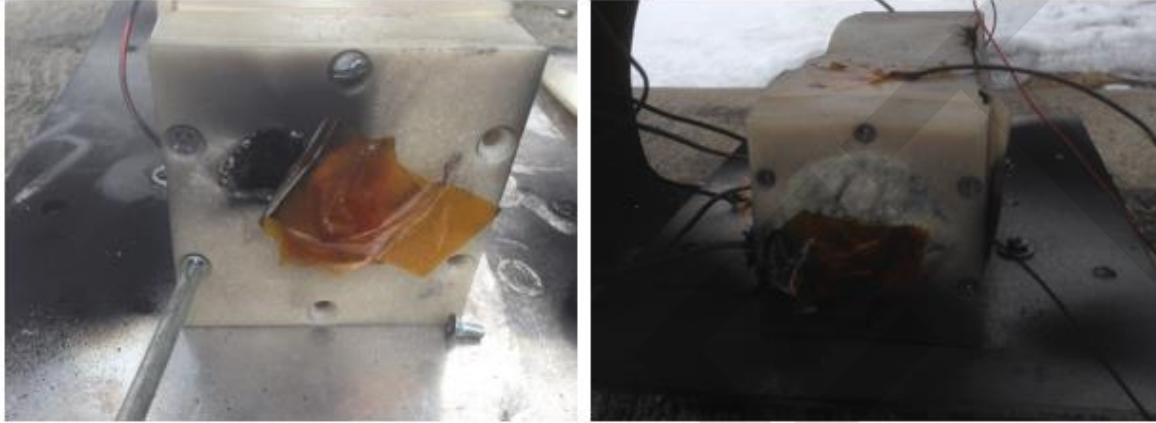


Figure 54. **Pyrophobic Material Results**

Following a long cool down period all the material including each cover and wall plate was removed and analyzed.



Figure 55. **Pyrophobic Material After Nail Puncture**

Figure 55 shows all the parts used to contain this cell nail puncture event. The material has obviously grown in thickness yet is clearly hasn't lost integrity. It would likely keep this event from impinging into another area, limiting thermal propagation and maintaining structural integrity.

## **PYROPHOBIC - OVERCHARGE WITH HOUSING**

Based on the previous test results for this material, the manufacturer recommended compliantly enclosing their product to take full advantage of the phase change functionality. In hopes of absorbing even more energy, an aluminum housing surrounded the Pyrophobic material and cell to simulate an enclosed battery system. The metal enclosure was made out of aluminum 6061 alloy and welded together to create a sealed enclosure. However, it was not completely closed since it had openings on the sides by the terminals to release the smoke and the flames, thus limiting the pressure buildup inside the enclosure to prevent an explosion.

The housing was bolted down on the same aluminum base that held all previous assemblies on the air press as seen in Figure 56.



**Figure 56. Pyrophobic – Overcharge with Enclosure Setup**

The cell was then overcharged as in previous tests and the results presented in Figure 57. This test started prior to a complete charge. Instead of fully charging, resting then resuming in an overcharge state the test started at approximately 50% SOC. This was a mistake on the part of the researchers performing the test but resulted in an overcharge venting event non-the-less. The typical voltage dip at the

start of thermal runaway was experienced but the peak voltage prior to venting was much higher than usual at 8.1VDC. It is also notable that the surface temperatures of the cells reached 100 °C right before the cell vented. This is substantially higher than typical tests. Likely because of the insulation effect the aluminum enclosure has on the cell and its surface mounted temperature sensors. Despite having higher values of voltage and temperature relative to other tests, the cell did not get extremely hot during the venting event or thereafter. All the temperatures excluding the one on the top of the cell by the center remained between 400-500°C which is a lower range than typical. The temperature measurements remained in this range for approximately ten minutes and then the cool down process started. It took around 1.5 hours to cool down to ambient temperatures, about the average.

During the cooling down process the temperatures captured by each sensor placed on the cell were similar and constituted a very homogenous profile although after the venting the material caught on fire.

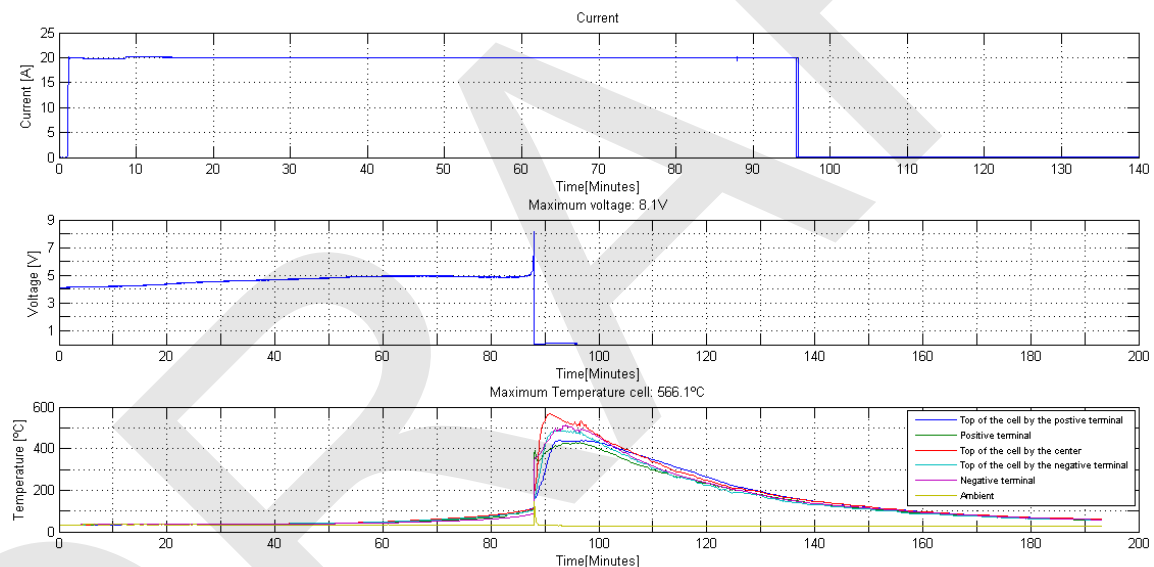


Figure 57. **Pyrophobic – Overcharge with Enclosure Data**

Figure 58 shows the machined opening, larger diameter hole, and the smaller opening cut by the venting gasses.



Figure 58. **Pyrophobic Enclosure Vent Opening**

Figure 59 shows the results of the material inside the enclosure. Clearly this material is more charred and not as strong or capable of holding a cell as the test performed without an enclosure.



Figure 59. **Pyrophobic Overcharge with Enclosure Material Results**

This test shows the aptitude of Pyrophobic material to absorb substantial amounts of energy, a desirable trait when selecting a material for battery pack designs. **However, it must be noted that the material can not be used to both absorb energy and maintain structural integrity.**

### **PET - OVERCHARGE**

The thermal response of a PET material used in a single cell test stand was also evaluated. This section details the setup and results of an overcharge event using PET to both hold and enclose a single cell. Figure 60 shows the setup for this test. As with previous tests, the cell is securely mounted to the air press and equipped with temperature, voltage and current sensors.



Figure 60. **PET – Overcharge Setup**

During this test extreme temperatures were reached, peaking at approximately 750 °C. Figure 61 shows the current, voltage and temperature data recorded during this test. Note, typical current and voltage profiles were seen. Leading up to the vent, a dip in voltages was experienced just as temperatures increased to thermal runaway values. An open circuit was realized when the cell began to vent.

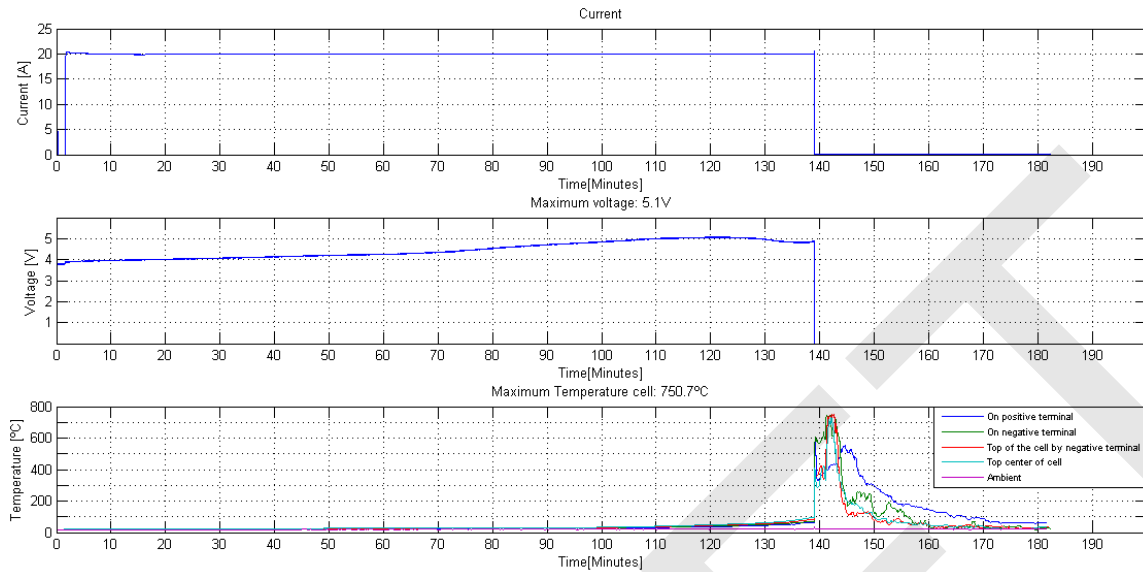


Figure 61. PET – Overcharge Data

Figure 62 shows the temperature data leading up to the venting event. Note the exponential rise in temperature starting around the 110-minute mark. Just around the same time as the typical voltage dip.

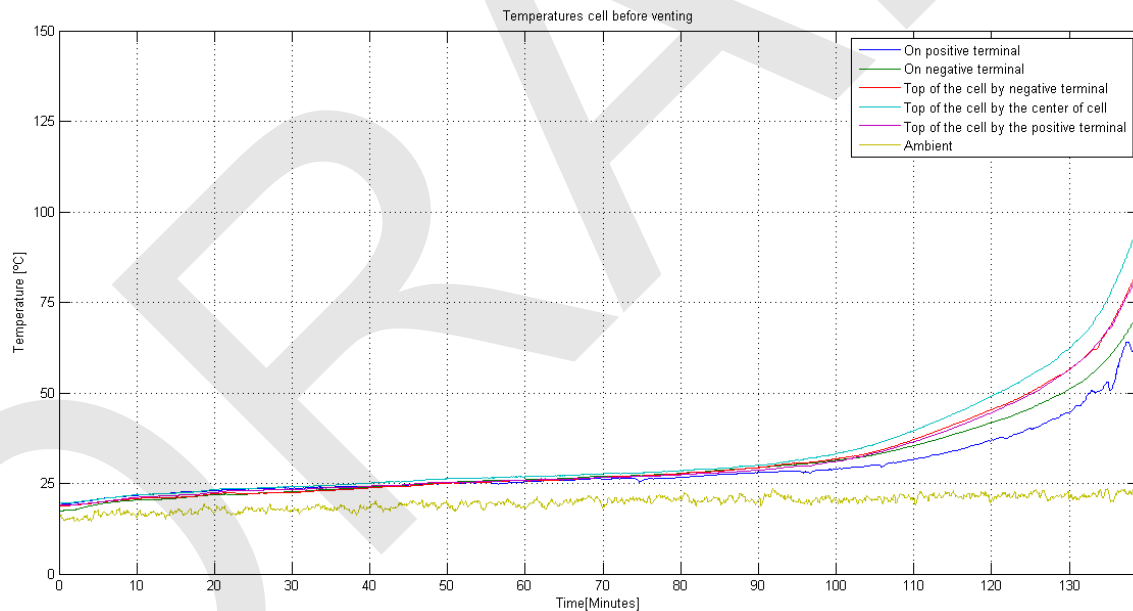


Figure 62. PET – Overcharge Temperature Data

Not all tests result in exactly the same temperature measurement distribution. Some show that the positive terminal is hotter than the negative. However, in this test since the PET material caught fire, as seen in Figure 63, most sensors detected extremely high and sustained values.



Figure 63. **PET – Material Result**

In this test, after the violent venting including flames, the material kept burning until completely gone. In fact, playing back the video recorded during the test, it took around ten minutes to burn the entire cell enclosure down to nothing. After which the enclosure cooled down very quickly because it basically disappeared after ten minutes and sensors then read ambient temperature. This fire surrounded the cell heating it and as a consequence the cell did not cool down as rapidly as the PET enclosure.

Figure 64 shows the remains after the PET enclosure melted down. The only part not damaged was the base which was made of a substantially thicker, 0.5in plate.



Figure 64. **PET – Material Result 2**

The conclusions of this test are that the PET material is neither capable of handling the temperatures, containing the event or remaining structurally intact.

### **PET - NAIL PUNCHURE**

Given the poor material results of the PET during and following its overcharge test, expectations were low for a nail puncture test using the same material.

Voltage and temperature data was gathered during this test. Figure 65 shows the logged data.

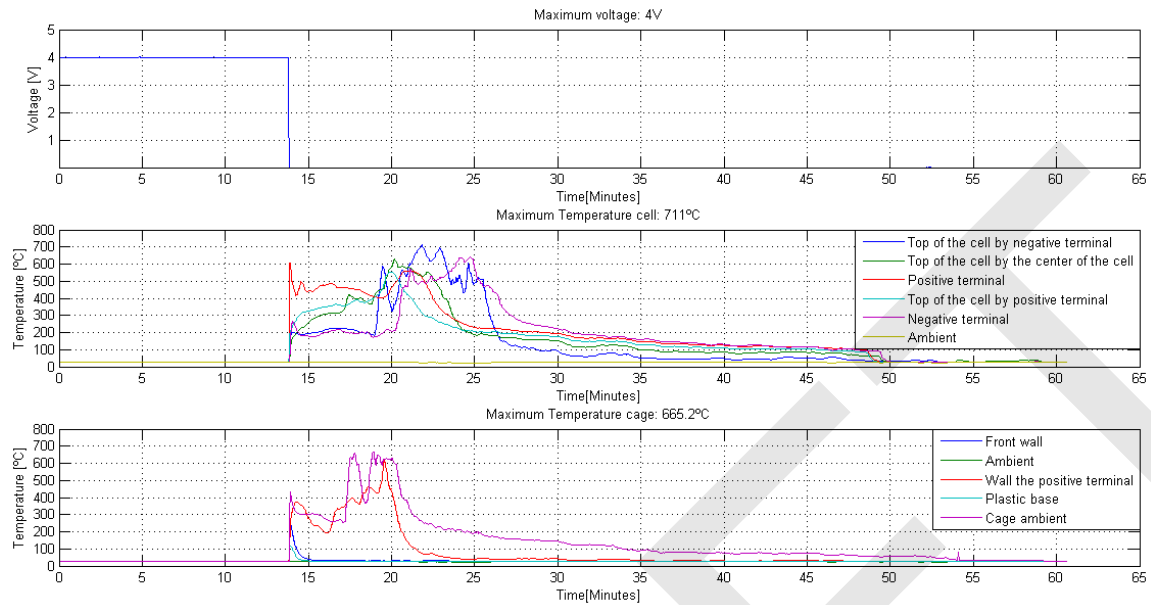


Figure 65. PET – Nail Puncture Data

The top voltage chart indicates that the cell was at an open circuit of 4VDC prior to the test. The voltage of the cell stayed stationary until it dropped due to the nail penetrated, which caused a short between the positive and the negative electrodes resulting in the typical cell temperature rise and ultimate fierce venting event.

Analyzing the response of the cell, notice that the positive terminal temperature climbed right after the nail went through the cell. It then remained fairly stationary while the other sensors responding slightly slower.

All the sensors except one on the top of the cell by the negative terminal achieved a maximum value between 500°C and 600°C and remained there for roughly five minutes until the cool down process started.

In a review of the recorded video some notable points stand out. The positive terminal was the first to reach the high temperatures recorded and was also the first side to experience a disc rupture, resulting in hot gasses venting and flame. This can be seen in Figure 66, note the right side represents the positive terminal.



Figure 66. **PET – Positive Venting First**

As with the previous PET tests the material caught fire and burned until completely gone. The fire lasted about ten minutes which according to the graph correspond to the period of time between the 15th and 25th minute when the cooling down profile started. The fire a few minutes after the nail puncture can be seen in Figure 67.



Figure 67. **PET – Nail Puncture Material Result**

The flames of the venting ignited the material by the terminals and then the fire propagated throughout the entire enclosure. Figure 68 shows that the enclosure

was nonexistent after a few minutes and only the cell case and plastic base remained.



Figure 68. **PET – Nail Puncture Results 2**

The results of this test were similar to that of the other PET/Acetal tests. The material is not capable of handling a thermal event from a large format 45Ah NCA cell.

## TEFLON - OVERCHARGE

Two Teflon overcharge tests were performed because the first was not successful. Several tests had to be repeated for various reasons but the results of this failure were rather interesting and are presented here as they provide valuable insight into the possibility of a failed burst disc.

### First Test – End Cap Failure

As with all other tests, a fully charged 45Ah cell was installed into a test stand made of the candidate material in an overcharge event. The first attempt at a Teflon test resulted in a structural failure because the entire cell end-cap burst instead of the burst disc. Shortly after the venting event started, the end-cap came off and the force of the venting gasses projected the cap about 7 meters from the test site. Cell casings are made by welding end caps to each end of a stainless steel tube. This weld failed and as a result ejected a substantial amount of electrode material. Figure 69 shows how far this material spread from the test site.



Figure 69. **Blast Radius**

The cell also ejected from the base and would have likely gone a great distance but hit a pile of snow, limiting its travel. This event gave the researchers an even greater respect for the power released during an event. It should be noted that each cell overcharge/nail puncture usually results in a violent venting event but the result of each event effects the cell casing slightly differently. In some cases, the burst disc fails and entire sections of the cell burst. A review of the test plan and setup was performed resulting in an increased distance between the test site and researchers/visitors.

## Second Test

The second attempt of this test resulted in the usual burst disc release and was a valid evaluation of the thermal behavior of the system. Figure 70 shows that the cell was over charged at constant 20 A. As a consequence, the voltage rose to 5.1 VDC just prior to the onset of the typical dip in voltage and increase in temperature rise rate.

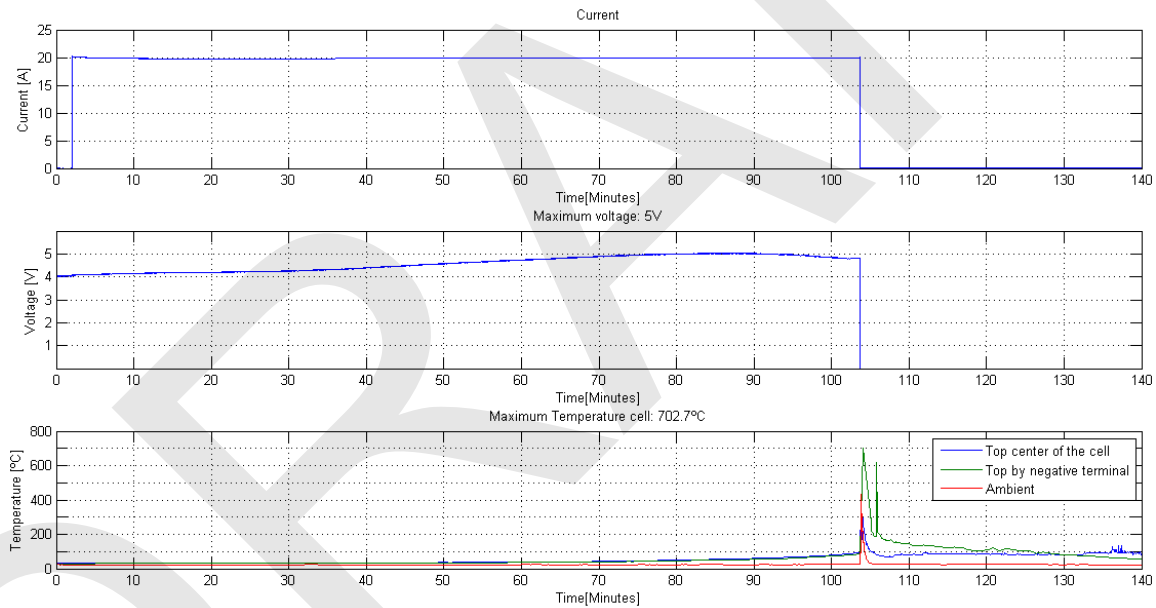


Figure 70. Teflon - Overcharge Data

In this case, venting occurred when the cell surface reached 100 °C. A peak temperature of approximately 700 °C was measured shortly after the event started. It is notable that during this test peak temperature cooled rather quickly. Also, because the Teflon material didn't burn, there was little sustained temperature readings following the test, unlike all other results.



Figure 71. Teflon Overcharge Material Results

Figure 71 shows the fire resulting from the overcharge event. Note, this fire only lasted about **43 seconds**. Figure 72 shows the temperatures measured by sensors mounted to the walls of the cell enclosure made of Teflon. Note, these temperatures were only above ambient for approximately 2 minutes. This was in contrast to all other tests where high temperatures are typically sustained for at least 10 minutes. Only one signal reported a temperature above 100 °C and is likely due to hot gasses venting from the cell.

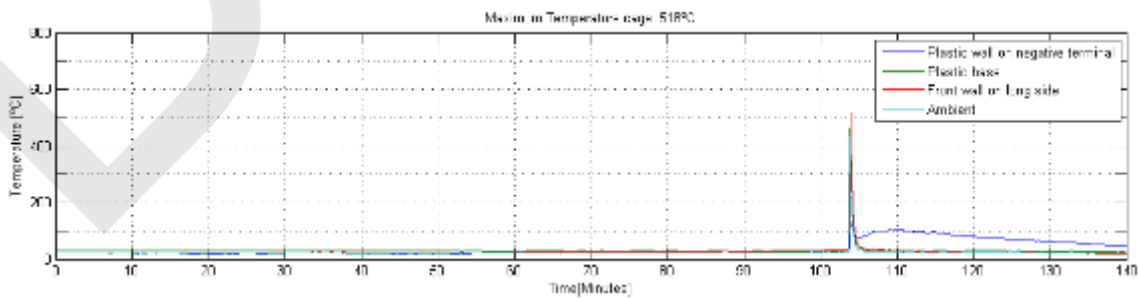


Figure 72. Teflon Overcharge Material Data

Figure 73 shows the results of the Teflon material after the cell and material cooled down to ambient.

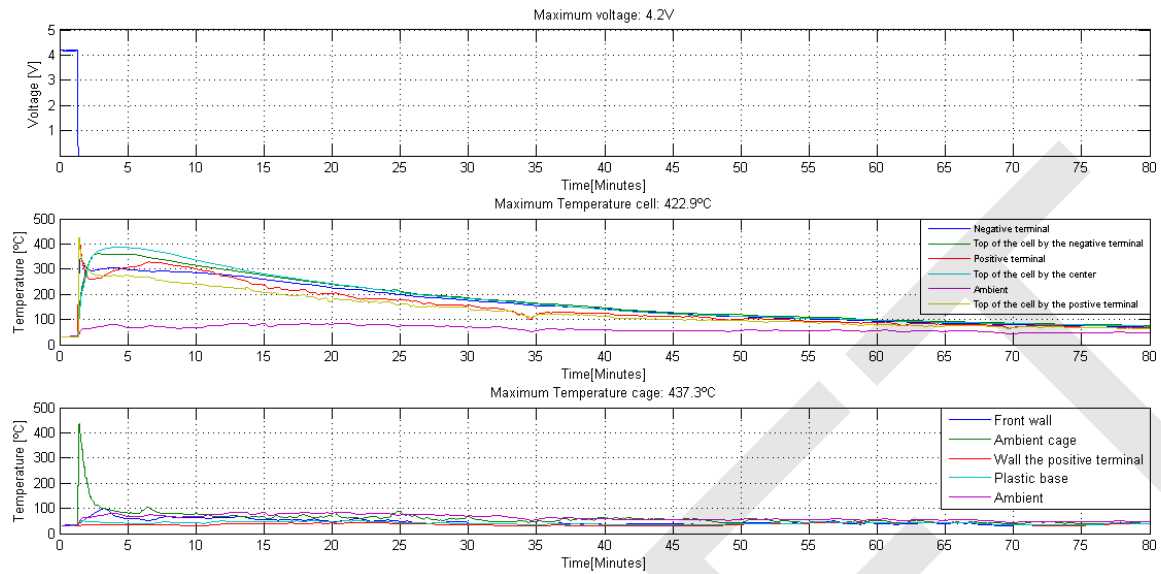


Figure 73. **Teflon Overcharge Material Results 2**

The results of this test show that Teflon is a viable material for use as a cell separator and even thermal barrier as it did not burn during this overcharge event. This single cell test required little material to secure the cell during testing but it is recommended by the researchers that a substantially thicker stock is used to ensure the cell remains secure after the event. Thickness should also be carefully considered for structural integrity in normal operation and high impact scenarios.

### **TEFLON - NAIL PUNCTURE**

As with all other nail puncture tests, a cell was fully charged and placed in a test stand made of the material under test. This cell then experienced a nail puncture and resulted in an internal short leading very quickly to a venting event. Figure 74 show the data recorded during this test.



**Figure 74. Teflon – Nail Puncture Data**

The top chart shows that the cell was fully charged and resting at an open circuit voltage of 4.2 VDC. This voltage dropped to zero once the nail punctured the cell casing, internally shorting the cell. The middle chart shows cell surface temperatures with peaks of approximately 420 °C and a cool down time of almost one hour. On the bottom chart material wall temperatures can be seen. This chart shows that besides a spike in the air temperature inside the cell enclosure, all measurements remain below 100 °C and mimic the cooling time of the cell.

Figure 75 shows the result of this nail puncture test. Note, the material is intact and shows little signs of damage, only a black coating of burned electrolyte.



Figure 75. Teflon – Nail Puncture Material Results

### **SINGLE CELL CONCLUSIONS**

The researchers conclude that the best packaging material will depend on your design scenarios and recommend Teflon for general applications. It's worth considering the Pyrophobic material for designs that require the absorption of energy and possibly using Teflon as a structural and barrier material and Pyrophobic to fill the gaps and absorb energy if necessary. In this case definitely consider your thermal management as there may be unintended reactions with the phase change material.

### **NAIL TIP TEMPERATURE MEASUREMENT**

To further understand the temperatures experienced inside a large format NCA cell during a nail puncture a special nail was fabricated. This nail was much larger

in diameter compared to the thin nail used on all other tests. This increase in diameter allowed space for a thermal pile. Many temperature sensors were packed into the tip of this large nail and a nail penetration test was performed to capture an internal cell temperature reading during such an event.

To this point, the only temperatures captured from the cell were actually from the casing which differed from internal temperatures due to the exothermic reactions.

Voltage and case temperature of the cell were also recorded in addition to six temperature sensors in the nail with one of them located at the very tip.



**Figure 76. Nail Tip Temperature Measurement Test Setup**

Figure 76 shows the test setup. Notice that the nail and the cell were lined up symmetrically to get the best approximation of electrolyte temperature.

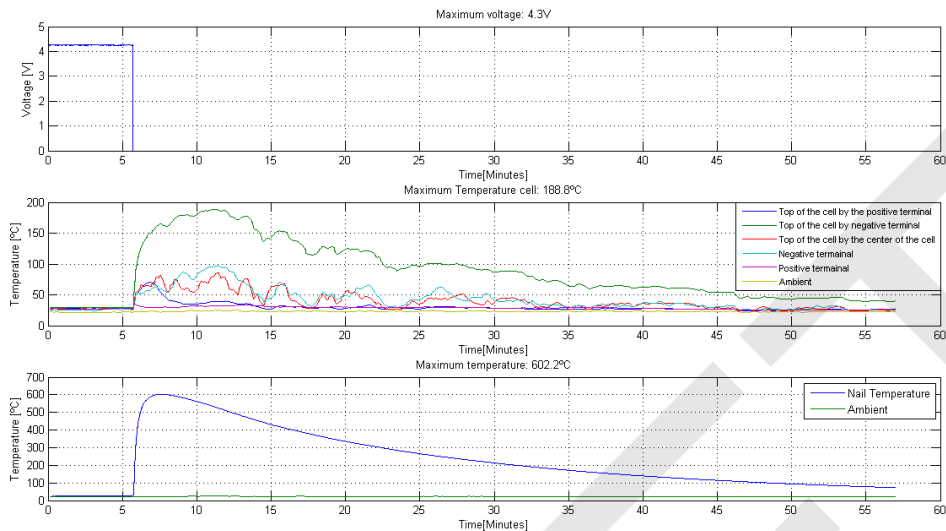


**Figure 77. Nail Tip Temperature Measurement Test Data**

Figure 77 presents data gathered during this test. As it has been mentioned before, six temperature sensors were in the nail and it turns out that all of them captured the same value so to simplify the graph cleaner just one signal is showed.

The top chart shows voltage recorded during this test. It also indicates when the event started, by displaying a sharp decrease in voltage. The second chart, shows cell casing temperature and note, the readings are relatively low compared to other similar tests. The highest temperature reached roughly 200°C meanwhile the others did not exceed 100°C. One reason may be that the cell had reached very low ambient temperatures beforehand.

The bottom graph showing nail tip temperature demonstrates that the temperature inside of the cell was very high in comparison to values captured on the housing, meaning that the majority of heat is released by the evacuation of electrolyte and other solid material through the hole made by the nail.

This larger diameter instrumented nail caused a more dramatic event relative to the smaller nails used in previous testing. This indicated that the severity of the puncture and short will vary the severity of the venting event. Note, in this test the steel end-cap of the positive terminal brock off and was projected several feet as seen in the Figure 78. The left image shows the internal construction of the cell. Visible are the long strips of foil rolled into a cylindrical jelly-roll shape that compose the different layers of the cell. The same picture also shows how the nail tip broke off in the cell as the air press lifted up. The image on the right demonstrates how savage the event was because the smoke and flames marked the ground.



Figure 78. **Cell and Surroundings After Test**

This concludes single cell testing.

DRAFT

## V. MODULE LEVEL TESTING DESIGN

This section details the design of the 20 cell modules and enclosures used in the test to failure scenarios. These high voltage packs were designed with ten/twenty batteries connected in series to produce a 36/72V nominal pack, 42/84V fully charged. In the design of a module, the component that holds each end of the cell, called the header, was the most critical component in the battery pack because of its structural and isolation requirements. In addition, the headers had to allow series connections between battery terminals. These components are necessary and must meet the high temperature demand set by the exhausting gasses if the pack is to remain intact or avoid complete vehicle fire.

SOLIDWORKS, a 3D CAD software package, was used to make mechanical designs and test feasibility. Later FEA and CFD analysis were performed on these systems.

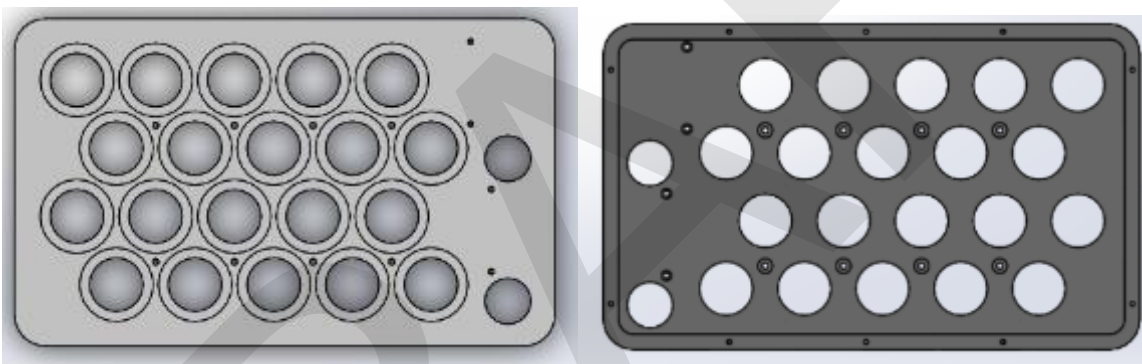


Figure 79. **Headers Designed for Module Testing**

Figure 79 shows a top and bottom view of the headers. Note, on the side of the header two, 1 in. holes were drilled through the header to pass main positive and main negative cables and to allow for small gauge cell voltage measurements wires. Finally, to secure down the cover a set of #6-32 threads were made on the outside lip of the header.

Figure 80 shows the assembled covers, headers and batteries. Two configurations of this module were built, one with and one without cell separators.

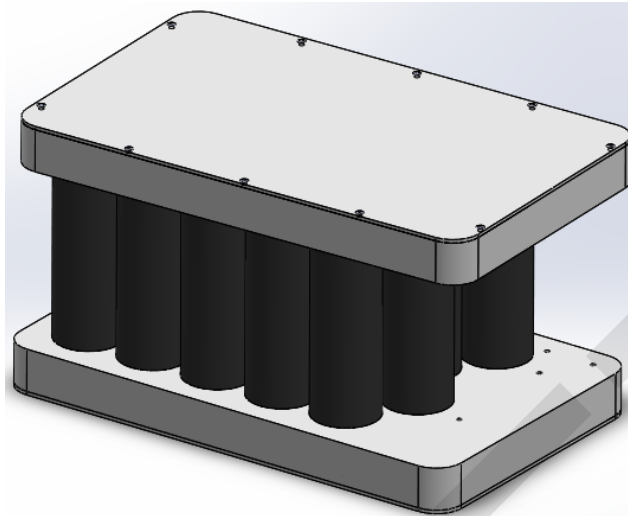


Figure 80. **CAD of the Battery Pack Assembled**

### **MANIFOLD DESIGN**

The manifold configuration was intended for evaluating the feasibility of evacuating and distributing the heat to prevent thermal runaway propagation between cells during a cell vent. To maximize and control the flow of electrolyte bursting out of the cells, 4 large openings were integrated. These openings, located at each terminal end of the cells, would allow for easy, low resistance flow of the hot gasses.

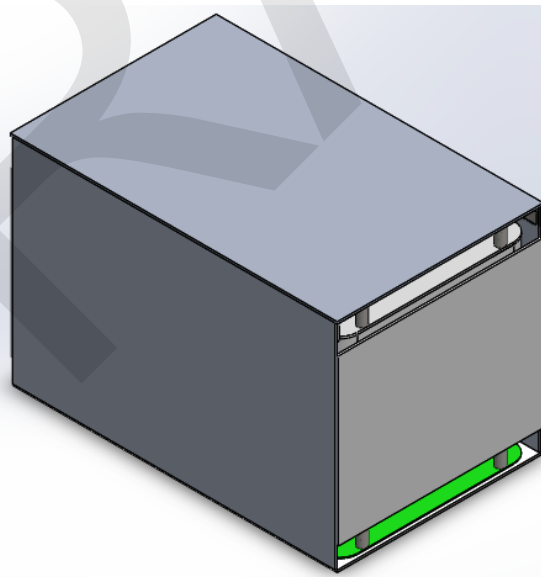


Figure 81. **CAD of the Manifold Design**

Figure 81 shows the manifold module design. To dissipate the heat and direct the hot gasses, steel plates were mounted on the top and bottom of this module enclosure. The melting point of the steel is  $1510^{\circ}\text{C}$  or roughly twice the aluminum's

so the steel was utilized to handle all the direct blast of the hot gasses. Stand-offs between the cover and steel plate create a gap to let the gasses easily flow out of the module.

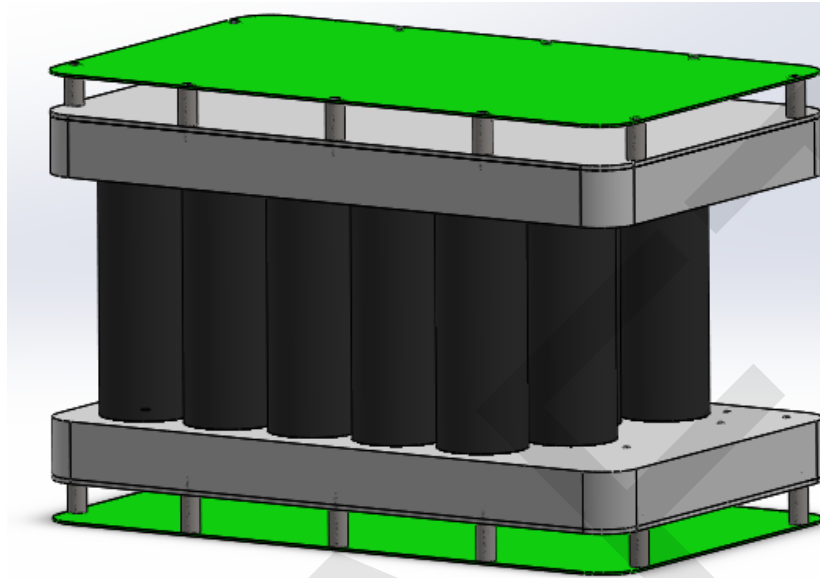


Figure 82. **CAD of the Inside Manifold Design**

Figure 82 shows the standoff and plate configuration inside the module enclosure.

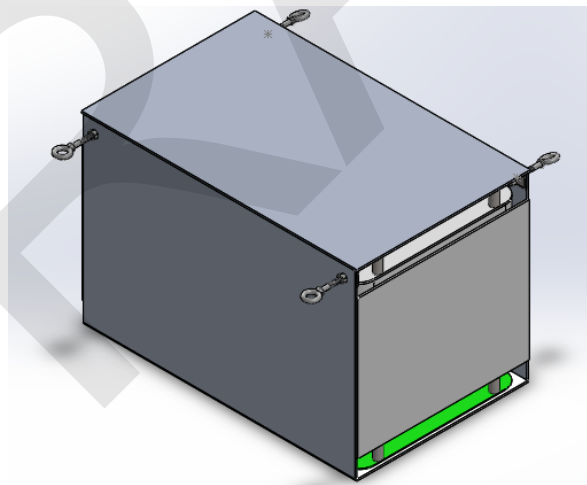


Figure 83. **CAD of the Manifold Design w/ Eyebolts**

Figure 83 shows the complete assembly with I bolts. These were used as anchors to stabilize the pack during testing.

## CELL SEPERATOR DESIGN

The cell separator configuration was intended to study/prevent thermal propagation between cells. The idea was to create a separate environment for each battery in order keep the heat/venting gasses from the cell in its own isolated area to limiting the heat transfer to adjacent cells. The separator configuration used only 10 cells to allow the necessary room for the separating materials. No mechanical resources were used to secure down the separator material, it we simply sandwiched between the two headers and secured via the threaded rods connecting the two headers together. Figure 84 shows the CAD of the separator design.

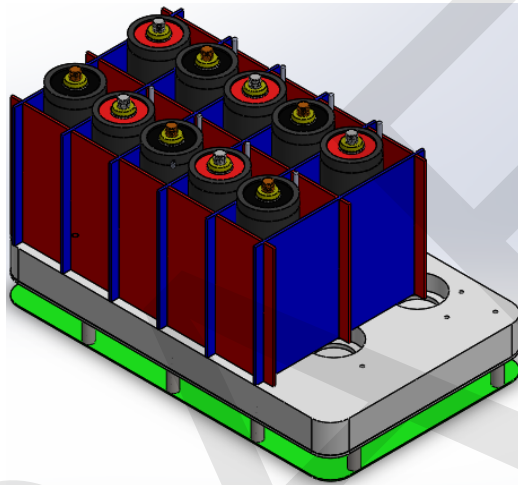


Figure 84. **CAD of Separator Design w/o Top**

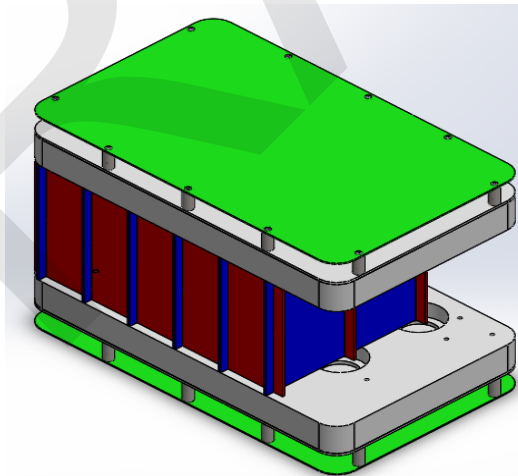


Figure 85. **CAD of the Walls Design**

Figure 85 shows a complete CAD image of a assembly ready for testing.

## PRESSURE RELEASE / CHECK VALVE

When one or more cells start venting in a completely closed battery pack, the copious amount of gas released builds up pressure that could even lead to an explosive scenario. To release pressure from the enclosure, this research team chose to incorporate a check valve. The check valve is designed to open once a pre-determined pressure is reached. A Matlab Simulink Module was created to simulate the increment of pressure as well as the check valve performance and determine the proper check valve.

The pressure inside the module is based on the volume of free space inside the module and the volume of gases emitted during the venting of at least one cell. For these calculations, it is assumed that the internal exothermic reactions boiled 100% of the electrolyte. Ideal gas laws were assumed. From the MSDS, the mass of electrolyte per cell is known and through the gas analysis already presented in Figure 4 the gas composition and percentages per volume are known. Therefore, multiplying the grams of electrolyte by the percentage of each element, the grams of each pure substance are calculated. Dividing these values by their respective molar mass, the mols of each pure substance are achieved. Adding these values, the mols in one battery are calculated. Even though this value results in a constant, it was added as a subsystem to the Simulink model as a means of keeping note.

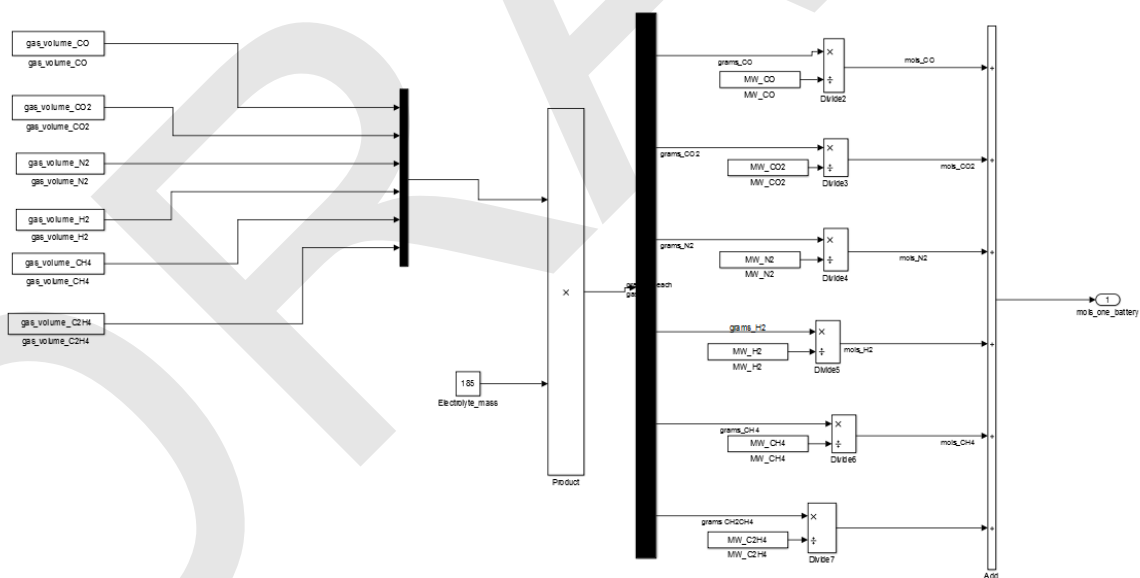


Figure 86. Moles of One Cell

Figure 86 show the Simulink calculation of mols Now, it is assumed that immediately after a cell vented, all the mols inside a cell were released as gas into the free space inside a module. Therefore, a trigger structure had to be created in order to simulate the venting process. It is assumed that the cell starts to vent at a tenth of a second and according to the experience gained through the previous

tests it was known that venting durations last for about 5 seconds.

Simultaneously, moles of air are being added to the moles of the cell to get the total moles inside the enclosure. Then, this value is divided by the seconds that the cell is venting to get the rate of moles/s. Later, the rate of moles/s is multiplied by the output of the switch that will be either one if the clock is between a tenth and five seconds because the cell is venting or zero when the clock is out of this range. However, the moles that are being released by the check valve have to be subtracted to know the remaining moles in the enclosure that build up s pressure. To simulate this increment of moles along the venting time, an integrator block is used. After the switch the “mols\_in\_the\_enclosure” variable is set as an output and graphed as well as is the trigger through the scope block. **Error! Reference source not found.** shows the trigger and its blocks.

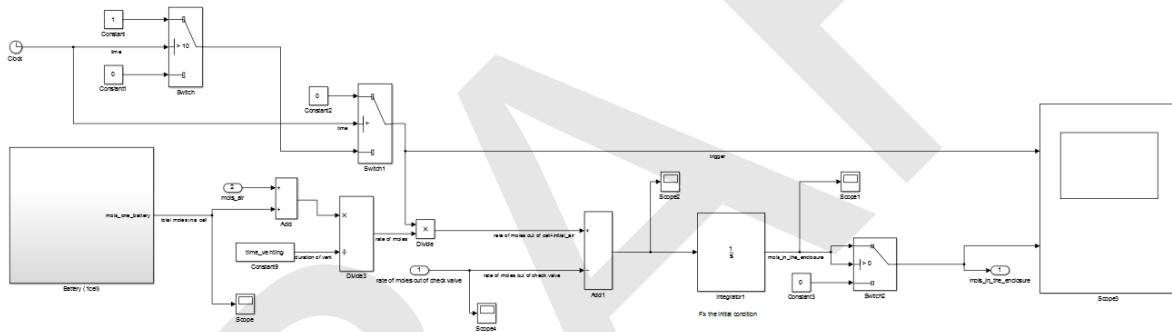


Figure 87. Trigger

Then, the variable mols\_in\_enclosure acts as an input to the next subsystem responsible for calculating the pressure generated for these moles using the equation of ideal gases.

The ideal gas law is used which states  $PV = nRT$  where:

P: Pressure (atm)

V: Volume (liters)

N: Number of mols (constant, no unit)

R: Gas constant (0.08205736 L·atm·mol<sup>-1</sup>·K<sup>-1</sup>)

T: Temperature (Kelvin)

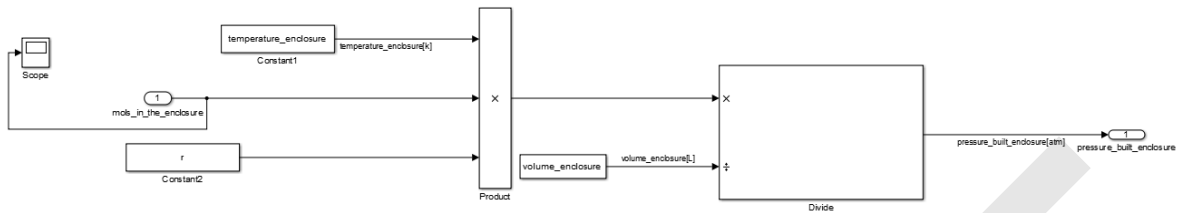


Figure 88. Enclosure Pressure Subsystem

Figure 88 shows the pressure calculation. Based on previous test, the temperature inside the enclosure is assumed to be 650°C. To get the volume, the volume of the plastic parts and cell have to be subtracted from the total volume of the enclosure. Then, the ideal gas law is applied to calculate the pressure that later on is used as an input to simulate the check valve operation. Figure 89 shows the subsystem accountable for replicating the check valve operation and quantifying the flow rate.

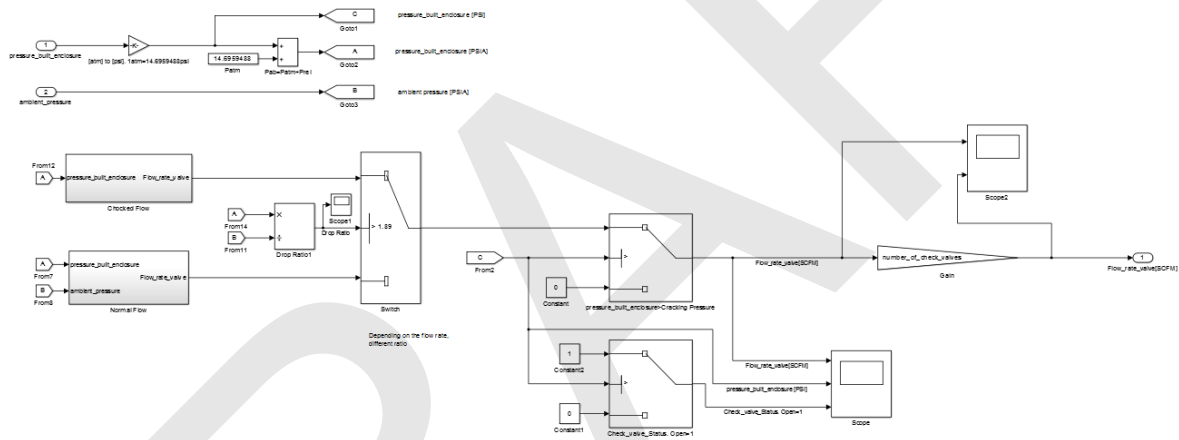


Figure 89. Check Valve Subsystem

The check valve flow rate changes depending on whether it is under normal flow or choked flow which is governed by a certain value of the pressure drop ratio. Below are equations to calculate each flow rate and the flow coefficient (Cv) of each case.

<b>NORMAL FLOW'S</b> <b>CRITICAL PRESSURE</b> <b>DROP RATIO:</b>	$\frac{P_1}{P_2} < 1.89$	: FLOW RATE LESS THAN THEORETICAL LIMIT	(EQ. 7)
<b>FLOW RATE (SCFM)</b> <b>(NORMAL FLOW)</b>	:	$Q = 16.05 \times C_v \sqrt{\frac{(P_1^2 - P_2^2)}{T(^{\circ}R) \times S_g}}$	(EQ. 8)
<b>FLOW COEFFICIENT</b> <b>(NORMAL FLOW)</b>	:	$C_v = Q \times (0.0623) \sqrt{\frac{T(^{\circ}R) \times S_g}{(P_1^2 - P_2^2)}}$	(EQ. 9)
<b>CHOKED FLOW'S</b> <b>CRITICAL PRESSURE</b> <b>DROP RATIO:</b>	$\frac{P_1}{P_2} > 1.89$	: FLOW RATE AT THE THEORETICAL LIMIT	(EQ. 10)
<b>FLOW RATE (SCFM)</b> <b>(CHOKED FLOW)</b>	:	$Q = 13.63 \times C_v \times P_1 \sqrt{\frac{1}{T(^{\circ}R) \times S_g}}$	(EQ. 11)
<b>FLOW COEFFICIENT</b> <b>(CHOKED FLOW)</b>	:	$C_v = \frac{Q \times (0.0734)}{P_1} \sqrt{T(^{\circ}R) \times S_g}$	(EQ. 12)
<b>NOTE: P<sub>1</sub> AND P<sub>2</sub> ARE IN UNITS OF PSIA</b>			

Figure 90. Flow Rate Equations. Source: Parker Valves Catalog 4135-CV

Where:

- P: Absolute pressure (PSIA)
- T: Temperature (degrees K)
- S<sub>g</sub>: Specific gravity (unit less)
- C<sub>v</sub>: Flow coefficient

The specific values of the gases are tabulated and since the substances that composed the gas as well as their percentage are known, the specific gravity can be calculated.

Given the pressure of the enclosure and the ambient pressure, the equations are implemented such that the output provides flowrate. Then, a switch is imposed to determine if the flow was normal or choked. In other words, if the pressure ratio was less than 1.89 the flow was normal, otherwise choked.

Another switch checked if the pressure in the enclosure was higher than the cracking pressure of the check valve. The cracking pressure is defined by the manufacturer and specifies the pressure at which the check valve is going to open. In this application, a very low cracking pressure was sought in order to start releasing the pressure as soon as possible. This value was sent to a gain representing number of check valves to model multiple check valves.

Finally, the output of this subsystem was the flow rate of the valve which was feed back to the trigger subsystem.

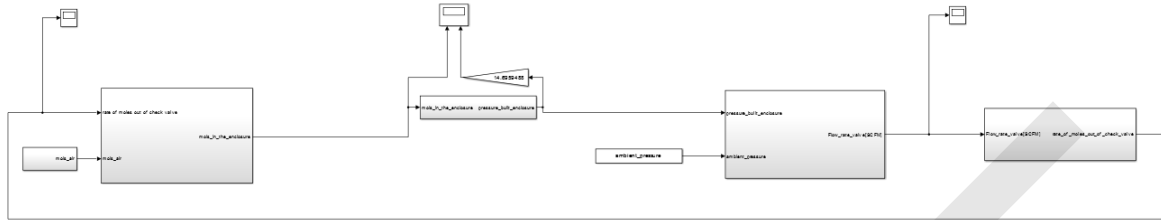


Figure 91. **Full Check Valve Model**

The simulation was run with a valve flow coefficient to 3.53. There are valves available with higher Cv's but they are expensive. The results are shown below.

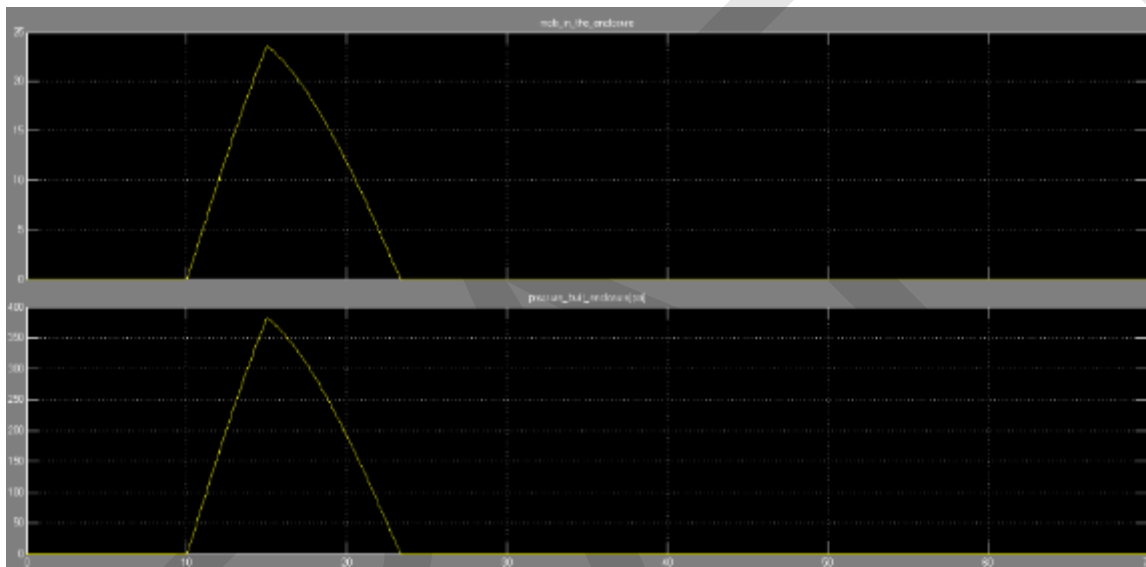


Figure 92. **Simulation Results**

Figure 92 shows simulation results. Note, the x axis in both charts is time in units of seconds while the top chart shows the total number of moles released by the cell and the bottom the pressure of the enclosure in units of psi.

At the first sight, it is seen that the peak of both signals match right at the same time. Analyzing the value of pressure, it turns out that it is surprisingly high and it's obvious that according to this results the box won't be able to withstand this much pressure and will end up exploding. To solve this problem, more check valves should be mounted or the use of check valves with higher flow rate should to be considered as well. The check valves necessary may need to be very large in diameter to achieve the required flow rate.

This was just a simulation and this results have to be verified. For this reason, the actual test was run to get real values and validate or disprove our assumptions and model.

## SECURING THE MODULE

Due to the sheer amount of energy released by the whole module, it is unsafe to leave unsecured during a destructive test. Based on prior single cell testing, it proved to this research team that tie downs to the ground were necessary to ensure the pack does not take off once cell venting occurs. The tie down system needed to be convenient to undo after completion of a test from a safe distance to avoid the potentially unsafe situation. To complete this goal tie downs were secured to the ground through a stake that could be lifted via a fork truck so as to minimize human interaction with the module. Eyebolts on each top corner of the enclosure were connected to a cable lifting loop and another cable to a ground stake as shown in Figure 93. Once the pack is forklifted up by the cables, it can be moved to a salt water bath, our storage and discharge container where used cells wait for hazardous chemical removal.



Figure 93. Handle to lift the Battery Pack up w/ the Forklift

## VI. MODULE LEVEL TESTING

This section goes into detail describing the tests conducted at the module level, and displaying the data that was collected during each test.

### **SINGLE CELL OVERCHARGE IN A MODULE WITH ACETAL HEADERS**

This was the first of three module level tests performed. The test served as a practice for the coming full module tests and also for obtaining information about the thermal response of the headers, the thermal runaway propagation between cells and the performance of design of the pack.

The test consisted of overcharging a single cell at 20 amperes with four bad cells on the corners of the Acetal headers. The enclosure used was the manifold design, an aluminum enclosure with a 1/16' steel sheet mounted on the top and bottom. Openings on side were included to release the smoke and the heat produced during the venting.

Voltage, current and temperatures were gathered over a CAN communication network. The temperatures sensors were distributed among the cells, headers, and covers. Below is detailed their locations:

- Center of cell that is being overcharged
- Enclosure Ambient
- Back right center of cell closest to overcharged cell
- Top right center of cell closest to overcharged cell
- Top right center of cell farthest away from overcharged cell
- Bottom right center of cell farthest away from overcharged cell
- Back left center of cell closest to overcharged cell
- Back left center of cell farthest away from overcharged cell
- Top left center of cell farthest away from overcharged cell
- Top left center of cell closest to overcharged cell
- Bottom header front
- Bottom header right
- Bottom header back
- Bottom header left

- Ambient
- Top cover center
- Top cover right
- Top cover back
- Top cover left

Unfortunately, the sensor on top left center of cell closest to overcharged cell got damaged and the data was irrecoverable, so this sensor won't be graphed.

To analyze the entire test and not miss any detail, the data will be presented progressively, starting with the information related to the cell that was being overcharged. The next figure shows the current, voltage, and temperature. The test plan for this event was to charge at a constant 20 amperes until the cell vented.

Figure 94 shows the voltage increased following the same trend as the previous tests. However, according to the data graph, the cell went off at 9.2V. This is technically impossible, so it means that something was wrong with the voltage sensor. Proof of that, is the increase of voltage right after the cell vented, which is technically impossible since if the cell has vented once it's not going to vent again.

In reference to the temperature, the data shows that the temperature increased as the cell was being overcharged, it hit the thermal runaway and then vented. As usual the cell temperature went up to about 700°C. Then, it cooled down to 200°C and then it ramped back up due to the burning Acetal headers.

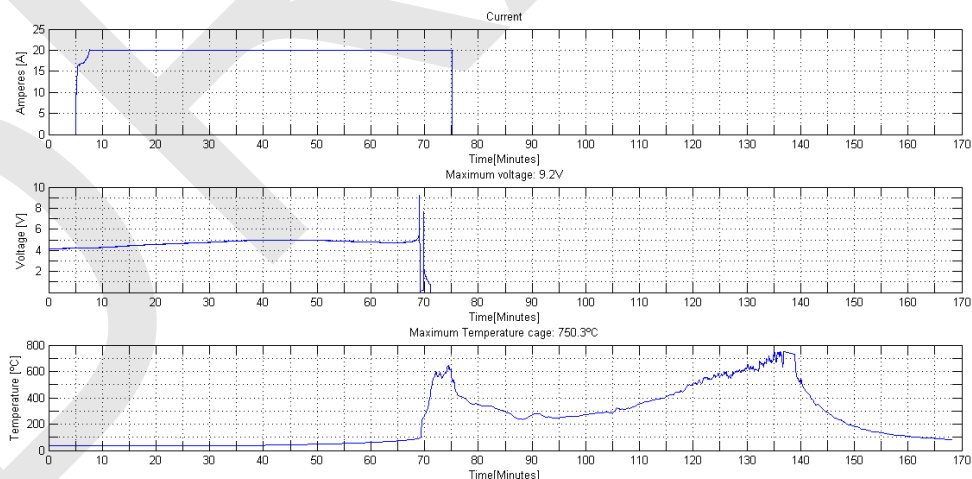


**Figure 94. Data - Cell Overcharge**

Each dummy cell had a couple temperature sensors attached to indicate if the

venting of the overcharged cell resulted in thermal propagation as well as the differences of temperatures between the farthest and closest sensor from the overcharged cell. Instead of graphing all the sensors at the same graph, the cells will be treated individually. Each graph in the Figure 95 represents the data of one dummy cell: the temperature sensors attached to it, the temperature of the overcharged cell as well as the ambient cage. The second graph just contains three signals because many sensors were damaged.

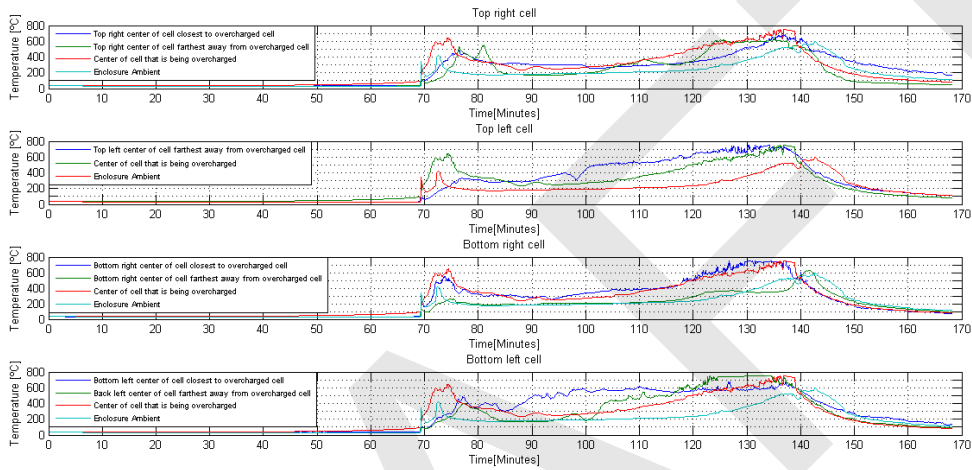


Figure 95. Data Dummies Cells

Each cell held two temperature sensors. The sensor closest to and or in direct view of the overcharged cell was always the first to increase. Shortly after the venting event both sensors of the same cell read very similar values. Eventually, all four dummy cells also vented due to the excessive heat inside the enclosure.

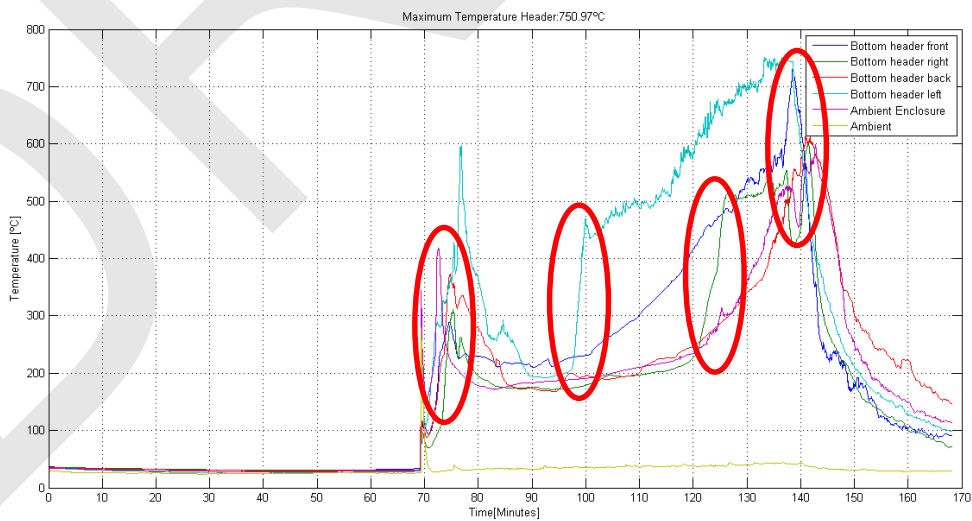


Figure 96. Bottom Header Temperatures

Figure 96 shows the bottom header temperature sensor readings. Analyzing the graph, it appears each sensor suddenly increased temperatures multiple times. This likely indicates when each dummy cell vented. So it would be convenient to treat each sensor individually and their data is shown in the Figure 97

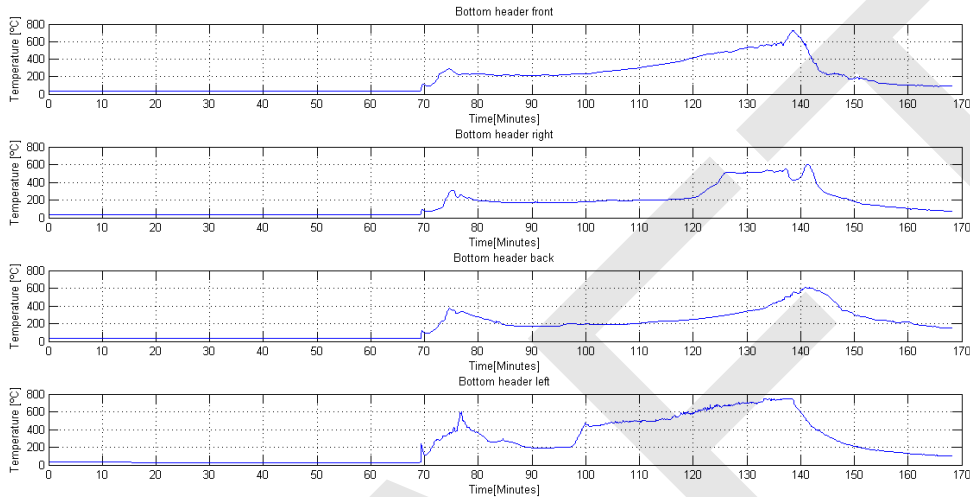


Figure 97. **Bottom Header Temperatures (Treated Individually)**

All the sensors recorded when the overcharged cell vented with a sudden increase of temperatures. Following the venting event one sensor cooled then rapidly increased its reading whereas the other sensors only continued to increasing their temperature gradually. Then, about 2 hours and 20 min. in all sensors experiences another increase in temperature. Likely another cell venting or internal fire.

To try to match the sudden increase of temperature with the cells venting, the next figure has four graphs which contain the data of each sensor of the header as well as the data of the couple closest cells. The data of the cell always correspond to closest sensor to the overcharged cell.

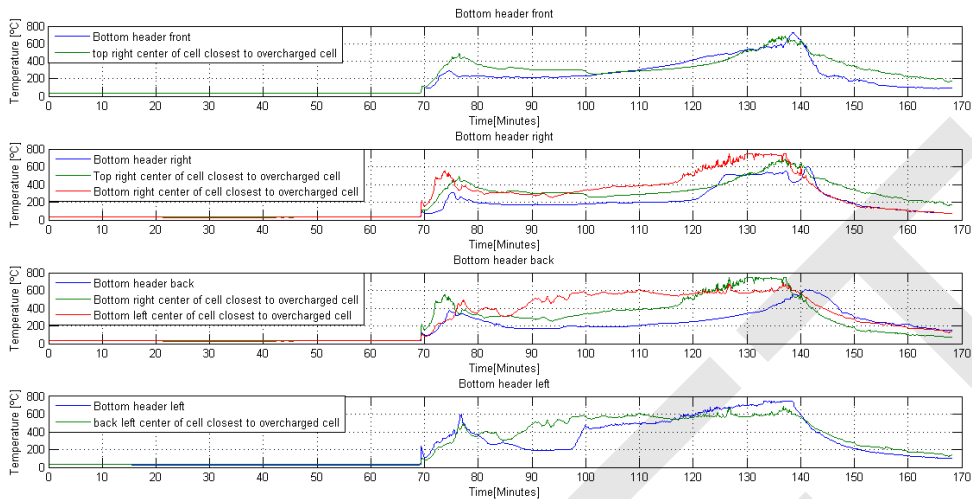


Figure 98. **Bottom Header and the Closest Cell Temperatures**

The data in Figure 98 doesn't clearly indicate when the individual cells would have vented. Again the highest temperatures were captured by the end of the test because the plastic of the headers burning.

The cover is the final part left to analyze. The overcharged cell caused a rise in all the temperature sensors to around 300-400°C. The majority of them kept going progressively up to around 700°C the shortly after started a cool process. Nevertheless, the sensors on the back, the center and right presented different responses. The first two mentioned, right after the cell went off experienced a brutal increase of temperature and then joined the other sensors. On the other hand, the one on the right always had lower values although higher than the melting point of Acetal (168°C).

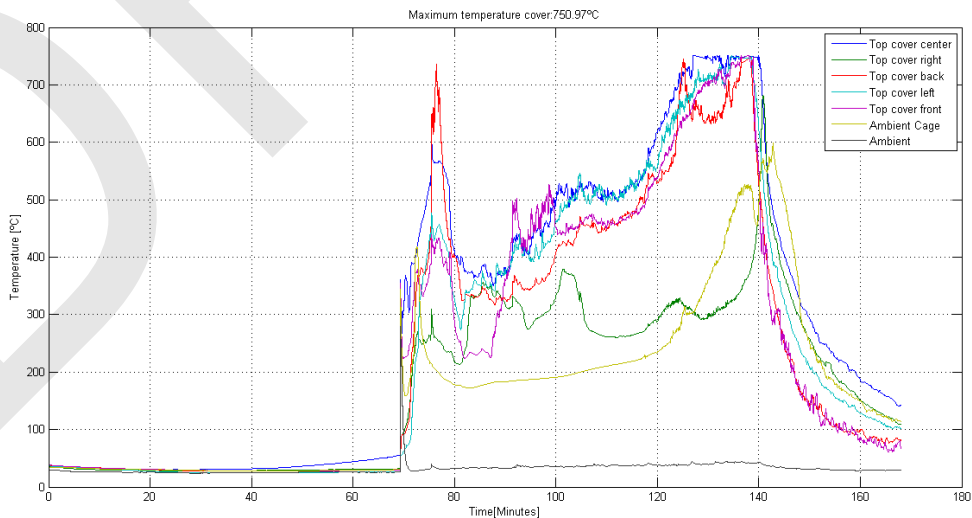


Figure 99. **Cover Temperatures**

Once everything cooled down to ambient temperature, the cleanup procedures started. The first surprise was that the front and the back sides of the enclosures Aluminum were melted as well as the sides as the Figure 100. It was likely caused by the heat of the plastic headers burning. On the other hand, the top and bottom steel plates successfully handled the direct impact and heat exposure of the cells venting gasses.



Figure 100. **Enclosure After the Test**

All cells were investigated and confirmed to have vented given that all burst disks were opened. Inside the enclosure only metal parts remained. No plastic part remained. No clear sign was left that the box ever contained any plastic before.

### **OVERCHARGE OF 20 CELLS IN STEEL ENCLOSURE**

In this test, the twenty cells were connected in series to obtain a high voltage battery pack with a nominal voltage of 72V. Our intention was to overcharge a single cell to avoid a really intense event where multiple cells began venting simultaneously. This scenario would more consistent with a BMS charging failure of a single cell due to a flawed voltage reading. It would also show the effect of thermal propagation from one failed cell to the other cells at normal state of charge. The method chosen was to start charging at 20 amps with all cells below 3.5 V except the one intended to vent which was fully charged at the nominal cell voltage of 3.6 V. In this way, only one cell is actually being overcharged.

The manifold design enclosure was used, the design with the openings on the side. However, adopting lessons learned from the previous single cell overcharge in a module, the aluminum enclosure was replaced with one entirely made out of Steel.

The headers used were made out of Acetal although it was already known that they will burn up eventually so their function was only to initially hold the batteries.

With the amount of energy in the pack and experience of the previous test, the

event was expected to be very intense. Test setup had to provide the maximum safety for the researchers as well as avoid any potential hazard. The first step taken was to move the observation and instrumentation trailer 250 ft away from the concrete test pad. The trailer contained the chargers as well as the laptop that logged data. Data and power lines were extended to reach the new trailer location.

In addition, the concrete pad was surrounded by three Jersey barriers to block any flying debris, although one side facing an open field was left open for access during setup and clean up. The pack was tied down using the cable system explained in the section Module Level Testing Design.

The cell voltages, temperatures and current were recorded through CAN., Two slave modules and a BMS were needed to capture the voltages. Starting at the main negative, the terminals of each battery were connected to the slaves. One slave measures ten cell voltages. Slaves are connected in an RS485 daisy chain to each other and to the BMS main board which provides all the cell voltages and pack voltage to the CAN network.

Several thermos-scanners were deployed, each supporting up to forty temperature sensors so that temperature distributions throughout the pack can be measured. All the sensors on the first thermo-scanner were attached to a surface of a cell starting from the most negative cell to the most positive. Sensors of the second thermo-scanner were distributed throughout the pack and enclosure as follows:

- Bottom header left
- Bottom header back
- Bottom header right
- Bottom header front
- Top cover left
- Top cover back
- Top cover right
- Top cover front
- Top of cover on center
- Top of steel enclosure
- Front of steel enclosure
- Left of steel enclosure

- Ambient inside pack
- Ambient

Figure 101 shows the battery pack at the start of testing, secured down and with all the data being logged prior to initiation of charge current. The current sensor was placed at the output of the charger in the instrumentation trailer on the power cables running out to the pack on the test pad.



Figure 101. **Battery Pack prior to Testing**

To run this test successfully required four attempts due to multiple problems that will be explained as the data of each test is presented. Figure 102 below shows the data of the first attempt. The top current chart shows the charger was unable to deliver the desired 20 A current output and current output also decreased as the voltage increased. The charger, which worked well for single cells tests, was obviously power limited at the pack level voltage. Several chargers were connected in parallel to in an attempt to increase the current capacity but this was unsuccessful as captured by the current trace around 100 minutes.

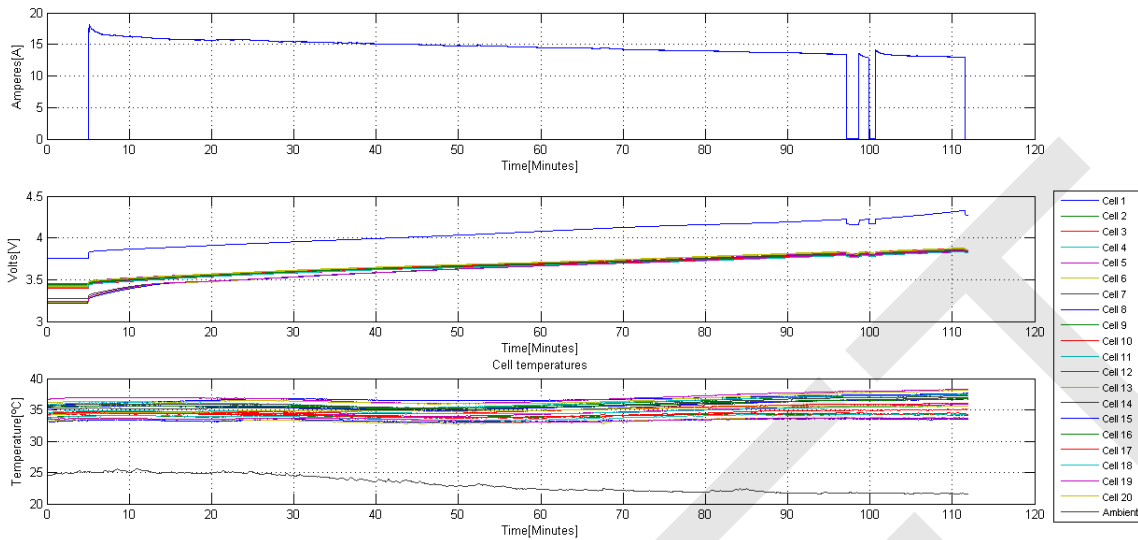


Figure 102. **Overcharge\_20\_cells\_steel\_enclosure- First try- Data**

The voltage chart shows that the fully charged target cell was clearly higher than the other cells during this first attempt. On the other hand, the cell temperatures stayed closely grouped together. This behavior was not expected since, according to the previous tests, it was known that a current of 14-16 A should significantly heat up the cells. It indicates that the cells were not getting the same amount current as the sensor read. The current drop could be caused by the long distance between the trailer and the pack and also because the gauge of the cable selected was unappropriated.

Because of the distance between the pack and the charger, the line had to be extended. In this case, the power line was composed by couple cables that had different gauges. One cable came out from the charger and the other one from the pack and met by the middle.

The cable that came out of the pack did not have the appropriate gauge, so decision taken was make shorter the line coming out of the pack and replace it with right gauge cable.

The next Figure 103 corresponds to the second try of the test. This time, the data was very useful to obtain remarkable information. First of all, that even though the charger was not pushing twenty amperes, the modification of the power line was worth it because the cells heated up more than the previous test. Secondly, that the BMS did not measure higher values than 4.5V although the voltages of the cells were higher. The last one, but not less important, is that despite the overcharged cell hit the one hundred Celsius it did not go off. It means that what really forces the cell to go off is a constant high current that keeps the exothermic inside the cells going on.

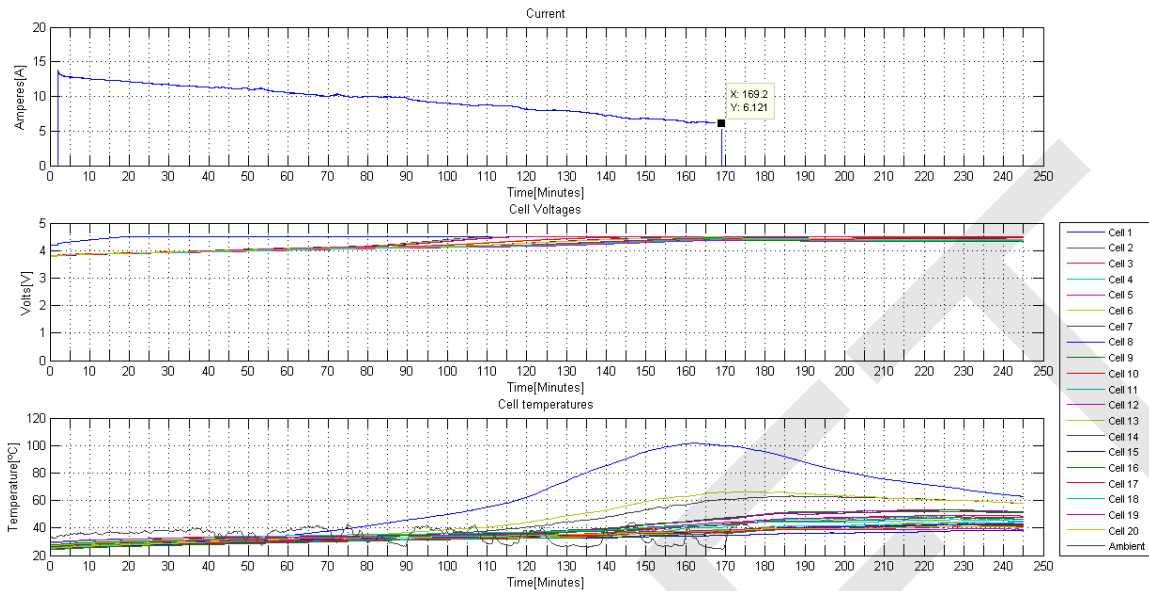


Figure 103. **Overcharge\_20\_cells\_steel\_enclosure- Second try- Data**

Therefore, it is obvious that there was a problem with the power supply since it was not capable of providing twenty constant amperes. It was replaced for another power supply, which according to its specs and the corresponding checks it was able to push twenty constant amperes. However, it fluctuated a lot so the next figure doesn't monitor the current data because it's not steady even though it was higher than twenty amperes.

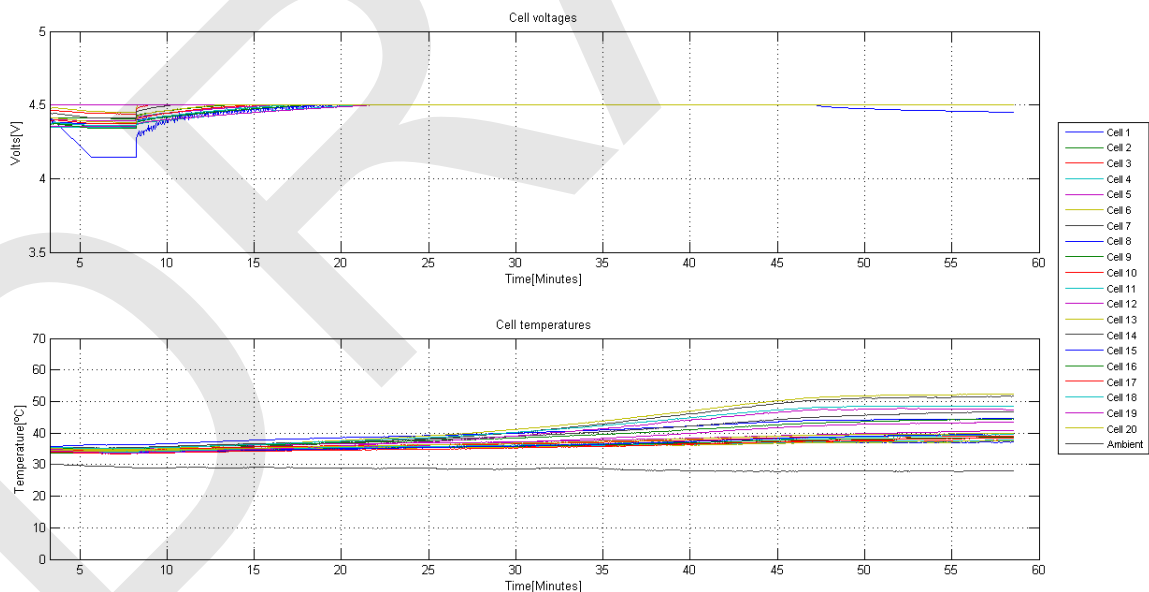


Figure 104. **Overcharge\_20\_cells\_steel\_enclosure- Third try- Data**

As the Figure 104 above shows, the pack did not go off again although all the

voltages were higher than 4.5V and the higher temperature was around 50°C. This temperature actually is within the safe condition of operation of the cell provided by the manufacturer and also according to what on the previous test, where the cell got around 100°C and nothing happened, this time not event should be expected.

However, the really remarkable information of the graph is that the current pushed was not heating the cells up. Fact, that demonstrates that the cells did not get much current due to there was a huge current drop between the main positive and negative coming out to the pack and the charger. The gauge of the wire was not appropriated and it caused losses by heat. The wire was replaced and at that point everything should be ready to force the pack to go off.

The Figure 105 summarizes the data of the test where the pack blew up. Again, the current data is not presented because it fluctuated a lot and the graph wouldn't be clear.

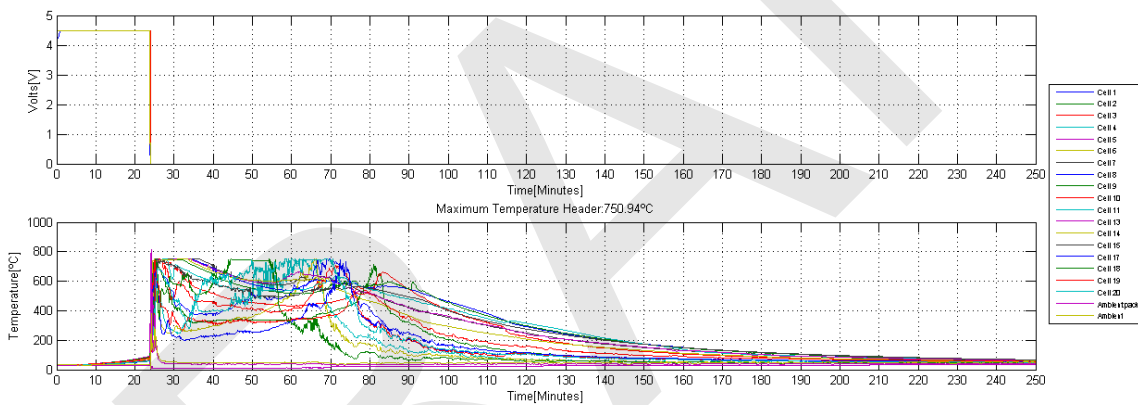


Figure 105. **Overcharge\_20\_cells\_steel\_enclosure- Data**

The following graph shows the voltages and the temperatures of the cells. The voltage it's just useful to make sure that the temperatures climbed as soon as the voltages dropped. Through both graphs can't be figured out which cell was the first to go off and the exact moment each cell vented.

Taking a look at the temperatures graph, first information that surprises is that the temperature was between two hundred Celsius and seven hundred Celsius for almost one hour and then it started cooling down that took another hour as well.

Nonetheless, the sensor that got the ambient inside the pack just got up to 300°C right when the first cell vented and after that it cooled down until it joined the ambient temperatures. This behavior it's very odd since the venting of cells were releasing a lot of heat. Hence, most likely the intensity of the event, the smoke or

flames kicked the sensor out of the pack and started reading ambient temperatures.

At the same time, the plastic parts of the battery pack were also being affected by the heat. The next Figure 106 presents the data of the sensors spread on the bottom header. Of course each plastic part of the pack caught fire and burned until it was gone. However, let's analyze the data available.

As a first time, couple sensors went up to 1200°C. It must be a consequence of that multiple cells went off right at the same exact moment. The other cells went up to more familiar values between 600-800 °C. After those peaks, the sensors got very different values and none of them followed the same trend. For some of them took longer to cool down meanwhile some of them take shorter.

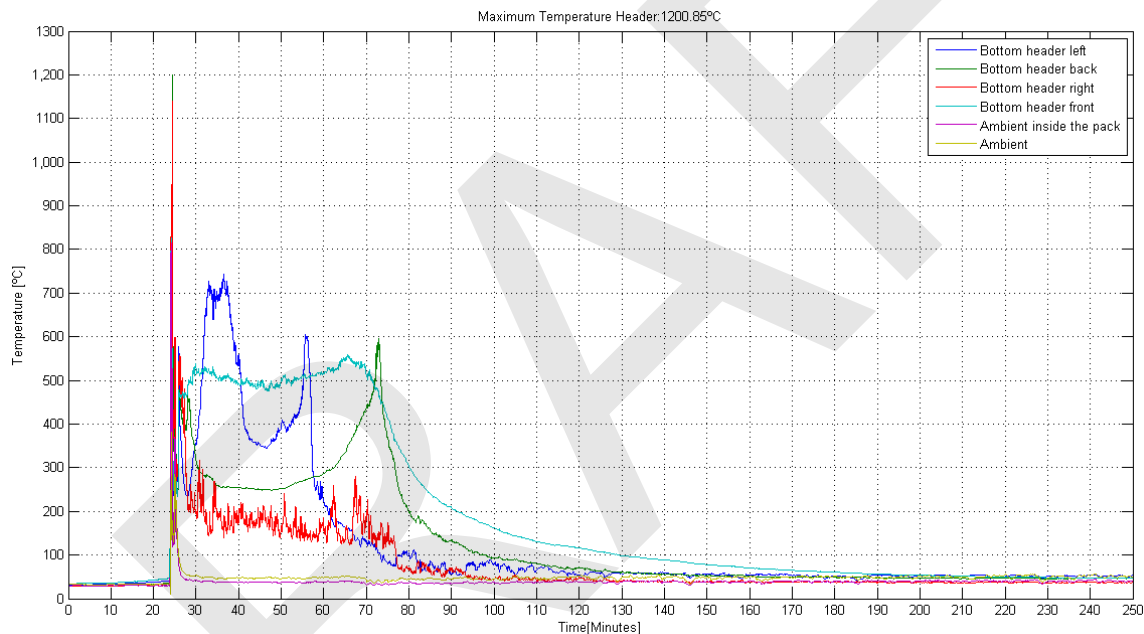


Figure 106. **Bottom Header Temperatures**

The covers, see Figure 107 below, also got up to 1200°C although the location does not match with the one on the header. The extreme heat damaged the sensor on the right and the one on center. Of course, the covers also burned down.

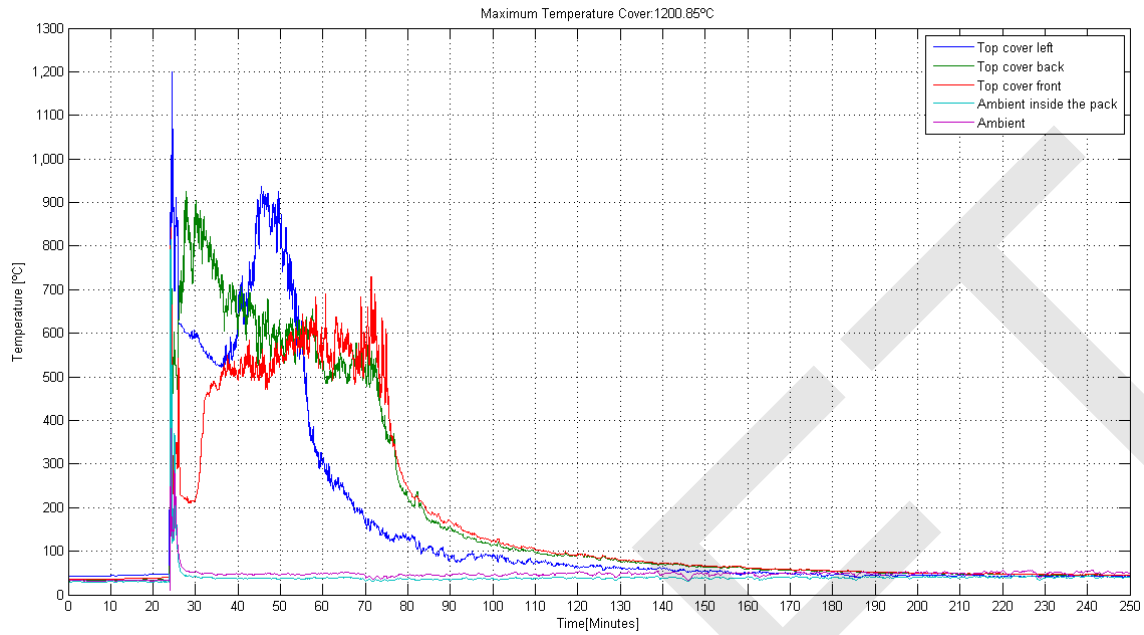


Figure 107. **Cover Temperatures**

According to the metal parts for the enclosure, as the next image shows, instead of getting as high as the cover and headers it got around 1000°C. Remember that the enclosure was made out of steel and its melting point it's higher than the temperature captured by the sensors. Therefore, the enclosure should present any sign of melting or any hole caused by the flames of the cell. Also, please notice that it cooled down so fast, basically because it was the outside layer of the pack, the one that received less heat and because it was in contact directly with the ambient temperature.

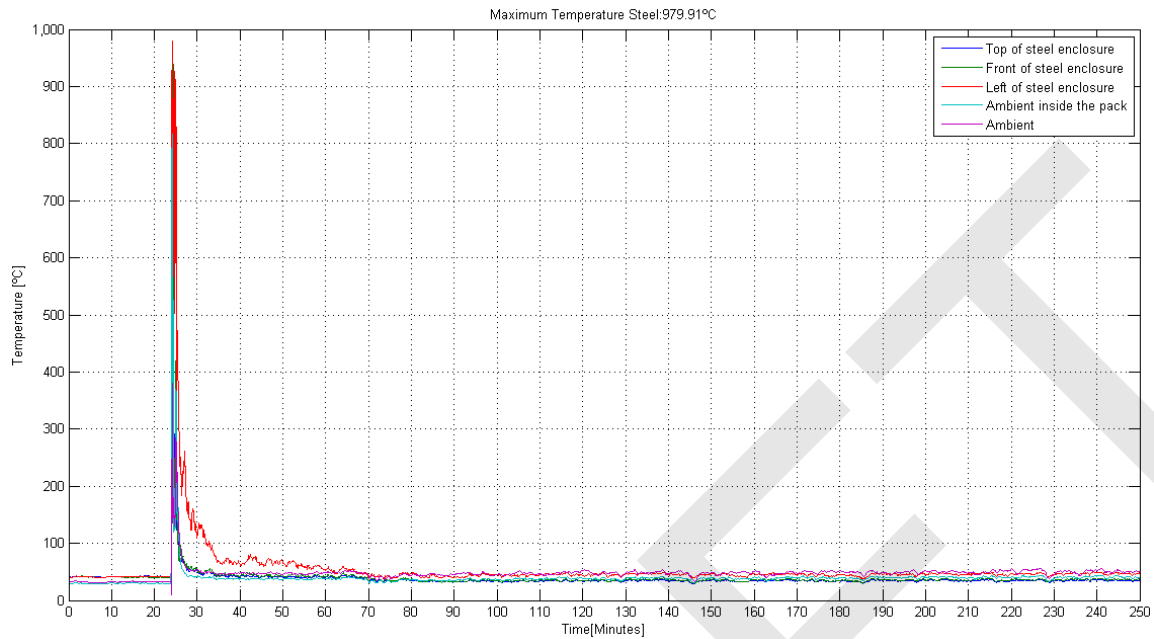


Figure 108. **Steel Temperatures**

After a reasonable time to let everything cool down, the pack was analyzed. The metal enclosure overcame the test really successfully since it did not get melted anywhere. The unique noticeable sign that it had been exposed to high temperatures was that each side bended a little bit and the steel got a different tonality.

Again, and how is expected according to the previous tests, the plastics parts didn't make it and burned down.

Moreover, all the cells had the venting's opened meaning that all of them vented. Their voltage was analyzed and they were null.

The Figure 109 is a screen shoot of the video recorded during the event. The picture demonstrates the brutality of the flames coming out of the openings of the pack. It wouldn't be unreasonable think that some batteries vented at the same time due to the effect of the thermal runaway propagation.



Figure 109. **Battery Pack Venting**

However, the thermal propagation was also palpable because multiple times, right after one cell had finish venting, another one started venting right away. Through the next sequence of images in the **Error! Reference source not found.**, the event is showed and explained.



Figure 110. **Sequence of the venting process**

On the top left of each picture there is the exact second the image was taken counting from the first cell that vented. As it has been mentioned before, the thermal propagation appeared several times and actually it did happen before the 30th second but the shots were not as clear as these ones.

The first picture of the sequence shows the venting of at least one cell and how all the flames come out of the openings. On the second one the venting was although as the plastic parts were still burning flames kept coming out. The fire and the high temperature forced another cell to vent as it is presented on the last picture of the sequence.

The venting of the twenty cells lasted around one minute and a half. After that, the pack kept burning for six more minutes.

From the images it is not appreciable but a huge dark cloud of smoke was generated. Unfortunately, it is very toxic, so it brings importance to the fact of treating the smoke as a potential hazard as well as the necessity of evacuating it rapidly to keep it away of the human beings.

The steel enclosure did a great job; it could handle those extreme temperatures without any problems. It did not melt and it could be even reused for another tests.

## **CHECK VALVE TEST**

A pack with twenty cells in a closed enclosure with a check valve was overcharged at twenty amperes to figure out the response of the batteries in a closed environment as well as verify is the operation of the check valve according to the pressure achieved in the pack to contrast the theoretical results obtained by the simulation tools with the real ones captured by a pressure mounted on the pack.

In this case, the pack replicated a full pack with one module in. In other words, the pack with the enclosure with the openings was inside a bigger closed enclosure as it was one module of the full pack.

Twenty cells connected in series to obtain a high voltage pack. Once again, one of these cells had a higher a SOC and charging the pack it was sought overcharge that particular cell meanwhile the other ones had a reasonable voltage.

The enclosure of the module was made out of steel and then it was housed in an external steel enclosure. Steel was chosen by both enclosures due to the great results from the last test.

To get the enclosure as hermetic as possible, the lid was bolted down to Aluminum L brackets throughout the contour of the lid.

In addition, right before closing the lid as the last time, sealing glue was spread around the contour to avoid any air gap.

Both ends of the check valve were male threaded. One side was threaded to the lid through a bung weld welded on the lid meanwhile to the other end was threaded to a tube that worked as exhaust to see the smoke coming out from the distance.

Couple more bung welds had to be welded to the lid as well. One for the pressure sensor and the other one for the air hose to calibrate and validate the operation of the check valve.

The check valve was carefully selected. Through Matlab Simulink the venting process was simulated for the battery pack under study to replicate the operation of

the check once one cell goes off to pick the appropriate valve and figure out the pressure build up in the pack along the time.

The pressure basically depended on if the cell vented, either the check valve it's open or closed or how much pressure is the valve capable of releasing as well as how much time it remained opened.

What really characterized this test was the fact that the pressure was also captured through CAN as the voltage of each cell, current and temperatures.

The check valve did work, but unfortunately just for a little while because too much pressure built up and the lid ended up popping up and the check valve and exhaust flew away as the next Figure 111 demonstrates.



Figure 111. **Check Valve Test Exhaust After Test**

However, this fact did not ruin the test because interesting results were obtained.

First of all, it is very remarkable that just one cell went off and the other ones did not get affected by the thermal runaway propagation. In fact, during the cleaning up tasks each voltage was measured and except the one that went off, the other ones held the SOC they had been charged to.

The flames produced in the venting did not ignited the plastic parts and just the area by the cell that vented melted but other than that, the plastic parts looked fine.

The steel enclosure that surrounded the module did not experiment any detriment and the external one, besides the lid, either.

## VII. CRASH TESTING

In contrast to the many standardized battery impact tests found in the literature, this pendulum based crash test was designed to simulate the specific and common scenario of a light vehicle impacting the side of a transit bus including the worst case scenario of the vehicle impacting directly at the point where a battery pack is mounted outside the bus frame rail. The intention was to include realistic vehicle speeds, vehicle mass, bumper dimensions, and dynamics of bus chassis and tires as will be seen later in the section. LTI regularly performs full scale crash tests of this type, but the cost of such a full scale test was beyond the scope of this project. A pendulum impact serves as a close approximation.

The impact test required significant preparation since everything must go perfectly on the first try. The tasks were split up as preparation of the truck to simulate a bus, preparation of the battery pack, and preparation of the test.

### **PREPARATION FOR THE TRUCK**

To simulate a small to medium transit bus, an 18,400 lb GVWR refrigerated box truck was selected from an inventory of available crash trucks at our test track. The particular truck used as shown in Figure 112 was used for on campus delivery by the Penn State Creamery and was not in running condition. This would not affect the goal of replicating the dynamics of the vehicle during an impact.



Figure 112. **18,400 lbs. GVWR Refrigerated Truck to Simulate Bus**

The box was removed from the truck for safety reasons since if the batteries burned the bed could also catch on fire. In addition, current buses do not use similar insulated materials for their side panels so it was incompatible to test it. Using a torch, the box was cut off, lifted by two forklifts, and then the truck was pulled from underneath the box as shown in Figure 113. All liquids were removed, the tires were filled up with air, and the exhaust was cut off.



Figure 113. **Refrigerated Box Remove from Crash Truck**

The bare truck chassis weighed in at 12,250 lbs. Several options were considered to add weight and the final choice was to mount two Jersey barriers at 4,750 lbs. each mounted on I beams sections welded to the frame as shown in Figure 114 and Figure 115. Heavy ratchet straps secured the Jersey barriers.



Figure 114. **I Beam Sections Welded to Chassis Frame**



Figure 115. **Jersey Barriers Mounted onto Truck Chassis**

At this point the truck was weighted again at 17,750 lbs. After taking into account that the weight of the battery pack would be 100 lbs., an extra 550 lbs. of sand bags were distributed throughout the back of the truck until the GVWR of 18,400 lbs. was achieved. At this point, the truck was moved to the pendulum test pad and be placed at the impact point.

## **PENDULUM**

Our track facilities include a 40 ft tall impact pendulum tower and test pad. In this case, the impact mass would simulate an SUV crashing into the side of a transit bus. The empty impact pendulum weighed in at 1,200 lbs. Given a typical SUV weighs between 3500 and 4500 lb, the pendulum was loaded with all twenty-eight available steel plates each weighing 100 lbs. achieving a total mass of 4000 lbs.

A front bumper for a 2006 Suburban was shortened to avoid a collision with the truck cab and back wheels. It was attached to the impact mass with steel tubes of similar proportions to the original Suburban frame. Figure 116 shows both square tubes were welded to a c-channel base and extra tabs were added to support the bumper from the main square frame tube similar to the vehicle design.



Figure 116. **Left, Top View of Bumper, Right Bottom View**

The bumper was mounted on the impact mass and the truck aligned for direct impact on the battery module as shown in Figure 117.



Figure 117. **Impact Mass Mounted Bumper and Battery Position**

## FREE SWING TEST

Goals of the free swing test were to insure the pendulum would impact the battery pack straight, accurately, and at the desired velocity. Exact location of the truck tires was marked on the test pad with spray paint, then the truck was moved off the test pad. Radar was set up to measure impact mass velocity. The radar is composed of two components: a laptop with software that monitors the velocity and the sensor to measure velocity of the moving mass. As Figure 118 below shows, the radar laptop was out of the pendulum trajectory while the sensor device was on the concrete test pad aligned with the approaching impact mass.



Figure 118. **Radar Alignment**

To determine exactly where the pendulum would impact the battery module, a sponge filled with yellow paint was attached to the bumper and a white cardboard target of the same dimensions as the battery pack was placed on the spot and height where the battery pack would be mounted on the truck as shown in Figure 119. Additional targets were placed in the positions of the truck cab and wheels to insure pendulum clearances.



Figure 119. **Pendulum Test Swing Setup**

The final setup step was to attach a measuring tape to the bottom of the impact mass to determine static height and lifted height above the ground. The static height was found to be 26 inches. The lifted height for a target impact speed can be determined through equating the potential and kinetic energy equations. Three free swings were performed, lowest speed first to test the releasing system and accuracy of pendulum swing. The pendulum was pulled up to a lifted height of 11.36 ft and a velocity of 18.5 mph was measured as validated by the following energy equations which predict a speed of 18.44 mph.

Pendulum weight = 4000 lbs. = mg

Gravity  $g = 32.2 \text{ ft/s}^2$

Pendulum mass =  $4000 \text{ lbs.} / 32.2 \text{ ft/s}^2 = 124.22 \text{ lb-s}^2/\text{ft}$

Potential Energy =  $mgh = 4000 \text{ lbs.} * 11.36 \text{ ft} = 45,453.3 \text{ lb ft}$

Kinetic Energy =  $mv^2/2 = PE$

$v = (2*PE/m)^{1/2} = (2 * 45,453.3 / 124.22)^{1/2} = 27.05 \text{ ft/s} = 18.44 \text{ mph}$

As a second test, the impact mass was raised to the maximum practical total height (limited by lift cable tension) of 21 feet and 1 inch and a velocity measured was 25.0 mph. A third try validated that the velocity at 21ft and 1inch was again 25.0 mph. This speed is typical of vehicles impacting the side of buses in urban environments, especially at intersections.

The last free swing was also used to validate the accuracy of bumper impact location relative to the battery box position. In Figure 120 below, the yellow paint mark indicates that the bumper impacted the battery position (simulated by the gray tape) within two inches of the original alignment. The fact that the pendulum im-

pacted lower than the static alignment is likely due to cable stretching under additional dynamic loading from swing velocity.



Figure 120. **Impact Accuracy of Pendulum to Battery Position**

### **BATTERY PACK PREPARATION**

The intention of this test was to simulate a full sized bus battery pack, but space limitations on the frame of the truck restricted the test to a single module with 20 cells. After making sure that all BMS and temperature data was logging properly, the pack was inserted into a steel box which was subsequently housed within an external Aluminum enclosure as shown in Figure 121. The aluminum enclosure was designed with flanges for mounting to the truck frame between the cab and rear wheels. A power connector was also attached to the pack to simulate a real pack as closely as possible.



Figure 121. **Aluminum Enclosure with Frame Mounting Flanges**

Figure 122 shows the battery module mounted to the truck frame between the cab and rear wheels. A thermocouple scanner was mounted to the truck frame and a data acquisition box was placed on the ground as far as cabling allowed.



Figure 122. **Battery Module Mounted on Frame with Data Acquisition**

Figure 123 shows the positions of video and high speed cameras placed to capture the crash event. The orange cone atop the pack is intended to serve as an inertial reference in the high speed video. The pendulum can be seen suspended a few feet away from the battery module prior to lifting.



Figure 123. **Camera Layout**

## **IMPACT TEST RESULTS AND CONCLUSIONS**

Test setup included camera placement and extending the pendulum release tether to 200 feet. Local fire departments were invited to observe the test. The area was

cleared of all personnel except one observer and the tow truck driver. The pendulum was pulled up to the 25 mph lifted height of 18.92 ft. Finally, the cameras were triggered and the area was cleared of all personnel to a radius of 200 feet. A horn blast was given and the release mechanism was triggered to drop the pendulum. The pendulum impacted the box and truck which was pushed back about one foot. No venting of cells was detected upon impact. As shown in, Figure 124 local fire fighters drilled on approaching the pack in full personal protective equipment (PPE) ready to apply water coolant as would be their practice in response to an actual traffic accident involving an electrified transit bus. They also deployed an infrared camera to remotely detect hot spots on the pack, an indication of thermal runaway. No excessive heat was detected. Afterwards, the pack was left undisturbed for at least 24 hours.



**Figure 124. Fire Fighters Approach Battery Pack after Impact**

The BMS collected voltage and temperature data on all 20 cells within the module during the simulated crash test in anticipation of venting and thermal events. Since no venting occurred, the voltage data was unchanged and only small perturbations in temperature occurred due to ambient conditions as shown in Figure 125. A slight temperature rise of 3C was detected on all cells at the time of impact. This was

likely due to mechanical energy and frictional work dissipated within the pack during the impact event. Cell 5 also demonstrated sensor bias and scaling which was unrelated to the crash event.

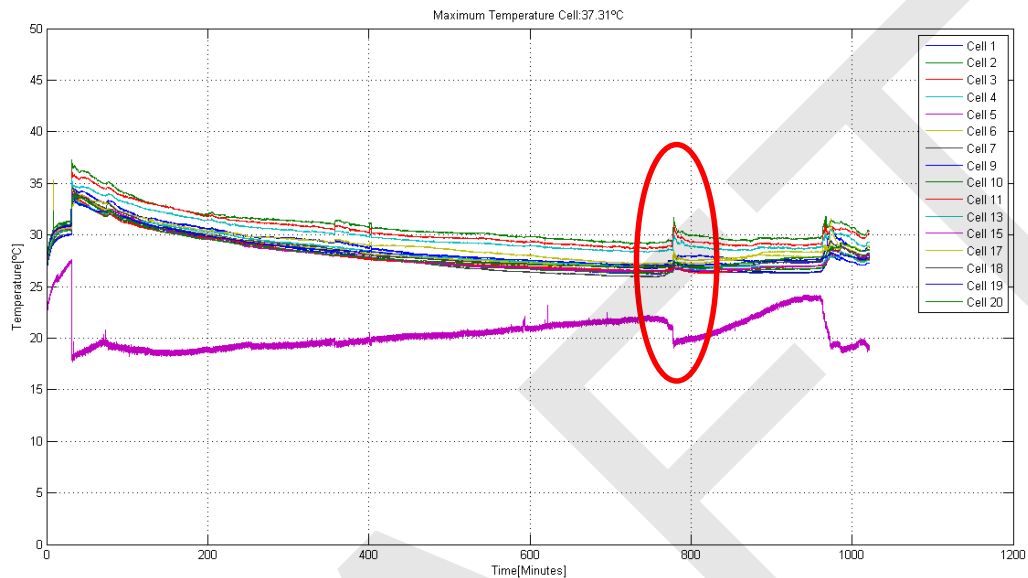


Figure 125. **Individual Cell Temperatures during Simulated Crash Event**

Upon inspection, it was noted that the center section of bumper deformed until the simulated SUV frame impacted the truck frame on either side of the battery module. The battery enclosure was significantly dented but not totally crushed as shown in Figure 126. Some truck frame deformation was detected. The impact momentum transferred to the truck moved the front axle back 13 inches and the rear axle back 11 inches. Almost all the energy was transformed into deformation of the bumper and into movement of the truck.



Figure 126. **Deformation of bumper and module enclosure**

Upon disassembly of the battery pack, it was noted that none of the battery cells were severely crushed or penetrated by any part of the pendulum. In this case, all four cells on the impact side of the pack showed some abrasion and slight denting

on the outside casings as shown in Figure 127. However, this impact represents a best case scenario with the bumper and vehicle dynamics absorbing much of the energy. This would not have been the case if a more ridged component of the impacting vehicle, such as the frame, had penetrated the pack. Here, no thermal runaway occurred within 48 hours before disposal. However, these dents are severe enough to have potentially resulted in either immediate or eventual internal shorting leading to thermal runaway. Delayed thermal runaway has occurred in some high profile cases. Individual cells retained their full voltage output. All cells from this pack were placed in a salt water bath to safely discharge prior to disposal.



Figure 127. **Dented battery cell**

This test demonstrated that the simulated shock of a 25 mph SUV collision directly into a battery module mounted outside a bus frame may not necessarily result in a venting event. In this case the bumper absorbed much of the energy by deformation, a significant energy portion was transferred into vehicle momentum, and the battery pack was not penetrated by any ridged vehicle components. The dual wall steel-aluminum enclosure and header also provided substantial strength and protection against crushing. A different outcome should be expected, however, if the collision had included battery pack penetration.

## VIII. ENVIRONMENTAL IMPACTS

In the case where NCA batteries onboard a bus vent, it is important to understand the gases released which may present an exposure risk to bus passengers and bystanders. Figure 4 showed the types and amounts of gases released during venting, most of which were common carbon oxides and hydrocarbons including  $\text{CH}_4$ ,  $\text{CH}_2$ , ethane, propane, butane,  $\text{H}_2$ , and higher hydrocarbons C3 and C5. A validation test of gases released was run during one of our cell nail puncture tests. Sample gases were collected near the event through a tube leading to a gas collection bag as shown in Figure 128.



Figure 128. **Sample Tube Leading to Gas Sample Bag**

The gas sample bag was processed at a Penn State laboratory using a GC-17A gas chromatograph manufactured by Shimadzu. The method used Flame Ionization Detection (FID) which is only effective at detecting hydrocarbons. The results are shown in Figure 129. Peaks were detected for several hydrocarbons including methane ( $\text{CH}_4$ ), methylene ( $\text{CH}_2$ ), ethane ( $\text{C}_2\text{H}_6$ ), propane ( $\text{C}_3\text{H}_8$ ), and butane ( $\text{C}_4\text{H}_{10}$ ). These gases (with the exception of methylene) were also present in the more comprehensive gas analysis depicted previously and presented here again in Figure 130 with the commonly detected gases highlighted.

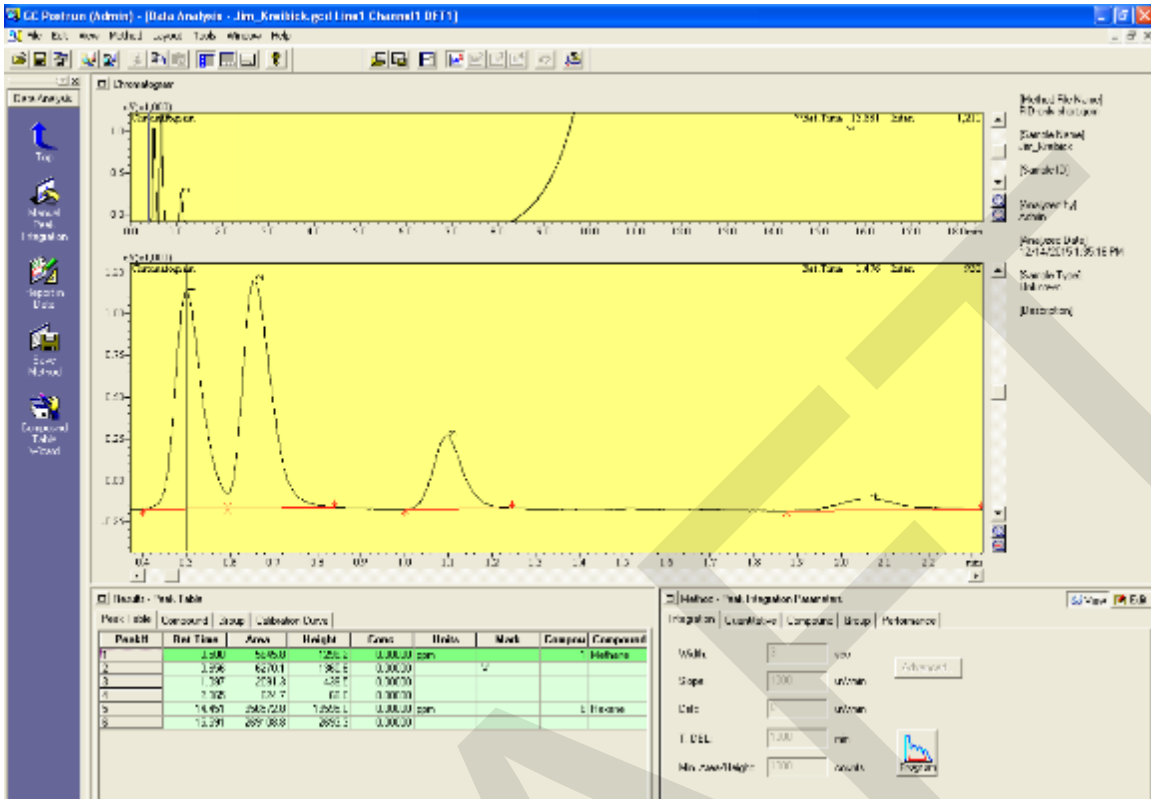


Figure 129. Gas Chromatography Results

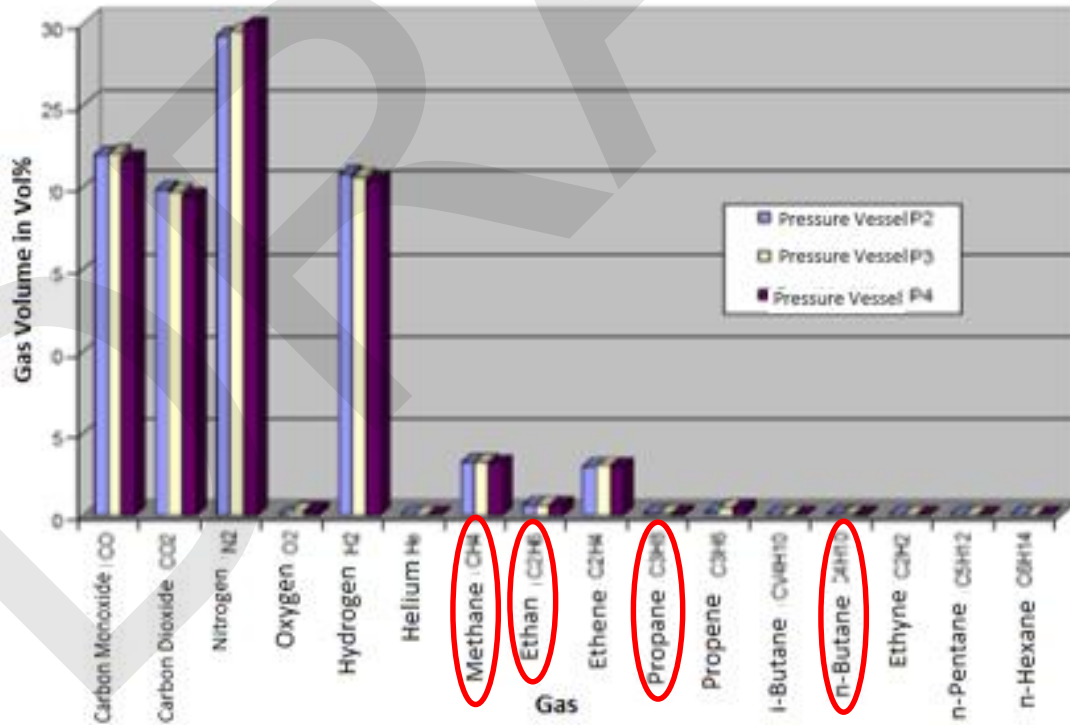


Figure 130. Molecules Present in Venting Gas

## IX. CONCLUSION

When considering the use of an NCA battery system in a transit bus application, material and structural design is critical to keep passengers safe. Common plastics such as Acetal and PET have acceptable structural properties but their rapid and sustained combustibility under the high temperatures of a nearby thermal event poses a risk of rapid and severe events. Teflon works well as a cell separator because its melting point is high enough to withstand the heat generated by the large format cells used in this testing. Pyrophoric and possibly other materials may also perform well. Aluminum enclosures cannot withstand the temperatures of venting or sustained fires afterwards. Steel performs very well and can also provide additional strength to resist crush and puncture.

Also, special consideration must be made for the possible over charge or cell puncture scenarios. This report presents the magnitude of these events cannot be contained by the typical battery system designs.

Expect high temperatures and extreme flow rates present in these thermal events. It is not possible to completely contain a thermal event but it may be possible to redirect the energy in a safe direction to provide passengers more time to evacuate the bus.

## X. SELECT ABBREVIATIONS AND ACRONYMS

A / Ah	Ampere / Ampere-Hour
BMS	Battery Management System
CAN	Controller Area Network
C	Degrees Celsius
C Rate	Battery Hourly Power Rate
DC	Direct Current
DP	Dual Polarization
DST	Dynamic Stress Test
EIS	Electrochemical Impedance Spectroscopy
EOL	End of Life
ESR	Effective Series Resistance
ESS	Energy Storage System
EV	Electric Vehicle
Hz	Hertz, a unit of frequency
kW / kWh	kiloWatt / kiloWatt-hour
LFP	Lithium Ion Phosphate
LTO	Lithium Titanate Oxide
mV	micro-Volt
NCA	Lithium Cobalt Oxide
OCV	Open Circuit Voltage
PHEV	Plug-in Hybrid Electric Vehicle
RTD	Resistance Temperature Detectors
RC	Resistor-Capacitor
VAC	Variable Alternating Current
V	Volt

## XI. BIBLIOGRAPHY

- American Public Transportation Association. (1997, 31 3). *American Public Transportation Association*. Retrieved from Standard Bus Procurement Guidelines: <http://www.apta.com/resources/reportsandpublications/documents/comterms.pdf>
- Ashis Arora, Noshirwan K. Medora, Thomas Livernois, and Jan Swart. (2010). *Electric and Hybrid Vehicles. Power Sources, Models, Sustainability, Infrastructure and the Market*. Amsterdam: G Pistoia.
- Dr. Lothar Wech, Richard Richter. (n.d.). *NHTSA*. Retrieved from CRASH SAFETY ASPECTS OF HV BATTERIES FOR VEHICLES : <http://www-nrd.nhtsa.dot.gov/pdf/esv/esv22/22ESV-000302.pdf>
- ECE, U. (2012). *UNECE*. Retrieved from Spectrum Of Road Safety Activities: [https://www.unece.org/fileadmin/DAM/trans/roadsafe/publications/Spectrum\\_of\\_Road\\_Safety\\_Activites.pdf](https://www.unece.org/fileadmin/DAM/trans/roadsafe/publications/Spectrum_of_Road_Safety_Activites.pdf)
- Fire Protection Engineering. (2012, October 7). *Lithium-Ion Battery Hazards*.
- Gerardo Olivares, Vikas Yadav. (n.d.). Retrieved from INJURY MECHANISMS TO MASS TRANSIT BUS PASSENGERS DURING FRONTAL, SIDE AND REAR: <http://www-nrd.nhtsa.dot.gov/pdf/esv/esv21/09-0427.pdf>
- Jennifer Chu. (2013, June 4). *MIT News Office* . Retrieved from Crash-testing lithium-ion batteries: <http://news.mit.edu/2013/crash-testing-lithium-ion-batteries-0604>
- National Fire Protection Association. (2014, December 9). *Tactical Considerations for Extinguishing Fires in Hybrid Electric Vehicles*.
- National Fire Protection Association. (2014, 9 December). *Youtube*. Retrieved from Tactical Considerations for Extinguishing Fires in Hybrid and Electric Vehicles: [https://www.youtube.com/watch?v=mtCk3srID\\_w](https://www.youtube.com/watch?v=mtCk3srID_w)

- National Fire Protection Association. (2015). *Emergency Field Guide*, Volume 4.
- National Highway Traffic Safety Administration. (n.d.). *National Highway Traffic Safety Administration*. Retrieved from Federal Motor Vehicle Safety Standards and Regulations: <http://www.nhtsa.gov/cars/rules/import/FMVSS/>
- Pistoia, G. (2010). Safety of Lithium-Ion Batteries for Hybrid Electric Vehicles. *Electric and Hybrid Vehicels: Power Sources, Models, Sustainability, Infrastructure and the Market*, 464-490.
- Transportation, N. Y. (1999, July). *DOT*. Retrieved from Title 17 Official Compilation of Codes, Rules and Regulations of the State of New York: <https://www.dot.ny.gov/divisions/operating/osss/bus-repository/busregs1.pdf>
- Wikipedia*. (2007, October 2). Retrieved from Federal Motor Vehicle Safety Standards: [https://en.wikipedia.org/wiki/Federal\\_Motor\\_Vehicle\\_Safety\\_Standards](https://en.wikipedia.org/wiki/Federal_Motor_Vehicle_Safety_Standards)
- Wikipedia*. (2013, January 28). Retrieved from New Car Assessment Program: [https://en.wikipedia.org/wiki/New\\_Car\\_Assessment\\_Program](https://en.wikipedia.org/wiki/New_Car_Assessment_Program)
- Wikipedia*. (2013, August 25). Retrieved from Insurance Institute for Highway Safety: [https://en.wikipedia.org/wiki/Insurance\\_Institute\\_for\\_Highway\\_Safety](https://en.wikipedia.org/wiki/Insurance_Institute_for_Highway_Safety)

## **XII. ABOUT THE AUTHORS**

### **Timothy Cleary**

Timothy Cleary is the director of the Battery Application Technology Testing & Energy Research Laboratory (BATTERY) at the Larson Institute at Penn State.

Timothy Cleary earned his B.Sc. and M.S. degrees in mechanical engineering from Penn State. He is involved in the U.S.DOE-sponsored Advanced Vehicle competitions serving as team leader for the 2007-2008 competition and currently an assistant faculty advisor to the current PSU team. In 2009-2010 he was a vehicle systems and simulation contracted engineer supporting U.S. DOE research in the area of pluggable hybrid electric vehicles. In 2010-2011 he gained Top Secret security clearance and assisted the U.S. Army's Seeker Effects Laboratory in performing infrared countermeasure testing. Currently the director of Penn State's Battery Application Technology Testing & Energy Research Laboratory (BATTERY), he concentrates his research in battery system development and application testing for advance chemistry automotive batteries ranging from starter to full electric buses.

### **Marc Serra Bosch**

Marc is an international student from Barcelona who was in an exchange program of his master's degree in investigation. He graduated in mechanical engineering at Institut Químic de Sarrià (IQS) and his interests are mostly focused on different aspects of the vehicle industry such as the implementation of alternative energies, active vehicle safety systems as well as the vehicle testing.

### **James A. Kreibick**

James A. Kreibick earned his BS in Electrical Engineering from Penn State. His studies focused on control systems and power systems. During his time at Penn State he was involved in the Penn State Advanced Vehicle team that participated in the EcoCar2 competition sponsored by General Motors and the Argonne National Laboratory. He also spent three years working on battery research with the Pennsylvania Transportation Institute that included two funded research projects from MNTRC and Norfolk Southern Corporation. These projects ranged from battery testing and hardware in the loop testing to battery modeling. He intends to join industry related to energy storage and power transmission.

## **Dr. Joel Anstrom**

Dr. Joel R. Anstrom is Director of the Hybrid and Hydrogen Vehicle Research Laboratory and the DOE Graduate Automotive Technology Education Program at the Thomas D. Larson Pennsylvania Transportation Institute at Penn State University. He is responsible for developing and managing transportation research projects that advance hybrid electric and fuel cell vehicles, hydrogen fueling infrastructure, and high-power in-vehicle energy storage. His research focus is modeling and demonstration of electric, hybrid electric, and fuel cell vehicles for efficiency and dynamic handling.

Dr. Anstrom earned B.S. and Ph.D. degrees in Mechanical Engineering from Penn State University and a Masters degree in Manufacturing Systems Engineering from the University of Texas at Austin.

### **XIII. APPENDIX A – DATA ACQUISITION SCRIPTS**

DRAFT

**XIV. APPENDIX B – DRAWINGS**

DRAFT

# XV. APPENDIX C – SPECIFICATION SHEETS



## HP 602030 NCA 45 Ah/ 162 Wh Lithium Ion Cell

### Physical and mechanical characteristics

Diameter	60 mm
Height	232 mm (203 mm without terminals)
Terminals	Positive terminal Al M12 L: 9 mm Negative terminal Cu M12 L: 9 mm
Weight	approx. 1500 g
Volume without terminals	0.57 l
Case material	Stainless Steel

### Chemical characteristics

Positive electrode	Lithium nickel cobalt oxide
Negative electrode	Graphite

### Electrical characteristics\*

Nominal voltage	3.6 V
Nominal capacity at 0.2 C	45 Ah
Minimum capacity	42 Ah
AC Impedance (1 kHz)	≈ 0.4 mOhm
DC Resistance (ESR) (2 s pulse discharge @ 20 C/ 50% SOC)	≈ 1.2 mOhm
Specific energy at 0.2 C	108 Wh/kg
Energy density at 0.2 C	282 Wh/l
Specific power (2 s pulse discharge @ 27.8 C/ 100% SOC)	2080 W/kg
Power density (2 s pulse discharge @ 27.8 C/ 100% SOC)	5440 W/l

### Operating conditions\*

Recommended charge method	Constant current - constant voltage
End of Charge	I = C/100
Maximum charge voltage	4.2 V
Recommended charge current	up to 45 A (1 C)
Continuous charge current	up to 180 A (4 C)
Maximum pulse charge current (15 s) (Max. SOC 80%, average current < 180 A)	270 A (6 C)
Recommended voltage limit for discharge	3 V
Lower voltage limit for discharge	2.7 V
Lower voltage limit for pulse discharge	2 V
Recommended discharge current	up to 90 A (2 C)
Maximum discharge current	up to 450 A (10 C)
Maximum pulse discharge current (2 s)	up to 1250 A (27.8 C)
Operating temperature	-30°C to +60°C
Recommended charge temperature	0°C to +40°C
Storage and transport temperature	-40°C to +60°C
Cycle life at 20°C and 100% DOD (0.5 C charge; 0.5 C discharge)	> 1000 cycles to 80% nominal capacity > 2000 cycles to 60% nominal capacity

\* Reference temperature 20°C

Doc HP 602030 NCA - 2009-06

Data in this document are subject to change without notice and are not binding.



GAIA Akkumulatorenwerke GmbH  
Montanlastr. 17  
99734 Nordhausen, Germany  
www.gaia-akku.com



Lithium Technology Corporation  
5115 Campus Drive  
Plymouth Meeting, PA 19462  
www.lithiumtech.com

High Power

## XVI. APPENDIX D - FMVSS STANDARDS

### FMVSS 201U

#### Test Procedure

A Free Motion Headform (FMH) impactor hits the upper interior parts with a velocity of 24 km/h (A-, B-, C-pillar, roof etc.).

#### FMH Impactor Data

Mass of FMH impactor: 4.54 kg

Head form according to SAE J 921 and J 977 including triaxial acceleration sensor.

#### Protection Criteria

$$\text{HIC Calculation} \quad \text{HIC} = \sup_{t_1, t_2} \left\{ \left[ \frac{1}{(t_2 - t_1)} \int_{t_1}^{t_2} a dt \right]^{2.5} (t_2 - t_1) \right\} \quad t_2 - t_1 < 36 \text{ ms}; a [g]; t [s]$$

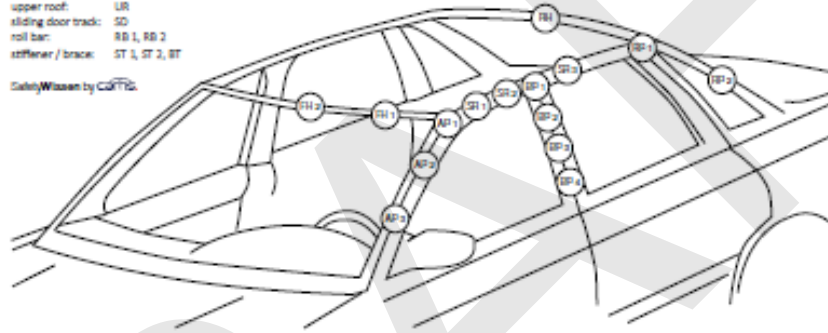
$$\text{HIC value for FMH} \quad \text{HIC}(d) = 0.75446 \text{ HIC} + 166.4$$

HIC(d) must not exceed 1000.

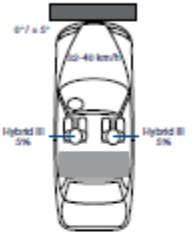
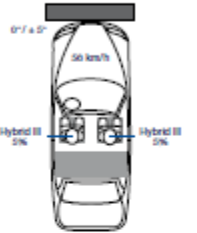
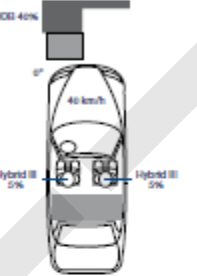
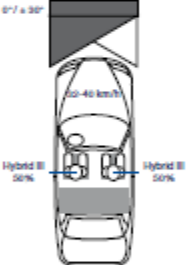
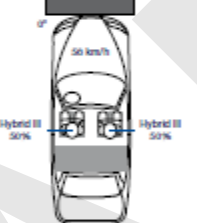
24 points defined for impact according Test Procedure TP-201 (each side, left and right)

other pillar: OP 1, OP 2  
 upper roof: UR  
 sliding door track: SD  
 roll bar: RB 1, RB 2  
 stiffener / brace: ST 1, ST 2, ST

SafetyWissen by carTIC



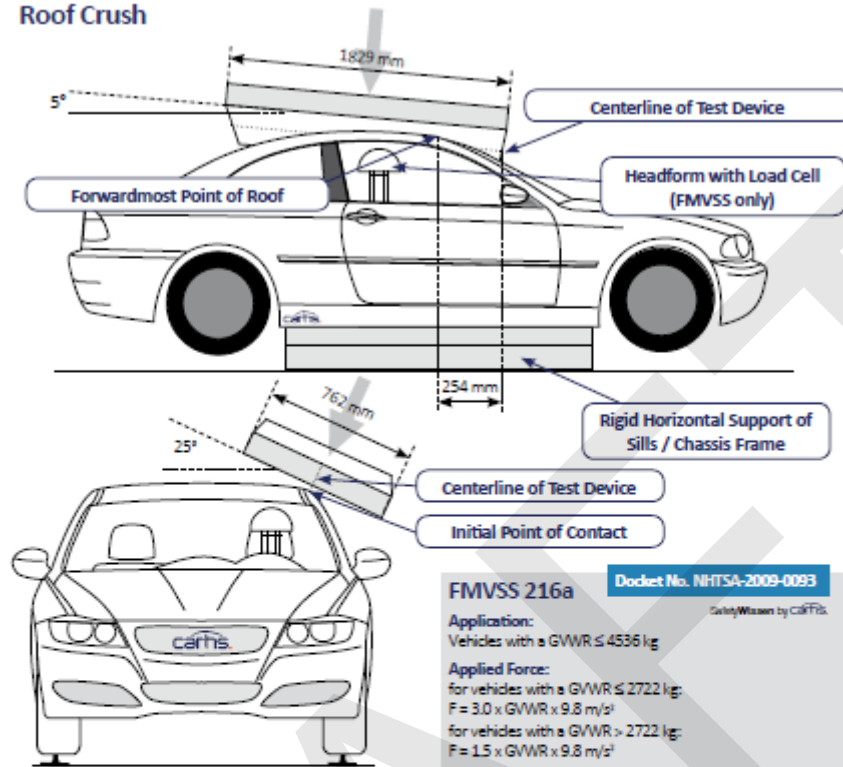
## FMVSS 208: Frontal Impact Requirements: In-Position

In-Position – Test Configurations			
	Full-Width Test		ODB Test
	unbelted 	belted 	
5 % Female Dummy	 <p>0°/7 ± 5° 32-40 km/h Hybrid III 50% Hybrid III 50%</p>	 <p>0°/7 ± 5° 50 km/h Hybrid III 50% Hybrid III 50%</p>	 <p>ODB 40% 0° 40 km/h Hybrid III 50% Hybrid III 50%</p>
50 % Male Dummy	 <p>0°/7 ± 50° 32-40 km/h Hybrid III 50% Hybrid III 50%</p>	 <p>0° 50 km/h Hybrid III 50% Hybrid III 50%</p>	<p>SafetyWaters by C&amp;FPG</p>

## FMVSS 208: Frontal Impact Requirements: Out of Position

Front seat	Dummy	Test configuration
Driver side	Hybrid III 5 % female	chin on airbag module in steering wheel chin on top of steering wheel
	CRABI 12m	in 23 defined CRS / positions
Passenger side	Hybrid III 3 y/o	chest on instrument panel head on instrument panel
	Hybrid III 6 y/o	chest on instrument panel head on instrument panel

## Roof Crush



**IIHS Testing Protocol Version II (Dec 2012)**

Platen Displacement: 127 mm  
 Feed Rate: 5 mm/s  
 Single Side Test: Lab selects worst case  
 Assessment: based on Strength-to-weight ratio (SWR) =  $F_{max} / m \times g$

SWR	Rating
$\geq 4.00$	Good
$\geq 3.25$ till $<4.00$	Acceptable
$\geq 2.50$ till $<3.25$	Marginal
$< 2.50$	Poor

A „Good“ rating in the roof crush test is a requirement for the Top-SafetyPick award.

**FMVSS 216a** Docket No. NHTSA-2009-0093

Application: Vehicles with a GVWR  $\leq 4536$  kg SafetyWitness by carfiis

Applied Force:  
 for vehicles with a GVWR  $\leq 2722$  kg:  
 $F = 3.0 \times GVWR \times 9.8 \text{ m/s}^2$   
 for vehicles with a GVWR  $> 2722$  kg:  
 $F = 1.5 \times GVWR \times 9.8 \text{ m/s}^2$

Feed Rate:  $\leq 13$  mm/s  
 Double Sided Test

Requirements:  
 Platen displacement  $\leq 127$  mm  
 Load on headform located at head position of 50% male  $\leq 222$  N

Phase-In for GVWR  $\leq 2722$  kg:

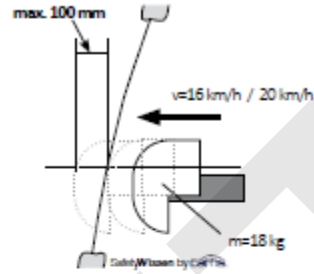
Manufacturing Period	%*
01.09.2012-30.08.2013	25%
01.09.2013-30.08.2014	50%
01.09.2014-30.08.2015	75%
on or after 01.09.2015	100%

\* in % of the production of the respective period or in % of the average production of the 3 previous years  
 Introduction for GVWR  $> 2722$  kg: 01.09.2016

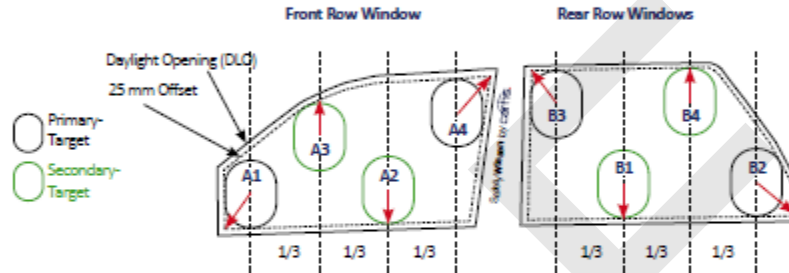
## FMVSS 226 - Ejection Mitigation

### Requirements:

- At up to 4 impact test locations on each side window in the first 3 rows of seats the head excursion may not exceed 100 mm
- Tests at two impact velocities: 16 km/h and 20 km/h
- Head protection systems (e.g. curtain airbags) must be fired before the impact:
  - at 20 km/h with a time delay of 1.5 s prior to the impact
  - at 16 km/h with a time delay of 6 s prior to the impact
- Tests are done without glazing or with pre-damaged glazing
  - pre-damage: perforation in a 75 mm grid pattern
- Valid for vehicles with GVWR ≤ 4536 kg
- Phase-In: 2013 - 2017



### Locating Targets:



Steps	Front Row Window	Rear Row Windows
1	Set Primary Target A1 in lower front corner	Set Primary Target B3 in upper front corner
2	Set Primary Target A4 in upper rear corner	Set Primary Target B2 in lower rear corner
3	Divide horizontal distance between A1 and A4 in thirds	Divide horizontal distance between B3 and B2 in thirds
4	Move A3 at the first third vertically upward	Move B1 at the first third vertically downward
5	Move A2 at the second third vertically downward	Move B4 at the second third vertically upward
6	Measure Distances $D_x$ (horizontal) and $D_y$ (vertical) of the target center points	
7	If $D_x (A2 - A3) < 135 \text{ mm}$ and $D_y (A2 - A3) < 170 \text{ mm}$ ⇒ Eliminate A3	If $D_x (B1 - B4) < 135 \text{ mm}$ and $D_y (B1 - B4) < 170 \text{ mm}$ ⇒ Eliminate B4
8	If $D_x (A4 - A3)$ [or A2 if A3 was eliminated in step 7] $< 135 \text{ mm}$ and $D_y (A4 - A3/2) < 170 \text{ mm}$ ⇒ Eliminate A3/2	If $D_x (B3 - B4)$ [or B1 if B4 was eliminated in step 7] $< 135 \text{ mm}$ and $D_y (B3 - B4/1) < 170 \text{ mm}$ ⇒ Eliminate B4/1
9	If $D_x (A4 - A2)$ [or A3 if A2 was eliminated in step 8] $< 135 \text{ mm}$ and $D_y (A4 - A2/3) < 170 \text{ mm}$ ⇒ Eliminate A2/3	If $D_x (B2 - B1)$ [or B4 if B1 was eliminated in step 8] $< 135 \text{ mm}$ and $D_y (B2 - B1/4) < 170 \text{ mm}$ ⇒ Eliminate B1/4
10	If $D_x (A1 - A4) < 135 \text{ mm}$ and $D_y (A1 - A4) < 170 \text{ mm}$ ⇒ Eliminate A4	If $D_x (B3 - B2) < 135 \text{ mm}$ and $D_y (B3 - B2) < 170 \text{ mm}$ ⇒ Eliminate B3
11	If only 2 targets remain: Measure absolute distance $D$ the center points of the targets	
12	If $D > 360 \text{ mm}$ , set additional 3rd target on the center of the line connecting the targets	
13	If less than 4 targets remain, repeat steps 1-12 with the impactor rotated by 90 degrees. If this results in a higher number of targets use the rotated targets.	
14	If no target is found rotate the impactor in 5 degree steps, until it is possible to fit the impactor in the DLO-offset. Then place the center of the target as close to the geometric center of the DLO as possible.	